Exxon Valdez Oil Spill
Restoration Project Final Report

Lingering Oil on Boulder-Armored Beaches in the Gulf of Alaska 23 Years After the *Exxon Valdez* Oil Spill

Restoration Project 11100112
Final Report

Gail V. Irvine
U. S. Geological Survey
Alaska Science Center
Anchorage, Alaska

Daniel H. Mann
Geography Program
School of Natural Resources
University of Alaska Fairbanks, Alaska

Mark Carls
Larry Holland
National Oceanic and Atmospheric Administration
National Marine Fisheries Service
Auke Bay Fisheries Laboratories
Juneau, Alaska

Christopher Reddy
Robert K. Nelson
Department of Chemistry and Geochemistry
Woods Hole Oceanographic Institution
Woods Hole, Massachusetts

Christoph Aeppli
Bigelow Laboratory for Ocean Sciences
East Boothbay, Maine

July 2014

Exxon Valdez Oil Spill
Restoration Project Final Report

Lingering Oil on Boulder-Armored Beaches in the Gulf of Alaska 23 Years After the *Exxon Valdez* Oil Spill

Restoration Project 11100112
Final Report

Gail V. Irvine
U. S. Geological Survey
Alaska Science Center
Anchorage, Alaska

Daniel H. Mann
Geography Program
School of Natural Resources
University of Alaska Fairbanks, Alaska

Mark Carls
Larry Holland
National Oceanic and Atmospheric Administration
National Marine Fisheries Service
Auke Bay Fisheries Laboratories
Juneau, Alaska

Christopher Reddy
Robert K. Nelson
Department of Chemistry and Geochemistry
Woods Hole Oceanographic Institution
Woods Hole, Massachusetts

Christoph Aeppli
Bigelow Laboratory for Ocean Sciences
East Boothbay, Maine

July 2014

Lingering Oil on Boulder-Armored Beaches in the Gulf of Alaska 23 Years After the *Exxon Valdez* Oil Spill

Restoration Project 11100112
Final Report

Study History: Project 11100112 is the latest in several projects that have addressed the status and recovery of oiled shorelines along national park coastlines in the Gulf of Alaska that were initially contaminated by the 1989 *Exxon Valdez* spill. Projects that have included earlier sampling of these sites include: R103B (which later became 93090), 94266, 99459, 00459 and 040708.

Abstract: Twenty-three years after the 1989 *Exxon Valdez* spill deposited oil mousse on rocky shores of national parks in the Gulf of Alaska, we reexamined our long-term study sites. We have been investigating the relationship of boulder stability to oil persistence, changes in surface and subsurface oiling over time, and the degree to which the oil has weathered. Repeat visits show that oil persistence is highly correlated with the stability of the boulder armors, which have remained largely intact for 20+ years, with few significant boulder movements. However, minor movements of boulders are common. Surface oiling continues to decline and is now at very low levels while subsurface oiling continues relatively unchanged at 4 of the 6 sites. New in 2011 and 2012 was the deployment of passive samplers at two sites; these revealed that oil constituents are being released into the water. Samples of nearby mussels did not conclusively show contamination by oil. For the first time since 1989, there was no apparent oiling at the most distant site from the spill origin; the extent of oiling was also reduced at the next most distant site. At the four remaining sites, the oil is present in depths previously recorded, and is only slightly weathered, although there are indications of microbial degradation at one site. Oil/sediment samples were analyzed by gas chromatography-mass spectrometry, and newer methods, which have allowed expanded views of the 23-year old oil. Comprehensive two-dimensional gas chromatographic (GC x GC) analyses have provided an order of magnitude increase in the discrimination of compounds found in the oil as compared to traditional GC analysis. Analysis of biomarkers by multiple techniques has suggested that oil at the Cape Gull site does not appear to be *Exxon Valdez* oil, or that the biomarkers have weathered in unexpected ways. At the Kashvik site, where no oil was observed, chemical analyses found a diesel or jet-fuel signal, which we interpret to be a secondary contamination of the site. Thin-layer chromatography-flame ionization detection analyses indicate no significant accumulation of recalcitrant oxygenated hydrocarbons at four of the sites, consistent with only minor oil weathering.

Key Words: armored beaches, *Exxon Valdez,* Gulf of Alaska, monitoring, oil, oil mousse, oil spill, PAH, persistence, petroleum hydrocarbon, weathering, biomarkers, passive samplers, mussels, *Mytilus trossulus*,

Project Data: The data collected by this project include: 1) description of oiling at selected shoreline sites in Kenai Fjords and Katmai National Parks and Preserves; 2) percent cover estimates of surface oiling within permanently marked quadrats; 3) bolt (boulder) movement data; 4) sampling of subsurface oiling via 'dip-stones'; 5) chemical analyses via gas-chromatography, mass-spectroscopy of oiled sediment samples collected by this project in 1992, 1994, 1999, and 2012; in 2012 additional analyses of oil/sediment samples by comprehensive two dimensional gas chromatography and thin-layer chromatography-flame ionization detection; 6) chemical analyses of passive samplers and mussel tissue from 2011 and 2012 to see if oil is being released into the water. Descriptions of oiling and associated quantitative data are expressed fully in the text and tables of the report (data are descriptive and tabular; tabular data is in Excel spreadsheets); Dede Bohn is the custodian of these data (U.S.G.S., Alaska Science Center, phone 336-721-3464, E-mail dbohn@usgs.gov). The hydrocarbon data are held as part of a larger database, The Exxon Valdez Oil Spill of 1989: State-Federal Trustee Council Hydrocarbon Database (EVTHD), 1989-2005. This database is housed at the Auke Bay Labs with Mark Carls as custodian (11305 Glacier Highway, Juneau, Alaska 99801-8626, phone 907/789-6019, fax 907/789-6094, E-mail mark.carls@ noaa.gov). Data are available on diskette in multiple formats.

Citation:

Irvine, G.V., D.H. Mann, M.G. Carls, L. Holland, C. Reddy, R.K. Nelson, and C. Aeppli. 2014. Lingering oil on boulder-armored beaches in the Gulf of Alaska 23 years after the *Exxon Valdez* oil spill, *Exxon Valdez* Oil Spill Restoration Project Final Report (Restoration Project 11100112), U.S. Geological Survey, Alaska Science Center, Anchorage, Alaska.

Executive Summary

In 1989, the *Exxon Valdez* oil spill contaminated approximately 2000 km of coastline, including more than 750 km of shoreline in the Gulf of Alaska, outside of Prince William Sound. The observed persistence of the oil on national park coasts for several years after the spill provided the impetus for this study. We have focused on investigating situations in which oil has persisted, analyzing why and how it persists, determining the rate of change in the chemical character of the oil, and the status of recovery of these oiled shorelines. In 2011 and 2012, we added several new components to our study in order to examine whether oil is being released from these sites and more detailed investigation of stranded oil chemistry using newer analytical methods. Our results are presented and discussed in two chapters, which along with associated figures, tables and appendices, comprise this report.

In Chapter 1, we examine field data on extent of both surface and subsurface oiling and processes controlling the long-term persistence of residual oiling. Five of the six sites are boulder-armored shores that can experience high wave energies. To investigate our hypothesis that boulder armor stability is key to the persistence of the oil, we have measured boulder movements at four of the sites. In 2011 and 2012, we deployed low-density polyethylene membrane devices (PEMDs) at two sites to determine if petroleum hydrocarbons were being released from the sites into the water column.

Stranded *Exxon Valdez* oil has persisted for twenty-three years on boulder-armored beaches that experience high wave energies in the Gulf of Alaska, 600 km from the spill origin. These shorelines were initially contaminated in the spring of 1989 by oil mousse, a viscous water-in-oil emulsion that can be transported long distances with little chemical weathering. In 1994, we established five permanent monitoring sites on the shores of Shelikof Strait in Katmai National Park and Preserve and one site in Kenai Fjords National Park. By 2012, no observable oil remained at the most distant site (Kashvik Bay) and very little oil remained at either the surface or in the subsurface at the second-most distant site (Cape Gull). At the other three sites on the Katmai coast (Cape Douglas, Kiukpalik Island, and Ninagiak Island), surface oil had declined to extremely low levels by 2012; however, subsurface oiling still persists in appreciable quantities at these three sites and shows remarkably little chemical weathering. The same is true at the McArthur Pass site in Kenai Fjords. The PEMDs detected the release of small amounts of petroleum products from these persistent oil patches into the water column. The reason these patches of subsurface oil have persisted on the Katmai coast is that they are protected beneath armors of boulders that shield both the underlying sediment and the stranded oil. Oil persists at the McArthur Pass site in Kenai Fjords because of the low wave energy at that site. Monitoring of boulder movements at the Katmai sites shows these armors have been surprisingly stable over the last two decades, even on beaches exposed to high wave energies. The percentage of boulders experiencing armor-disrupting movements has been relatively small (<10%) regardless of wave exposure. The main geomorphic changes on these beaches have involved individual boulders shifting in place within the surrounding armor and the occasional transient infilling of armors by smaller-sized sediment (pebbles and cobbles). The long-term persistence of slightly weathered oil in this geomorphic setting suggests that boulder-armored beaches should be emphasized in all shoreline assessments aimed at predicting oil persistence and planning response activities after oil spills. The 23-year persistence of slightly weathered oil on these macrotidal, high wave-energy shorelines illustrates the challenges facing the remediation of oil spills in high-latitude settings. The release of oil from these sites, albeit in small quantities, may still be posing toxic threats to local fauna.

Chapter 2 focuses on the chemistry of the stranded oil/sediments in 2012, with more limited data from historical samples presented. We investigated the extent of weathering in oiled sediment collected beneath stable boulder armors or in bedrock crevices from six locations. Sample extracts were analyzed with traditional gas chromatography, comprehensive two-dimensional gas chromatography (GC×GC), as well as thin layer chromatography (TLC-FID) to chemically describe the oil on a molecular and bulk level. To confirm that the oil residues were indeed from the *Exxon Valdez* cargo, hopane and sterane biomarkers were employed. Surprisingly, stranded oil at two shoreline sites could not be confidently matched to *Exxon Valdez* oil, but instead indicated another oil source and/or the occurrence of substantial biomarker transformations. Chemical analyses suggest that evaporation has been the main weathering process and reveal only minor amounts of biodegradation of the stranded *Exxon Valdez* oil, even though the oil has been exposed in the environment for 23 years. In line with the absence of advanced oil degradation, no major increase of oil degradation products was found. We conclude that weathering of the oil at most of our Gulf of Alaska monitoring sites has been very slow. Most of the 2012 samples were chemically very similar to 11-day old samples collected from Prince William Sound in 1989, even after transport for hundreds of kilometers and 23 years of being stranded on beaches; only in the abundances of n-alkanes did they differ. We suspect that the preservation of the oil was primarily due to the formation of oil mousse within days after the spill, prior to its long-distance transport. The stranding of the oil on stable, boulder-armored shores or on a low-energy bedrock/boulder beach further protected the oil and slowed oil degradation processes.

Our study of oil persistence at these six Gulf of Alaska sites represents the only long-term study outside of Prince William Sound, and the longest consistent study of oil persistence spill-wide. Because we are studying more exposed shorelines and all of the oiling of these sites was by oil mousse, our results provide insights not gained from studies within Prince William Sound.

Chapter 1

Evaluation of the Long-Term Persistence of *Exxon Valdez* Oil on Gulf of Alaska Beaches

Gail V. Irvine[1], Daniel H. Mann[2], Mark Carls[3], Larry Holland[3]

[1]U. S. Geological Survey, Alaska Science Center, Anchorage
[2]Geography Program, School of Natural Resources, University of Alaska, Fairbanks
[3]National Marine Fisheries Service, Auke Bay Laboratories, Juneau, Alaska

Abstract

Stranded *Exxon Valdez* oil has persisted for twenty-three years on boulder-armored beaches that experience high wave energies in the Gulf of Alaska and are distant from the spill origin. These shorelines were contaminated in the spring of 1989 by oil mousse, a viscous water-in-oil emulsion transported long distances with little chemical weathering. In 1994, we established five permanent monitoring sites on the shores of Shelikof Strait in Katmai National Park and Preserve and one site in Kenai Fjords National Park. By 2012, no observable oil remained at the most distant site (Kashvik), and very little oil remained at the surface or the subsurface at the second-most distant site (Cape Gull). At the other three sites on the Katmai coast (Cape Douglas, Kiukpalik Island, and Ninagiak Island), surface oil had declined to very low levels by 2012; however, subsurface oiling still persisted in appreciable quantities and showed remarkably little chemical weathering. The same was true at the McArthur Pass site in Kenai Fjords. In 2011 and 2012, we deployed low-density polyethylene membrane devices (PEMDs) at the Cape Douglas and the Kiukpalik Island sites and detected the release of small amounts of petroleum products into the water column. These patches of subsurface oil have persisted on the Katmai coast because they are protected beneath natural boulder armors that shield both the underlying sediment and the stranded oil. Oil persists at the site in Kenai Fjords, which is a bedrock shoreline without a boulder armor, probably because of the relatively low wave energy at that site. Monitoring of boulder movements at the Katmai sites shows these armors have been stable over the last two decades, even on beaches exposed to high wave energies. The percentage of boulders experiencing armor-disrupting movements over 18 years has been relatively small (<10%) regardless of wave exposure. The main geomorphic changes on these beaches have involved individual boulders shifting in place within the surrounding armor and the occasional transient infilling of the armors by smaller-sized sediment (pebbles and cobbles). The long-term persistence of slightly weathered oil in this geomorphic setting emphasizes the need to pay special attention to boulder-armored, gravel beaches when planning responses to oil spills. The release of oil from these sites, albeit in trace quantities, could pose a toxic threat to local fauna if a large-scale disruption of the boulder armor occurred.

Key Words: oil spill; geomorphology; boulder-armored beaches; *Exxon Valdez*; Gulf of Alaska; monitoring; oil mousse; PAH; oil persistence; petroleum hydrocarbons; passive samplers

1. Introduction

When the T/V *Exxon Valdez* ran aground in March 1989, the oil it spilled (Fig. 1) was not expected to persist for decades on shores of the Gulf of Alaska (Hayes et al., 1977, 1979). Most crude oil spilled in temperate and subarctic seas persists on rocky shorelines for only a few weeks to a few months (Owens et al., 2008). Although <1% of the *Exxon Valdez* oil remained on shorelines twelve years after the spill (Short et al., 2004), today pockets of unweathered oil still remain decades after the spill (Nixon et al., 2013). What is more, some of this oil persists on shorelines that are exposed to high wave energies (Irvine et al., 1999; Short et al., 2004; Nixon et al., 2013), despite the fact that the longevity of stranded oil usually displays a strong, inverse correlation with wave energy (Vandermulen, 1977; Gundlach and Hayes, 1978; Vandermuelen, 1977).

Studies conducted in the aftermath of the *Exxon Valdez* oil spill (EVOS) in 1992 have added greatly to our understanding of the processes affecting stranded oil on high latitude shorelines. One of the most important advances has been a fuller appreciation of the role that shoreline geomorphology plays (Owens et al., 2008; Hayes et al., 2010; Nixon et al., 2013), where the term "geomorphology" refers to both the landforms (e.g., beach berms, barrier beaches, spits, offshore bars, and beach-boulder armors) and the processes (e.g., wave action, relative sea-level changes) that create and maintain these landforms through time. Specifically, we have learned much more about the interactions between oil persistence and the geomorphology of gravel beaches. "Gravel" is any unconsolidated sediment composed of a diverse mixture of particle sizes ranging from granules (median clast diameter = 2-4 mm on the Wentworth scale) to large boulders (>256 mm). Hence there are "pebble gravels," "cobble gravels," and "boulder gravels," among others. Gravel beaches are widespread at high latitudes, particularly in formerly glaciated regions like southern Alaska. In Prince William Sound, 47% of all shorelines are gravel beaches (Hayes et al., 2010).

Gravel beaches provide particularly complex settings for the preservation of stranded oil because of their dynamic natures and porous substrates (Hayes et al., 2010). Even before the *Exxon Valdez* spill, gravel beaches were recognized as posing complications in any simple scheme of assigning environmental sensitivity ratings to oil spills because of their high porosities (Gundlach and Hayes, 1978). While the multi-decadal persistence of stranded oil is unusual on the surface of gravel beaches (Owen et al., 2010), significant potential exists for oil persistence in the subsurface.

Oil can persist in the subsurface of a gravel beach if three conditions are fulfilled: 1) there is sufficient pore volume, 2) groundwater is unable to flush the subsurface oil (Li and Boufadel, 2010), and 3) the subsurface oil reservoir is protected from wave disturbance (Nixon et al., 2013). All three of these necessary conditions are strongly affected by geomorphic features that operate at relatively fine spatial scales of centimeters to meters. Foremost among these oil-preserving, geomorphic features are boulder armors that protect subsurface oil from wave action (Irvine et al., 1999; Hayes et al., 2010; Nixon et al., 2013).

Boulder armors develop on any coarse-grained gravel beach exposed to ocean waves (see Section 2.1). These armors shield underlying layers of smaller-sized particles (gravelly mixtures of cobbles, pebbles, granules, and sand) from wave disturbance (Orford et al., 2002; Hayes et al., 2010). The importance of armored beaches in the EVOS region became apparent after it was noticed that oil was retained on gravel beaches if the shoreline was covered by cobble or boulder armors despite high wave energies (Irvine et al., 1999; Irvine et al., 2006; Hayes and Michel, 1999; Nixon et al., 2013). In the years after 1989, it became increasingly apparent that the natural removal of stranded oil from wave-exposed, boulder-armored shorelines was occurring more slowly than initially predicted (Irvine et al., 1999). Boulder armors have turned out to be one of the main geomorphic correlates of stranded oil persistence in the EVOS region (Nixon et al., 2013).

To better understand the processes controlling the persistence of stranded oil on armored, high-energy beaches in the Gulf of Alaska (GOA), in 1994 we began a long-term monitoring study of five, coarse-grained, gravelly, boulder-armored beaches in Shelikof Strait contaminated with *Exxon Valdez* oil in 1989 (Schoch, 1993; Irvine et al., 1999, 2006, 2007; Short et al., 2007). In addition, we studied oil persistence on a bedrock/boulder beach in Kenai Fjords National Park and Preserve located closer to the spill origin (Fig. 1).

Our long-term research questions have been: What are the frequency and scale of geomorphic disturbance at these sites, and how do they relate to the persistence and chemical weathering of stranded oil? Analyses describing the chemical state of the oil in 2012 are presented in Chapter 2 of this report. In this chapter, we present new data obtained in 2012, twenty-three years after the spill, concerning the continued persistence of the *Exxon Valdez* oil, the dynamics of the boulder armors, and whether oil is being released at these sites.

2. Study Area

A detailed description of the study area's geomorphology on the Gulf of Alaska coastline is given in Irvine et al. (2007). In brief, a long history of tectonism and glacial erosion has created intricate, bedrock-controlled shorelines with numerous coarse-grained gravel beaches. Because of its intricate plan adjacent to the open sea, this coastline experiences a wide range of wave energies in a milieu of rapidly changing, storm-wave conditions influenced by strong currents, a 3-5 m tidal range, directionally variable winds, and wave run-ups reaching 7-9 m (AEIDC, 1977; Wilson and Overland, 1986). Buoy Station 46077 in the central Shelikof Strait records mean significant wave heights of 0.9 m in summer and 1.5 m in winter, with an annual range of 0 to 5.5 m. Average wave periods are 4-5 seconds with maximum periods of 7-12 seconds (NOAA, 2013). The Katmai and Kenai coastlines are directly influenced by the Alaska Coastal Current, whose counterclockwise flow transported *Exxon Valdez* oil from the spill point in Prince William Sound (PWS) to distant points in the GOA (Fig. 1) (Royer et al., 1990). Current speeds range seasonally from 20 cm-sec^{-1} to 100 cm-sec^{-1} (Reed and Schumacher, 1986). Our study sites in Shelikof Strait (Fig. 1; Appendix A) are located in a stormy, macrotidal, subarctic coastal environment. They are coarse-grained gravel beaches possessing well-developed boulder armors. The McArthur Pass site is more sheltered and is predominately a bedrock shoreline with a thin veneer of cobbles and boulders.

2.1. Background: Boulder Armors on Beaches

Armoring at the surface of unconsolidated sediment containing multiple clast sizes is a widespread phenomenon in stream beds and on shorelines (Oak, 1984; Wilcock and DeTemple, 2005; Hayes et al., 2010). Armors of interlocking boulders (clast diameters >256 mm) develop naturally on rocky shorelines when the finer particles (e.g., silt, sand, pebbles, and cobbles) are winnowed away by wave action, deflating the shore face and leaving behind a lag of boulders too large for currents to move (Fig. 2). These boulders then protect underlying sediment from further winnowing (Orford et al., 2002; Hayes et al., 2010). In some settings, the process of winnowing may be supplemented by kinetic sieving in which finer particles are sifted downward through the armor by the kinetic energy of water currents and shifting boulders (Isla, 1993). On beaches, boulder armors are often packed together, with the projections of one boulder fitting into the concavities of its neighbors (Shelley, 1968), and larger boulders trapping smaller ones between them (Hills, 1970). The fitting together of boulder armors occurs as the boulders shift and roll in place until they achieve a packing of very high stability (Isla, 1993).

On GOA shorelines, boulder armors occur in the intertidal zone on relatively low-angle surfaces, often at the upper margin of the low-tide terrace (Figure 3 in Hayes et al., 2010). This is probably the case because current velocities are highest here and result in the sweeping of clasts either shoreward onto the storm berm or alongshore. There are numerous exceptions to this scheme, particularly on rocky shorelines where bedrock outcrops control the distribution of unconsolidated sediment (Appendix A). Boulder armors are widespread on Gulf of Alaska shorelines even where relative sea level changed suddenly during the Great Alaskan Earthquake in 1964, demonstrating that armor formation can be very rapid (Hayes et al., 2010). Probably because relative sea level change was slight along the Katmai coastline during the 1964 earthquake and because wave energies are higher there, boulder armors there tend to be better developed than in PWS.

Despite their wide distribution on shorelines around the world, natural boulder armors are little studied, as are boulder beaches in general (Paris et al., 2011). Artificial boulder armors are frequently used to stabilize eroding beaches (Dean and Dalrymple, 2004); however, natural and artificial armors are distinctly different phenomena (Oak, 1984, 1986). Boulder armors that possess a tightly fitted fabric are highly resistant to wave attack, and some are thought to have remained stable for thousands of years (Bishop and Hughes, 1989). On the beds of rivers, coarse-grained armors greatly reduce how much sediment is moved downstream as bedload and tend to induce geomorphic stability despite large scale fluctuations in sediment supply (Mueller and

Pitlick, 2013). Similarly, boulder armors on shorelines probably represent equilibrial geomorphic features that develop into progressively more stable entities over time, to the point where most wave events cannot disturb them or the sediment beneath them (Hayes et al., 2010).

3. Methods

3.1. Site Selection, Oil Characterization, and Oil Sampling

The six study sites (Fig. 1) were selected in 1992 on the basis of being known sites of persistent *Exxon Valdez* oiling (Schoch, 1993); one site in Kenai Fjords National Park (McArthur Pass) and the other five sites in Katmai National Park and Preserve. The five sites located in Shelikof Strait are boulder-armored, gravel beaches that have underlying bedrock abrasion platforms at shallow (0-1 m) depths. The site at McArthur Pass is a bedrock shoreline with a thin covering of locally quarried cobbles and boulders. All six sites were cleaned by Exxon personnel between 1989 and 1992 using manual techniques and several were treated with bioremediation fertilizer. No hot-water washing was done at any of these sites.

Initial oiling at the Cape Douglas site (CD-003A) was described as "heavy" in 1989 by both Exxon and Alaska Department of Environmental Conservation observers. Oil mousse covered an area of 30 x 40 m there in April, 1990 (Irvine et al., 1999). Approximately 24 m^3 of mousse was removed from this site by hand in 1990, and bioremediation fertilizer applied. Initial oiling at the Kiukpalik Island site (SK-101) was described as "medium" in 1990, with the oiled area covering 5 x 100 m. Approximately 33 m^3 of mousse was removed from this site in 1990, and bioremediation fertilizer was applied. Initial oiling of the Ninagiak Island site (HB-050B) was described as “medium" in 1990, and the oil covered an area of 5 x 10 m. Approximately 0.6 m^3 of mousse was removed by hand in 1992. No fertilizer was applied here (Irvine et al., 1999). Initial oiling at the Cape Gull site (K-0922-CG-001) was described as "heavy" in 1989, and it covered an area of 12 x 100 m in 1990. A large amount of mousse was removed by hand from this site and adjacent beaches (~412 m^3). No fertilizer was applied at Cape Gull. Initial oiling at the Kashvik site (KA-002) was described as "moderate" in 1989 and was estimated to cover 20 x 100 m in 1990. Approximately 22 m^3 of mousse was removed from this site in 1989 and another

20 m^3 in 1990. No fertilizer was applied at the Kashvik site (Irvine et al., 1999). These estimates of the amount of oil removed should be considered very approximate.

We estimated the extent of subsurface oiling by examining naturally occurring “dip stones” that were dislodged with a hammer, measured, and then reinserted into the ground. These dip stones came from areas outside the quadrats, but within each study site. Dip stones function like a dip stick in that the stone, once dislodged from the substrate, is a sampler of subsurface oil (Fig. 3). The ideal dip stone extends beyond the depth of the oil (e.g., is clean on its lowest point), which allows the depth of the oil and its state (e.g., asphalt, mousse, etc.) to be determined.

We use the following terms to describe surface and subsurface oil: 1) mousse -- thick emulsified oil, usually brown in color; 2) asphalt -- heavily oiled sediments held together cohesively in a highly-weathered oil matrix; 3) tar -- thick oil layer ≥ 1mm thick, able to be scratched off; 4) coat -- oil that ranges from 0.1 to <1.0 mm thick and that can be easily scratched off a stone with a fingernail; and 5) stain -- oil that is < 0.1 mm thick that cannot be easily scratched off with a fingernail.

Detailed site maps are presented in Irvine et al. (1997) and in Appendix A of this report. Appendix B lists Global Positioning System (GPS) data for each site. Details of the Kenai Fjords NP&P site at MacArthur Pass (MR-1) are given in Irvine et al. (2006). Oiling and boulder movement data through 2005 are described in Irvine et al. (2007), and additional descriptions of oil chemistry in Short et al. (2007). Our sampling methods in 2012 followed the same methods begun in 1994 and re-employed in 1999, 2005, and 2011-2012 (estimation of surface and subsurface oil, and boulder movements), as well as new methods used in 2011 and 2012 (passive samplers and mussel tissue analyses).

3.2. Surface and Subsurface Oil

We assessed percent surface-oil cover within permanently marked quadrats measuring 40 x 50 cm. Quadrat locations were marked by two corner bolts placed in boulders. The cover estimates of three different observers were averaged to give a final estimate of oil percent cover in each quadrat. The number of quadrats at each site ranged from 12 to 26. We tested the single-tailed hypothesis that the percent cover of surface oil has decreased over time at each site using a Regional Kendall test (Helsel and Frans, 2006). This nonparametric method tests whether there is a monotonic temporal trend to the data. Because we have a lower limit on surface oil at zero percent, quadrats which have reached this lower limit and remained at zero percent for multiple years will not fit a monotonic model. To account for this issue, we removed from the analysis years in which a quadrat has remained at zero percent surface oil. We followed the method of Helsel and Hirsch (2002) to account for ties between years.

3.3. Boulder-Stability Measurements

We assessed boulder movements by re-surveying bolt locations in the boulders comprising the study sites' armors. These same bolts were used as corner markers for the surface-oiling quadrats. We measured changes through time in three parameters: 1) distance between each bolt and the survey station’s temporary bench mark (tbm) established in 1994, 2) the bearing (azimuth) relative to the original bearing measured between the survey station and each bolt in 1994, and 3) the elevation of each bolt relative to its 1994 elevation. This technique is relatively crude and is now outmoded by recent advances in GPS technology. Although some boulder movements will not be detectable by these measurements, they are sufficient to detect movements of individual, large boulders and reveal major disruptions of the site's boulder armor. Because boulders can shift their positions within the surrounding matrix of the armor, the movements we measured refer to changes in bolt positions and not necessarily to lateral or vertical displacements of entire boulders.

We estimated errors for boulder-movement measurements in two ways. First, we re-surveyed an index bolt multiple times during the same visit to a site. Second, we placed some bolts at each site in bedrock and included measurements of these bedrock-bolts in our re-surveys. The error estimates represent the largest error obtained in re-measurement. Distance measurements have the greatest potential error because of the relatively primitive method we used (tape measure). Azimuth (bearing) changes are the most insensitive measurement because bolts are not triangulated, but instead are surveyed from a single datum. At site MR-1 in

McArthur Pass, most of the bolts were affixed to bedrock outcrops and so are not of interest in regards to armor stability. The typical long-axis diameter of the boulders composing the armor at the Cape Douglas, Kiukpalik Island, Ninagiak Island sites is approximately one meter (Appendix A). The boulders in the armor at the Cape Gull site are smaller, approximately 50 cm in long-axis diameter. For the northern three Katmai sites, we define a "significant" movement -- one that could potentially compromise the integrity of the boulder armor-- as a >1m change in distance, and/or a change in elevation >25 cm, and/or a >10 degree change in bearing. At Cape Gull where the boulders comprising the armor are relatively small, we consider a "significant" movement as a distance change of >50 cm, and/or change in elevation >25 cm, and/or a >10 degree change in azimuth. For all sites except Cape Gull, "minor" movements considered to be those ranging between the error involved in making each measurement and the limit determining a "major" change (see above). Thus "minor" shifts in boulder positions are indicated by 12-100 cm changes in horizontal distance, and/or 5-25 cm in height, and/or 3-10 degrees in azimuth. At Cape Gull, where boulders are smaller than at the other sites, we consider "minor" movements to be 12-50 cm in horizontal distance, and/or 5-12 cm in height, and/or 3-5 degrees in azimuth.

At all four Katmai sites, a bolt/boulder that is missing on a subsequent survey date is noted and the percentage of missing bolts computed. Not finding a bolt/boulder could result from breakage and/or loss of the bolt or from the bolted boulder rolling in place and hiding the bolt; it could also result from displacement (loss) of the boulder itself. In those instances where burial by sand or gravel occurs and obscures bolt and boulder positions, the bolts/boulders are not considered missing and no data on the affected areas is taken until the boulders emerge again.

3.4. Exposure ratings of sites

We characterize wave exposure at the study sites using methods detailed in Howes et al. (1994). F_{max} is the maximum fetch distance in any direction that waves can approach a shore segment. F_{em} is the effective modified fetch calculated at three different angles relative to the strike of the shoreline segment. The categorical ratings are: very exposed sites = F_{max} >1000 km;

exposed = F_{max} 500 -1000 km; semi-exposed = F_{max} 50-500 km; semi-protected = F_{max} 10-50 km; protected = F_{max} <10 km; and very protected = F_{max} <1 km.

3.5. Vicissitudes of Shoreline Studies in the Gulf of Alaska

Monitoring beaches in Shelikof Strait is complicated by intermittent sedimentation events and by hazardous beach landings. In 1994, we were unable to mark boulders at the Kashvik Bay site because a 20-40 cm thick layer of cobbles had been deposited over the boulder armor there sometime between 1992 and 1994, obscuring both the location of the stranded oil and our marker bolts. In August 2005, we were unable to land at the Kashvik site due to high seas. At the Ninagiak Island site in 2005, recent deposition of a 10-20 cm thick layer of pebbles interfered with our describing the surface oil cover and boulder movements. At the Kiukpalik Island site in 2005, recent deposition of cobbles amongst the boulder armor prevented a thorough description of percent surface oil cover and curtailed our collection of oil samples for chemical analysis. In 2011, stormy weather prevented boat access to most of the sites.

3.6. Detection of Oil Constituents in the Water Column

To test whether oil constituents were still being released into the water in 2011 and 2012, we deployed passive samplers (low density polyethylene membrane devices, PEMDs) at two oiled sites (Cape Douglas and Kiukpalik Island) and at nearby control sites where no oil had ever been observed. These passive samplers are polyethylene strips encased in protective metal housings bolted to boulders (Fig. 4). In May 2011, we placed ten PEMDs in the oiled area of the Cape Douglas site and set one PEMD as a para-reference 29 m outside the oiled area. On the same trip, nine PEMDs were deployed in the oiled area of the Kiukpalik Island study site, and four reference PEMDs were deployed at an unoiled area >250 m away. Deployment time was 34 days at Cape Douglas and 29 days at the Kiukpalik Island site. On the recovery trip, the para-reference at Cape Douglas was found unbolted but wedged in a crevice under a nearby boulder. Additional PEMDs were deployed on 7/7/2012 at the same locations used previously at the Cape Douglas and Kiukpalik Island sites, unless a bolt was missing, in which case the 2012 PEMD was placed as close as possible to the original 2011 location. At the Cape Douglas site, four reference PEMDs were placed approximately 75 m from the oiled area. PEMDs were collected from Cape Douglas on 8/3/12 after 27 days and from Kiukpalik Island after 28 days.

As an alternative method of detecting biologically available hydrocarbons, we collected and chemically analyzed naturally occurring mussels (*Mytilus trossulus*) in 2011 and 2012 at the same sites where PEMDs were deployed. One or two samples consisting of 20-30 mussels were collected by hand at each site in each of these years, placed in chemically clean jars, then in a chilled cooler in the field and frozen on return to the vessel. Since mussels live at a lower tidal elevation than the oiled areas at these two sites, they were collected approximately 30m from the oiled areas.

3.7. Chemical Methods

Hydrocarbons were extracted from water and mussel tissue with dichloromethane, then dried, fractionated, purified and processed by gas chromatography-flame ionization detection (GC-FID) and gas chromatography-mass spectrometry (GC-MS). Mussels were dissected so that the tissue did not contact external shell surfaces, mechanically macerated for three minutes with a Tekmar "tissuemizer," spiked with 500 μL of deuterated surrogate recovery standard (Appendix C, Supplemental 1), and then extracted with dichloromethane in a Dionex accelerated solvent extractor (Larsen et al. 2008). The extract was dried with sodium sulfate and concentrated to 1 ml in hexane. The sample was fractionated into aliphatic and aromatic compounds on a chromatography column (10 g of 2% deactivated alumina over 20 g of 5% deactivated silica gel). The aliphatic compounds were eluted with 50 ml pentane, and aromatic compounds were eluted with 250 ml of a 1:1 mixture of pentane and dichloromethane. Aromatic fractions were further purified by a high pressure liquid chromatograph equipped with phenogel size-exclusion column (22.5 mm x 250 mm, 100 angstrom pore size). Both the aliphatic and the aromatic fractions were reduced to 1 ml in hexane, spiked with internal standards (dodecylcyclohexane and hexamethylbenzene, respectively) and stored at -20º C pending analysis.

The PEMDs were wiped clean to remove gross surface contamination, placed in centrifuge tubes, and then spiked with 500 µl of a solution equivalent to half the concentration of the deuterated surrogate recovery standard, PAHs only (Appendix C, Supplemental 1). The spike solvent (hexane) was allowed to evaporate, and then hydrocarbons were extracted from the PEMDs in a sonic bath containing 100 ml of a 80:20 mixture of pentane:dichloromethane for 120 minutes (three 20 min sonications with a 30 min rest between each). The PEMDs were immediately rinsed with pentane as they were removed from the final sonication. The extracts were dried with sodium sulfate and concentrated to 1 ml hexane. The extracts were purified on a chromatography column (1.5 g 5% deactivated silica gel). Samples were eluted with 22 ml of a 1:1 mixture of pentane and dichloromethane. Extracts then were spiked with the internal standard, hexamethylbenzene and stored at -20ºC pending analysis.

Aromatic fractions were analyzed for PAHs by GC-MS. The data were acquired in selected ion monitoring (SIM) mode and concentrations were determined by the internal standard method (Short et al. 1996; Carls et al. 2004). Experimentally determined method detection limits were generally 0.1 ng/g in tissue, 0.3 ng/g in sediment, and 0.4 to 7.9 ng/g in PEMDs. The accuracy of the PAH analyses was about ± 15% based on comparison with National Institute of Standards and Technology values (SRM1944), and precision expressed as coefficient of variation was usually less than about 20%, depending on the PAH. Surrogate recoveries averaged 52, 88, and 92% in tissue, sediment, and PEMDs respectively. Total PAH (TPAH) concentrations were calculated by summing concentrations of individual PAH (Table 1). Concentrations are reported as µg / g wet weight and µg/device in PEMDs. Relative PAH concentrations were calculated as the ratio of PAH_i / TPAH. Because unusually high P0 concentrations were encountered in several PEMDs - an apparent artifact - we analyzed TPAH in PEMDs after removing the P0.

Aliphatic fractions (tissue extracts only) were analyzed for n-alkanes using GC-FID. Analyte concentrations were determined by the internal standard method. Experimentally determined method detection limits were generally 3 ng/g in tissue and < 1 ng/g in sediment. The accuracy of the alkane analyses was ± 15% based on a spiked blank processed with each set of samples, and precision expressed as coefficient of variation was usually less than about 20%. Surrogate recoveries averaged 72 and 74% in tissue and sediment. Total alkane concentrations were calculated by summing concentrations of individual calibrated alkanes (Table 2). Concentrations are reported as µg / g wet weight in tissue and µg/device in PEMDs. Relative alkane concentrations were calculated as the ratio of alkane_i /total alkanes. The unresolved complex mixture (UCM) was determined from the difference between the total FID response area and resolved peak areas.

3.7.1. Measurement interpretation

Composition of PAH in PEMDs and mussel tissue was modeled to characterize source attributes (petrogenic or pyrogenic) using revised methods of (Carls 2006); values ranged from -1 (pyrogenic) to +1 (petrogenic). For PEMDs, source modeling was restricted to fluorenes (F0-F4), dibenzothiophenes (D0-D4), and phenanthrenes (P0-P4); lighter (naphthalenes) and heavier compounds evidently were not sufficiently accumulated, likely because of depletion of the lighter compounds or low aqueous solubility of the heavier compounds. Tissue modeling also included naphthalenes (N0-N4), fluoranthene/pyrenes (FL, PYR, FP0-FP4), and chrysenes (C0-C4).

Alkane composition was modeled to identify the presence or absence of oil in mussel tissue. The first step was to determine if oil was present. Normal alkanes *n*-C12 through *n*-C36 were examined, and if the concentration of each individual *n*-alkane was > 0 then it received a score of 1, else 0. These scores were summed and divided by the number of observations. If this value was > 0.6, then a petrogenic signal may be present and F = 1 (if ≤ 0.6, F = 0; else 0). The second step was to determine if concentration patterns were consistent with the source oil. Even pairs and odd pairs were compared in the range *n*-C26 to *n*-C36. Even-even and odd-odd comparisons were chosen to mitigate possible interference from alkanes produced by plants (Wang and Fingas 2003). If the concentration was smaller in the larger compound it was assigned a score of 1; if it was larger, −1, else 0. These scores were summed and divided by the number of pairs; if this value > 0.6 then concentration declined with molecular weight and H = 1 (else 0). Alkane concentration[1] potentially associated with whole oil was estimated as $C = \sum (Alk_i - Alk_{max\ control})$ and the fraction of alkanes associated with oil, D, was $F \cdot H \cdot (C / cAlk)$, where Alk is the ith alkane concentration and cAlk is total calibrated alkane concentration. Values for D ranged from 0 to 1.

Alkane composition was also examined for the presence of prominent odd-numbered compounds indicative of a contemporary plant source. The fraction of odd alkanes was $Z = \sum (C21 + C23 + \dots C35) / \sum (C21 + C22 + \dots C36)$. Odd scores were assigned as -1 if $Z \geq 0.9$, -0.75 if $Z \geq 0.85$, and -0.5 if $Z \geq 0.8$.

Composition of all PAHs in PEMDs was also analyzed by Principal Components Analysis (PCA), thus providing independent insight into the presence (or absence) of oil and weathering. Concentration data were normalized before analysis (PAH_i / TPAH) to understand composition similarities and differences. PCA was completed with Minitab using correlation matrices.

4. Results

4.1. Surface Oil

Surface-oil percent cover showed a progressive, statistically significant decline at all sites between 1994 and 2012 ($p < 0.001$; Regional Kendall test) (Fig. 5). In 2012 the most striking, overall changes were apparent at the Kashvik and Cape Gull sites. At the Kashvik site, no oil - neither surface nor subsurface - was observed in 2012. For logistical reasons, we were not able to establish permanent quadrats at the Kashvik site, but a thorough search of the site and the digging of small pits along the approximate line of the original transect established in 1992 revealed no oil detectable by either sight or smell. At the Cape Gull site in 2012, no surface oil was observed in the permanent quadrats, and only a few isolated and extremely small patches of oil were observed elsewhere at this site. At all sites with permanent quadrats, including the McArthur Pass site (Appendix D), surface oil cover in 2012 ranged from 0% to ~3%, which represents a striking decrease compared to the 16-26% cover observed in 1994.

---

[1] Sediment and tissue only; alkanes were not measured in PEMDs

Accompanying the decline in surface oil, the diversity of surface oiling types has progressively declined since monitoring began in 1994. In 1994 we observed stain, coat, tar, soft asphalt, interstitial tar and mousse, as well as rainbow and gray sheens (Appendix D). By 2012, surface oiling within the permanent quadrats was almost entirely asphalt with embedded sediment and occasional patches of tar.

4.2. Subsurface Oil

In 2012, a thorough search found no subsurface oil remaining at the Kashvik site, although it was still present at the other five sites. At the Cape Gull site in 2012, we found only one small patch of subsurface oil covering < 60 cm^2. No dip stones were sampled at Cape Gull in 2012 because no suitable ones could be located. The depths of subsurface oiling at the remaining four sites do not appear to have changed appreciably between 1994 and 2012 (Table 3, Appendix E). The mean depths of oiling for those four sites, as measured by dip stones, ranged from 3.0 to 5.2 cm, while the maximum oil depth was > 9 cm at both Cape Douglas and Kiukpalik Island (Table 3). The depth of subsurface oil tends to be least at the McArthur Pass site because much of the site has bedrock exposed at the shoreline surface and there is very little unconsolidated sediment there (Appendix A).

4.3. Stability of the Boulder Armors

At McArthur Pass where much of the site is exposed bedrock, boulder movements were not studied. At the Kashvik Bay site, the boulder armor, along with the surface and subsurface oil, were largely covered by recently transported cobbles when we first visited the site in 1994, so we were unable to mark boulders adjacent to oiling there. Observations of boulder movements are as follows.

4.3.1. Cape Douglas

Of the 25 bolts placed in boulders in 1994, four had disappeared by 2012 (Fig. 6). Over the three intervals between surveys, 4-8% of the marked boulders shifted their positions by more than 1 m in distance, or by >25 cm in elevation, or by >10 degrees in the azimuth relative to the datum (Table 4). Bolt L disappeared between the 1994 and 1999 surveys. Bolt/boulder M moved almost 2 m horizontally between 1994 and 1999, before disappearing after the 2005 survey. Bolt/boulder N disappeared after the 1999 survey. We suspect that some or all of the missing four bolts are hidden under boulders that rolled in place rather than being moved elsewhere on the shoreline. We found no evidence for major armor-disrupting wave events over the 18 years we followed the boulders at this site. In contrast, minor movements (<1 m change in distance, <25 cm change in height, and <10 degree azimuth changes) were frequent and affected 5-26% of the marked boulders during each interval between surveys (Fig. 6). Some boulders were more stable than others, probably reflecting how tightly they were packed.

4.3.2. Kiukpalik Island

Three bolts out of the initial 18 were lost at this site over the 18-year survey interval (Table 4, Fig. 7). Bolt A disappeared sometime after the 1994 survey, bolt J disappeared after 2005, and bolt P disappeared after 1999. As at Cape Douglas, we suspect that some or all of these missing bolts were hidden when boulders rolled in place. Over the three intervals between surveys, only 5-6% of the marked boulders underwent "significant" position changes. Bolt/boulder C moved the furthest with a 122-cm change in distance from the datum between 1999 and 2005 (Fig. 7). There is no evidence for major, armor-disrupting events at this site (Table 4). On the other hand, minor movements occurred frequently, with up to 63% of the bolts undergoing minor position changes between surveys. As at Cape Douglas, some boulders experience a greater frequency of "minor" movements than others.

4.3.3. Ninagiak Island

Sometime between 1999 and 2005, much of this site was covered by pebbles and small cobbles, obscuring the survey area so we were unable to re-locate a number of our bolts in 2005. Most but not all of these pebbles had been removed by 2012, allowing assessment of boulder stability between 1999 and 2012. Of the 23 boulders we marked in 1994, 4-5% had experienced "significant" position changes by 2012 (Table 4, Fig. 8). There were no significant changes in distances over this interval, but bolt F changed its height by 90 cm between both 1994 and 1999 and again between 1999 and 2012. Three bolts were not found in 2012: N, O, and X, resulting in a 13% loss rate for bolts at this site over the 18-year survey period. Up to 30% of the marked boulders showed evidence for minor movements between surveys (Table 4). As seen at the other sites, individual boulders varied in their relative stabilities as revealed by their tendency to show minor position shifts (Fig. 8). As at the preceding two sites, there is no evidence for catastrophic, armor-disrupting wave events at the Ninagiak site over the 18 years we tracked boulder positions there.

4.3.4. Cape Gull

We placed 12 bolts at the Cape Gull site in 1994. In 2012, all were still accounted for. Only one marked boulder, K, experienced significant position shifts during each survey interval (Table 4). Between 10 and 40% of marked boulders routinely experienced "minor" position shifts at Cape Gull (Table 4). Overall, this site has one of the most stable armors, despite the generally smaller diameters of its boulders.

4.4. Exposure Ratings of Sites

The study sites range from “exposed” to “protected”. Both the Cape Douglas (F_{em} = 453 km, F_{max} = 880 km) and Kiukpalik Island sites (F_{em} = 500 km, F_{max} = 600 km) are classified as “exposed”; the Ninagiak (F_{em} = 120 km, F_{max} = 75 km) and Kashvik sites (F_{em} = 50 km, F_{max} = 200 km) are “semi-exposed”; and the McArthur Pass (F_{em} = 2 km, F_{max} = 3 km) and Cape Gull sites (F_{em} = 2.6 km, F_{max} = 2.5 km) are “protected”.

4.5. Hydrocarbons in Passive Samplers and Mussels

4.5.1 Passive samplers (PEMDs)

Composition of PAHs present in about half of the passive samplers deployed in oiled areas at Kiukpalik Island and Cape Douglas was consistent with crude oil (Table 5). Petrogenic PAHs accumulated in all nine PEMDs placed in the oiled area at the Kiukpalik Island site in 2012 and possibly in one PEMD deployed there in 2011. The PCA also indicated this subset of PEMDs was oiled (Table 5). Oil was not detected in blank PEMDs or in any controls on Kiukpalik Island. At Cape Douglas, source modeling indicated oil was present in 14 of the 20 PEMDs placed in oiled areas. PCA also indicated twelve of these were oiled and suggested oil was present in two additional samples (Table 5). Of the twelve samples identified as being oiled based on both methods, five were from 2011 and seven were from 2012, with five of the oiled PEMDs coming from the same locations each year. Source modeling suggested oil in one Cape Douglas control in 2012, though this was not supported by PCA results and was disregarded.

Total PAH concentration in passive samplers was consistent with exposure history. Concentrations were lowest in the laboratory blanks and site controls and significantly elevated in PEMDs placed within the oiled areas ($P_{\text{Kruskal-Wallis}} < 0.001$; Dunn's *a posteriori* method; Fig. 10). There were hints of contamination by a non-oil source in some field blanks, but TPAH concentration was not significantly elevated. All passive sampler data formed a continuous point cloud in PCA space except for a single blank (Fig. 11). We assume this trip blank was contaminated by an unknown source because it contained an unusual set of higher molecular weight PAHs; therefore, we did not analyze it further. Total PAH concentration in this anomalous trip blank was greater than in all other blanks. Some samples from Cape Douglas and Kiukpalik Island overlapped the blanks and others extended away from this grouping, consistent with conditions ranging from uncontaminated to contaminated (Fig. 11).

4.5.2 Hydrocarbons in Mussels

Oil was not detected in mussels at Cape Douglas and Kiukpalik Island in 2011 and 2012. Petrogenic PAHs consistent with dissolution were not detected in mussels in either year (Table 6, Fig. 12). Alkane composition at Cape Douglas and Kiukpalik Island weakly supported contamination in 2011; alkanes in the *n*-C22-*n*-C32 range were reminiscent of, but not identical to, corresponding composition in the more weathered sediment samples (Fig. 13). Hints of insoluble alkanes in mussel tissue plus failure to find dissolved PAHs suggested possible accumulation of oil droplets by feeding but a follow-up analysis of hopanes and steranes failed to confirm the presence of whole oil. In addition, the UCM was absent in mussel tissue. Alkane patterns in both 2012 samples were reminiscent of background patterns in sediment that did not contain oil. Thus, the weight of evidence does not support mussel contamination in 2011 and 2012.

5. Discussion

5.1. *Exxon Valdez* Oil Still Persists on Some Gulf of Alaska Beaches

For the first time since 1989, no observable oil could be located in 2012 at the Kashvik site (though see Irvine et al. 2014 [Chapter 2]). This site is the most distant (~640 km) from the spill's origin (Fig. 1). At the second-most distant site, Cape Gull, surface and subsurface oil had declined to very low levels by 2012. At the other four sites (Ninagiak Island, Kiukpalik Island, and Cape Douglas in Katmai National Park; and McArthur Pass in Kenai Fjords National Park), surface oil declined to low levels (≤ 3%) by 2012; however, patches of subsurface oil still persisted at these four sites to depths similar to what they were in 1994. This subsurface oil persists despite the passage of 23 years in a relatively high-energy, wave environment and despite manual cleanup efforts in the years immediately after the 1989 spill.

5.2. Stability of Boulder Armors

The potential oil-cleansing effects of Shelikof Strait's stormy seas appear to have been effectively countered by the sheltering effects of boulder armors at three of the monitored sites. Observations of boulder movements at the Cape Douglas, Kiukpalik Island, and Ninagiak Island sites over the last 18 years indicate their boulder armors have been quite stable. Among the 76 boulders we initially marked, only ten (14%) of the marker bolts were lost, and we suspect that most of these were lost because the boulders they mark simply rolled in place and covered them. Between each survey at the four boulder-armored beaches we monitored, fewer than two boulders at each site experienced "significant" positional shifts (Table 4). At most we estimate that <10% of the boulder armor at any of these four sites was disrupted by waves during the 18 years of this study. There is no indication that the boulder armors at Cape Douglas, Kiukpalik Island, Ninagiak Island, and Cape Gull have been disrupted and re-organized since 1989 when the *Exxon Valdez* oil was stranded.

In contrast to the overall stability of the armor they comprise, individual boulders undergo frequent minor shifts in their positions within their surrounding armor framework. Up to half of the marked boulders exhibited "minor" shifts in position between survey periods. Even though large boulders are frequently rocked and rotated by waves, the overall armor remains intact. Small shifts in the positions of individual boulders may actually enhance long-term armor stability by fitting boulders together and locking them more securely. These minor shifts probably do little to disturb the underlying, finer sediment and the stranded oil. Our results show clearly that well-developed boulder armors on coarse-grained, gravel beaches are capable of physically protecting and chemically preserving oil mousse for several decades and probably longer in stormy, high latitude settings. By providing actual field data on armor stability and the persistence of oil beneath them, these results strengthen the modelling inferences of Nixon et al. (2013) that describe spatial correlation between boulder armors and persistent *Exxon Valdez* oil.

5.3. Oil in Water and Mussels

Polycyclic aromatic hydrocarbons from *Exxon Valdez* oil sequestered in Gulf of Alaska sediment in 2011 and 2012 (Irvine et al., 2014 [Chapter 2]) were biologically available in some sites at low dissolved concentrations 22 to 23 years after the spill. Hydrocarbons that accumulated in passive samplers at the Cape Douglas and Kiukpalik Island sites in 2011 and 2012 were consistent with a petrogenic source and by inference this source was *Exxon Valdez* oil sequestered at these sites. In contrast, oil was not present in controls or blank PEMDs. Dissolved oil was not observed in mussels living near these two sites, likely because they were lower in the intertidal zone than stranded oil deposits and about 30 m distant.

The PEMD data from Cape Douglas and Kiukpalik Island suggest that aqueous dissolved PAH concentrations are very low but are chronically present. Total PAH concentrations were <1000 ng/g in 96% of the PEMDs. The PEMDs are capable of concentrating PAHs from water by a factor of roughly 10^3 to 10^5 (Carls et al. 2004). Thus, the maximum aqueous TPAH concentration in the water column at the time of membrane exposure was probably less than or equal to 1 part-per-billion and may have been only a few parts per trillion. At such low concentrations, high spatial variation in oil attaching to the PEMDs is to be expected, especially when the effects of tide- and wind-driven currents are taken into account. Low-level, intermittent releases of oil into the water column under varying sea conditions probably explain why dissolved oil was found at the Kiukpalik Island site in 2012 but not in 2011. It is interesting to note that in 2011 a storm occurred just after we deployed PEMDs at the Cape Douglas site, which prevented us from deploying them at the Kiukpalik Island site for almost a week. It is possible that the minor shifts in boulder positions caused by that single storm accounted for the inter-site differences (higher at Cape Douglas) we observed in hydrocarbon levels of the PEMDs in 2011.

5.4. Boulder Armors, Oil Release, and Oil Weathering

The persistence of stranded oil on shorelines is strongly influenced by the long-continued interactions of ocean waves with geologic substrates that occur across spatial scales ranging from millimeters to kilometers. Gravel beaches are particularly problematic settings for oil stranding (Hayes et al, 2010) because their high porosities can sometimes store large amounts of subsurface oil (Gundlach and Hayes, 1978; Owens et al., 2008). As shown in our earlier work (Irvine et al. 1999, 2006, 2007) and that of others (Hayes et al. 2010, Nixon et al. 2013), another important aspect of coarse-grained gravel beaches relating to spilled oil is the sheltering effect of boulder armors. None of our study sites possess deep, subsurface deposits of porous gravel containing fluid oil, but many of them continue to shelter oil mousse located immediately below surface armors. At these sites, boulder armors have protected relatively small volumes of oil mousse, despite 23 years of wave action on the Gulf of Alaska coast. Armor stability is much greater than we thought at the beginning of this study, and while the frequency of armor-disrupting storm events is unknown, our data indicate it is greater than two decades in Shelikof Strait.

We suspect that the boulder armors we have tracked in Shelikof Strait are more stable than most armors in PWS because they were not disturbed as much by coseismic changes in relative sea level during the 1964 earthquake and because the average clast size of the armors in Shelikof Strait tends to be larger than on most beaches in PWS. In other words, our three sites in Shelikof Strait where appreciable subsurface oil persists (Cape Douglas, Kiukpalik Island, and Ninagiak Island) may represent the ideal setting for the effective geomorphic shielding of subsurface oil within the region affected by the EVOS.

Clearly, boulder armors can protect and preserve stranded oil for several decades, but what is just as surprising is the relatively unweathered condition of the oil (see Irvine et al., 2014 [Chapter 2]). The fact that low but detectable levels of hydrocarbons continue to leak out of these sites is surprising given the length of time since the oil spill, the distance from the spill site, and the high wave energies these sites have experienced over the last 23 years. What is more, our observations of oil release into the water column occurred in summer, the season when wave energies are typically lowest. Oil release from these sites may well be significantly greater in other seasons when storms are stronger and more frequent.

How dangerous in terms of environmental pollution are patches of remnant, subsurface oil sheltering under boulder armors on Gulf of Alaska shorelines? The intermittent release of trace concentrations of hydrocarbons is unlikely to pose significant risk to the nearby biota, unless sudden and catastrophic disruption of the boulder armors occur, which our observations suggest is unlikely. Risks would be higher for sensitive forms such sessile eggs or larvae, for sessile organisms restricted to the vicinity of the remnant oil, or for organisms that accumulate hydrocarbons - and then by extension to their predators. At the four sites where appreciable oil remains, this oil is situated high in the intertidal zone, which means fewer biota are exposed than if it were lower in the intertidal zone. Invertebrate taxa, notably littorine snails, are present at all of our study sites, and we have observed black oystercatchers using some of the sites. Thus there could be routes of exposure from invertebrates to their vertebrate predators.

Given the much reduced volume of oil that contaminated Gulf of Alaska shorelines in 1989 compared to Prince William Sound (Wolfe et al., 1994) and subsequent loss of most of the oil from the GOA coastline since the spill (Michel et al. 2011), our sites represent small, localized pockets of long-term contamination and low-level hydrocarbon release. Widespread oil pollution from these sites is unlikely. The primary significance of these sites and of this study relates to future oil spills, namely as examples of how the geomorphic processes characteristic of rocky, macrotidal coastlines interact with oil spilled in high-latitude seas. Their most general significance is as a cautionary note concerning our ignorance about the complex legacy of contaminants in coastal environments.

6. Conclusions

In 1994, we began monitoring six beaches in the Gulf of Alaska that were contaminated by oil mousse from the *Exxon Valdez* oil spill in 1989. The five study sites located in Shelikof Strait all possess boulder-armors overlying finer-grained sediment. Four of these sites experience moderate to high wave energies and are distant (up to 640 km) from the spill origin in PWS. We have periodically revisited these beaches over the last 23 years to re-assess surface and subsurface oiling, to evaluate the stability of the boulder armors, and to sample the oiled sediments for hydrocarbon analysis. In 2012, we failed to find any observable oil at Kashvik, our most distant site, and we found much-reduced surface and subsurface oil at the second most remote site, Cape Gull. Our results show a clear decline in surface oil at all sites but reveal the continued persistence of subsurface oil at the Cape Douglas, Kiukpalik Island, and Ninagiak Island sites, as well as at the McArthur Pass site in Kenai Fjords National Park.

The persistence of oil for 23 years on the high wave-energy beaches in Shelikof Strait has two causes: initial oiling by weathering-resistant mousse and its subsequent sheltering under stable boulder armors. There has been remarkably little chemical weathering of the subsurface oil at the Cape Douglas, Kiuikpalik Island, Ninagiak Island, and McArthur Pass sites (Irvine et al., 2014 [Chapter 2]). Measurements of oil release into the water column in 2011 and 2012 using passive samplers show low but definite rates of hydrocarbon contamination emanating from the Cape Douglas and Kiukpalik Island sites. We measured oil release to the water column in summer when wave energy is least. The observed rates of oil release in summer are so small that they probably pose little threat to nearby biota, but it is possible that winter storms trigger higher rates of release. If an unusually powerful storm completely disrupts the boulder armor, it will trigger a much larger, short-lived release of hydrocarbons.

Tracking the movements of boulders indicates that most of the shifts in the armors on these beaches have been minor, suggesting no storm events have occurred since 1989 that have been capable of disrupting the integrity of the armors at any of our four boulder-bolted sites on the Katmai coast. The underlying oil deposits cannot be physically dispersed by wave action unless the overlying armors are disrupted. Instead of significant boulder movements, the main geomorphic changes on these beaches have been the transient infilling of boulder armors with finer grained particles. This transient infilling had no effect on the subsurface oil, though it may have reduced surface oiling through abrasion. Although the oil still sequestered high in the intertidal zones of these beaches probably poses minimal threat to biota, our results highlight the potential threats posed by heavily oiled beaches that possess stable boulder armors following future spills. These results indicate the importance of considering shoreline armoring effects in oil spill response efforts and in subsequent monitoring efforts.

7. Acknowledgments

We appreciate and acknowledge the initial work by Carl Schoch and Joel Cusick (National Park Service), the previous involvement in our studies of Jeffrey W. Short, and the support of T. Scott Smeltz, Carson Baughman, Carissa Turner, Erica Madison, Yvette Gillies, Sharon Kim, Jeff Mondragon, Jennifer Mondragon, Johnny Zutz, Marie Larsen, Jeep Rice, Billy Choate, Collette Choate, Bill Albrecht, John Rogers, Mike Yourkowski, Michael Parks, and Lydia Rabottini. Helicopter support was provided by Pathfinder Aviation and Maritime Helicopters. Funding was provided primarily by the *Exxon Valdez* Oil Spill Trustee Council, with additional support from the U.S. Geological Survey (Alaska Science Center), the National Oceanic and Atmospheric Agency (NOAA), and the National Park Service. The findings and conclusions are those of the authors and do not necessarily reflect the views or position of the *Exxon Valdez* Oil Spill Trustee Council. Any mention of trade names is for descriptive purposes only and does not represent endorsement by the U.S. government.

8. Literature Cited

Arctic Environmental Information and Data Center, National Climatic Center (AEIDC, NCC), 1977. Climatic Atlas of the Continental Shelf Waters and Coastal Regions of Alaska. Vol. 1, Gulf of Alaska. NOAA RU No. 347, 439 pp.

Alaska Department of Environmental Conservation (ADEC), 1991. Evaluation of impacted shorelines in the Kodiak/Alaska Peninsula regions. Final Report 1989-1991. Alaska Department of Environmental Conservation, Oil Spill Response Center, Anchorage, Alaska.

Bishop, P., Hughes, M., 1989. Imbricate and fitted fabrics in coastal boulder deposits on the Australian east coast. Geology, 17, 544-547.

Brower, W.A. Jr., Diaz, H.F., Pretchtel, A.S., 1977. Marine and coastal climatic atlas. In: Climatic Atlas of the Outer Continental Shelf Waters and Coastal Regions of Alaska, Vol. 1, Gulf of Alaska. Arctic Environmental Information and Data Center (AEIDC), University of Alaska, Anchorage, National Climatic Center, Environmental Data Service, Asheville, North Carolina, National Oceanic and Atmospheric Administration. Anchorage: AEIDC, University of Alaska, 23-439pp.

Carls, M. G., 2006. "Nonparametric identification of petrogenic and pyrogenic hydrocarbons in aquatic ecosystems." Environmental Science & Technology, 40(13), 4233-4239.

Carls, M. G., L. G. Holland, et al., 2004. "Monitoring polynuclear aromatic hydrocarbons in aqueous environments with passive low-density polyethylene membrane devices." Environmental Toxicology and Chemistry, 23(6), 1416-1424.

Dean, R.G., Dalyrymple, R.A., 2004. *Coastal Processes with Engineering Applications*. Cambridge University Press, Cambridge.

Gundlach, E.R., Hayes, M.O., 1978. Vulnerability of coastal environments to oil spill impacts. Marine Technology Society Journal, 12 (4), 18-27.

Hayes, M.O., Brown, P.J., Michel, J., 1977. Coastal morphology and sedimentation, lower Cook Inlet, Alaska, with emphasis on potential oil spill impacts. Technical Report 12-CRD (pp 107). University of South Carolina, Department of Geology, Coastal Research Division.

Hayes, M.O., Michel, J., 1999. Factors determining the long-term persistence of *Exxon Valdez* oil in gravel beaches. Marine Pollution Bulletin, 38 (2), 92-101.

Hayes, M.O., Michel, J., Betenbaugh, D.V., 2010. The intermittently exposed, coarse-grained gravel beaches of Prince William Sound, Alaska: comparison with open-ocean gravel beaches. J. of Coastal Research, 26 (1), 4-30.

Hayes, M.O., Gundlach, E.R., D'Ozouville, L., 1979. Role of dynamic coastal processes in the impact and dispersal of the *Amoco Cadiz* oil spill (March 1978) Brittany, France. In: Proceedings of the 1979 International Oil Spill Conference, Los Angeles, CA, 193-198.

Helsel, Dennis R., Frans, L. M., 2006). Regional Kendall test for trend. *Environmental Science and Technology*, 40 (13), 4066-4073.

Helsel, D. R., Hirsch, R. M., 2002. *Statistical methods in water resources* (Vol. 323). Reston, VA: US Geological Survey.

Hills, E.S., 1970. Fitting, fretting and imprisoned boulders. Nature, 226, 345-347.

Howes, D.E., Harper, J.R., Owens, E., 1994. Physical Shore-Zone Mapping System for British Columbia. Queen's Printer Government Publications Centre, Vancouver, British Columbia.

Irvine, G.V., Aeppli, C., Carls, M., Nelson, R.K., Holland, L., Reddy, C.M., Mann, D.H., 2014. *Exxon Valdez* oil persists on Gulf of Alaska beaches after 23 years: Using new methods to look at old stranded oil. Chapter 2, in *Exxon Valdez* Oil Spill Restoration Project Final Report (Restoration Project 11100112), U. S. Geological Survey, Anchorage, Alaska.

Irvine, G.V., Mann, D.H., Short, J.W., 1997. Geomorphic position, weathering, and possible biotic impacts of oil mousse persisting on a high energy coastline distant from the *Exxon Valdez* spill. *Exxon Valdez* Oil Spill Restoration Project Final Report (Restoration Project 94266), U. S. Geological Survey, Anchorage, Alaska.

Irvine, G.V., Mann, D.H., Short, J.W., 1999. Multi-year persistence of oil mousse on high energy beaches distant from the *Exxon Valdez* spill origin. Marine Pollution Bulletin, 38 (7), 572-584.

Irvine, G.V., Mann, D.H., Short, J.W., 2006. Persistence of 10-year old *Exxon Valdez* oil on Gulf of Alaska beaches: the importance of boulder-armoring. Marine Pollution Bulletin, 52, 1011-1022.

Irvine, G.V., Mann, D.H., Short, J.W., 2007. Monitoring lingering oil from the *Exxon Valdez* spill on Gulf of Alaska armored beaches and mussel beds sixteen years post-spill. *Exxon*

Valdez Oil Spill Restoration Project Final Report (Restoration Project 040708), U. S. Geological Survey, Anchorage, Alaska.

Isla, F. I., 1993. Overpassing and armoring phenomena on gravel beaches. *Marine Geology, 110* (3), 369-376.

Larsen, M. L., L. Holland, et al., 2008. Standard operating procedures for the analysis of petroleum hydrocarbons in seawater, marine sediments, and marine faunal tissue at the Auke Bay Laboratory. Juneau, AK, NOAA, NMFS, Alaska Science Center, Auke Bay Laboratories, 81 pp.

Livingstone, D. R., 1991. Organic xenobiotic metabolism in marine invertebrates. *Advances in comparative and environmental physiology*. R. Gilles. New York, NY, Springer-Verlag. 7, 45-185.

Michel, J., Hayes, M. O., 1999. Weathering patterns of oil residues eight years after the *Exxon Valdez* oil spill. Marine Pollution Bulletin, 38 (10), 855-863.

Michel, J., Hayes, M.O., Brown, P.J., 1978. Application of an oil vulnerability index to the shoreline of lower Cook Inlet, Alaska. Environmental Geology, 2, 107-117.

Michel, J., Nixon, Z., Hayes, M.O., Irvine, G.V., Short, J.W., 2011. The distribution of lingering subsurface oil from the *Exxon Valdez* oil spill. Proceedings of the 2011 International Oil Spill Conference, 2011-27, 14 pp.

Mueller, E.R. and Pitlick, J., 2013. Sediment supply and channel morphology in mountain river systems: 1. Relative importance of lithology, topography, and climate. Journal of Geophysical Research: Earth Surface, 118, 1-18.

Nixon, Z.; Michel, J.; Hayes, M.O.; Irvine, G.V., and Short, J., 2013. Geomorphic factors related to the persistence of subsurface oil from the *Exxon Valdez* oil spill. In: Kana, T.; Michel, J., and Voulgaris, G. (eds.), Proceedings, Symposium in Applied Coastal Geomorphology to Honor Miles O. Hayes, Journal of Coastal Research, Special Issue No. 69, 115–127. Coconut Creek (Florida), ISSN 0749-0208.

National Oceanographic and Atmospheric Administration, 2013. National Buoy Data Center http://www.ndbc.noaa.gov/station_history.php?station=46077. Accessed April 2014.

Oak, H.L., 1984. The boulder beach: A fundamentally distinct sedimentary assemblage. Annals of the Association of American Geographers, 74, 71-82.

Oak, H.L., 1986. Process inference from coastal-protection structures to boulder beaches. Geografiska Annaler 68A, 25-31.

Orford, J.D., Forbes, D.L., and Jennings, S.C., 2002. Organizational contriols, typologies, and timescales of paraglacial gravel-dominated coastal systems. Geomorphology 48, 51-85.

Paris, R., Naylor, L.A., and Stephenson, W.J., 2011. Boulders as signatures of storms on rocky coasts. Marine Geology 283, 1-11.

Reed, R.K., Schumacher, J.D., 1986. Physical Oceanography. In: Hood, D.W., Zimmerman, S.T. (Eds.), The Gulf of Alaska: Physical Environment and Biological Resources, National Oceanic and Atmospheric Administration, Washington, DC, 57-75pp.

Royer, T.C., Vermersch, J.A., Weingartner, T.J., Niebauer, H.J., Muench, R.D., 1990. Ocean circulation influencing the *Exxon Valdez* oil spill. Oceanography 3 (2), 3-10.

Schoch, C., 1993. 1992 Stranded oil persistence study on Kenai Fjords National Park and Katmai National Park and Preserve. Interim Status Report, Coastal Programs Division, National Park Service, Anchorage, Alaska.

Shelley, D., 1968. Fitting boulders: The result of an important shore process. Nature, 220, 1020-1021.

Short, J.W., Heintz, R.A., 1997. Identification of *Exxon Valdez* oil in sediments and tissues from Prince William Sound and the Northwestern Gulf of Alaska based on a PAH weathering model. Environmental Science & Technology, .31(8), 2375-2384.

Short, J.W., Irvine, G.V., Mann, D.H., Maselko, J.M., Pella, J.J., Lindeberg, M.R., Payne, J.R., Driskell, W.B., Rice, S.D., 2007. Slightly weathered *Exxon Valdez* oil persists in Gulf of Alaska beach sediments after 16 years. Environmental Science and Technology, 41, 1245-1250.

Short, J.W., Jackson, T.J., Larsen, M.L., Wade T.L., 1996. Analytical methods used for the analysis of hydrocarbons in crude oil, tissues, sediments, and seawater collected for the Natural Resources Damage Assessment of the *Exxon Valdez* oil spill. In: Rice, S.D., Spies, R.B., Wolfe, D.A., Wright, B.A. (Eds.), Proceedings of the *Exxon Valdez* Oil Spill Symposium. American Fisheries Society Symposium 18, pp. 140-148.

Venkatesan, M.I., 1988. Occurrence and possible sources of perylene in marine sediments – a review. Marine Chemistry 25, 1-27.

Wang, Z. D. and Fingas, M. F., 2003. Development of oil hydrocarbon fingerprinting and identification techniques. Marine Pollution Bulletin, 47 (9-12), 423-452.

Wang, Z., Fingas, M., Owens, E.H., Sigouin, L. and Brown, C.E., 2001. Long-term fate and persistence of the spilled *Metula* oil in a marine salt marsh environment: Degradation of petroleum biomarkers. Journal of Chromatography A, 926 (2), 275-290.

Wang, Z., Hollebone, B.P., Fingas, M., Fieldhouse, B., Sigouin, L., 2003. Characteristics of spilled oils, fuels, and petroleum products 1. Composition and properties of selected oils. Report Number EPA/600/R-03/072, Environmental Protection Agency, Research Triangle Park, North Carolina.

Wilcock, P.R. and DeTemple, B.T., 2005. Persistence of armor layers in gravel-bed streams. Geophysical Research Letters, 32, L08402, doi: 10.1029/2004GLO21772.

Wilson, J.G., Overland, J.E., 1986. Meteorology. In: Hood, D.W., Zimmerman, S.T. (Eds.), The Gulf of Alaska: Physical Environment and Biological Resources. National Oceanic and Atmospheric Administration, Washington, DC, 31-54pp.

Wolfe, D. A., M. J. Hameedi, et al. 1994. The fate of the oil spilled from the *Exxon Valdez.* Environmental Science & Technology, 28 (13), 560A-568A.

Table 1. Measured polycyclic aromatic hydrocarbons (PAH) and abbreviations (Abbr). Asterisk indicates PAHs used in the EVO weathering model (Short and Heintz, 1997; Chapter 2).

Abbr	PAH	Abbr	PAH
N0	Naphthalene	ANT	Anthracene
N1	C-1 Naphthalenes	FLU	Fluoranthene
N2	C-2 Naphthalenes	PYR	Pyrene
N3	*C-3 Naphthalenes	FP1	C-1 Fluoranthenes/Pyrenes
N4	*C-4 Naphthalenes	FP2	C-2 Fluoranthenes/Pyrenes
BPH	Biphenyl	FP3	C-3 Fluoranthenes/Pyrenes
ACN	Acenaphthylene	FP4	C-4 Fluoranthenes/Pyrenes
ACE	Acenaphthene	BAA	Benzo(A)Anthracene
F0	Fluorene	C0	*Chrysene
F1	C-1 Fluorenes	C1	*C-1 Chrysenes
F2	*C-2 Fluorenes	C2	*C-2 Chrysenes
F3	*C-3 Fluorenes	C3	C-3 Chrysenes
F4	C4 Fluorenes	C4	C-4 Chrysenes
D0	Dibenzothiophene	BBF	Benzo(b)Fluoranthene
D1	*C-1 Dibenzothiophenes	BKF	Benzo(k)Fluoranthene
D2	*C-2 Dibenzothiophenes	BEP	Benzo(e)Pyrene
D3	*C-3 Dibenzothiophenes	BAP	Benzo(a)Pyrene
D4	C-4 Dibenzothiophenes	PER	Perylene
P0	*Phenanthrene	ICP	Indeno(1,2,3-cd)Pyrene
P1	*C-1 Phenanthrenes/Anthracenes	DBA	Dibenzo(a,h)Anthracene
P2	*C-2 Phenanthrenes/Anthracenes	BZP	Benzo(ghi)Perylene
P3	*C-3 Phenanthrenes/Anthracenes		
P4	*C-4 Phenanthrenes/Anthracenes		

Table 2. Measured alkanes and abbreviations (Abbr).

Abbr	Alkane	Abbr	Alkane
C9	C9- (*n*-Nonane)	C22	C22- (*n*-Docosasne)
C10	C10- (*n*-Decane)	C23	C23- (*n*-Tricosane)
C11	C11- (*n*-Undecane)	C24	C24- (*n*-Tetracosane)
C12	C12- (*n*-Dodecane)	C25	C25- (*n*-Pentacosane)
C13	C13- (*n*-Tridecane)	C26	C26- (*n*-Hexacosane)
C14	C14- (*n*-Tetradecane)	C27	C27- (*n*-Heptacosane)
C15	C15- (*n*-Pentadecane)	C28	C28- (*n*-Octacosane)
C16	C16- (*n*-Hexadecane)	C29	C29- (*n*-Nonacosane)
C17	C17- (*n*-Heptadecane)	C30	C30- (*n*-Triacontane)
Pris	Pristane	C31	C31- (*n*-Hentriacontane)
C18	C18- (*n*-Octadecane)	C32	C32- (*n*-Dotriacontane)
Phy	Phytane	C33	C33- (*n*-Tritriacontane)
C19	C19- (*n*-Nonadecane)	C34	C34- (*n*-Tetratriacontane)
C20	C20- (*n*-Eicosane)	C35	C35- (*n*-Pentatriacontane)
C21	C21- (*n*-Heneicosane)	C36	C36- (*n*-Hexatriacontane)

Table 3. Subsurface oiling indicated by the depth of oil cover on dip stones in 1994, 1999, 2005 and 2012 at the study sites. SE = standard error.

Sites	Year	Max. oil depth (cm)	Mean depth (cm)	SE	n	% clean
McArthur Pass	1994	2	**1.4**	0.32	8	25
	1999	4	**2.4**	0.38	6	0
	2005	6	**2.1**	0.32	16	6
	2012	>8	**3.0**	0.31	19	0
Cape Douglas	1994	9	**3.5**	0.71	19	26
	1999	>8	**3.7**	0.49	20	5
	2005	10	**4.6**	0.40	20	0
	2012	>9	**4.7**	0.49	20	0
Kiukpalik Is.	1994	11	**4.5**	0.94	19	32
	1999	14	**5.7**	0.74	18	0
	2005	NA[1]				
	2012	>9	**5.2**	0.48	20	0
Ninagiak Is.	1994	7	**3.5**	0.72	18	33
	1999	8	**2.1**	0.55	20	40
	2005	4.5	**3.8**	0.88	6	17
	2012	>6	**3.5**	0.40	12	0
Cape Gull	1994	7	**1.6**	0.59	19	68
	1999	8	**2.3**	0.62	17	41
	2005	>3	**1.5**	0.41	10	40
	2012	*[1]				
Kashvik	1994	NA[1]				
	1999	8	**3.6**	0.41	15	0
	2005	NA[2]				
	2012	*[2]				

Notes:
NA[1] - Site could not be assessed due to infilling of site with cobble/boulders
NA[2] - Site not visited
*[1] – Cape Gull – No oil found in quadrats; one very small patch of subsurface oil (sampled for analysis)
*[2] – Kashvik – No observable oil at the site (see Results)

Table 4. Summary of boulder movement at the study sites on the Katmai coastline. For all sites except Cape Gull, "minor" movements are those 12-100 cm in horizontal distance, and/or 5-25 cm in height, and/or 3-10 degrees in azimuth. "Significant" movements are those >1 m in horizontal distance, and/or >25 cm in height, and/or >10 degrees in azimuth. At Cape Gull, where boulders are smaller than at the other sites, we consider "minor" movements to be 12-50 cm in horizontal distance, and/or 5-12 cm in height, and/or 3-5 degrees in azimuth. Minor movements probably represent boulders shifting in place within the boulder armor they are part of, while "significant" movement represent disruption of the armor.

Survey Interval / Type of Movement	***Distance, "minor" (n, %)***	***Distance, "significant" (n, %)***		***Height, "minor" (n, %)***	***Height, "significant" (n, %)***		***Azimuth, "minor" (n, %)***	***Azimuth, "significant" (n, %)***	***Bolts missing (n, %)***	***Number of bolts tracked***
1994-1999										
Cape Douglas	3, 12%	2, 8%		6, 24%	1, 4%		3, 12%	1, 4%	*2, 8%*	25
Kiukpalik	5, 28%	0		0	0		6, 24%	0	*1, 6%*	18
Ninagiak	5, 19%	0		3, 13%	1, 4%		0	1, 4%	*0*	23
Cape Gull	4, 40%	0		2, 20%	0		0	0		10
1999-2005										
Cape Douglas	3, 13%	1, 4%		6, 26%	1, 4%		3, 13%	0	*3, 13%*	23
Kiukpalik	4, 24%	1, 6%		4, 17%	1, 6%		10, 43%	0	*2, 12%*	16
Cape Gull	0	1, 10%		1, 10%	1, 10%		0	1, 10%	*0*	10
1999-2012										
Ninagiak*	1, 5%	0		6, 30%	1, 5%		2, 10%	0	*3, 13%*	20
2005-2012										
Cape Douglas	2, 10%	0		2, 10%	0		1, 5%	0		20
Kiukpalik	5, 31%	0		3, 19%	1, 5%		10, 63%	0		16
Cape Gull	0	0		2, 20%	1, 10%		0	1, 10%		10
*Ninagiak site was largely buried by pebbles prior to 2005 survey and exhumed before 2012 survey.										

Table 5. Polycyclic aromatic hydrocarbon (PAH) concentration minus P0 and composition in passive samplers (PEMDs). Type identifies field blanks (b) and controls (c), SIN is sample identification number. Total PAH is adjusted by method detection limit (MDL); analyte concentrations below MDL were set to zero. The model is a non-parametric source model and was restricted to fluorenes, dibenzothiophenes, and phenanthrenes (see Methods). These model results were scored as consistent with oil (asterisk) or not (blank). Similarly, Principal Component Analysis (PCA) results consistent with oil were marked with an asterisk. Conclusions (concl) for the presence of oil were 'yes,' 'possible,' or 'no.'

				TPAH			**Oil?**	
Date	**Location**	**type**	**SIN**	**ng/g**	**model**	**Model**	**PCA**	**Concl**
5/3/11	Blank, lab	b	20110301	44	0.00			no
5/3/11	Blank, lab	b	20110302	8	0.00			no
6/25/12	Blank, lab	b	20120754	0	0.00			no
8/15/12	Blank, lab	b	20120755	123	-0.10			no
6/16/11	Blank, field	b	20110316	45	-0.27			no
6/16/11	Blank, field	b	20110321	49	-0.30			no
6/16/11	Blank, field	b	20110331	692	-0.40			no
5/13/11	Blank, field	b	20110337	21	-0.03			no
5/18/11	Blank, field	b	20110338	38	-0.03			no
5/18/11	Blank, trip, #1	b	20110339	24	0.10			no
5/18/11	Blank, trip, #2	b	20110340	95	-0.03			no
5/18/11	Blank, trip, #3	b	20110341	880	0.03			no
7/7/12	Cape Douglas	b	20120702	175	-0.40			no
7/7/12	Cape Douglas	b	20120703	144	-0.57			no
7/7/12	Kiukpalik Is.	b	20120701	90	-0.07			no
8/4/12	Kiukpalik Is.	b	20120732	427	-0.70			no
8/3/12	Cape Douglas	c	20120714	25	0.37			no

8/3/12	Cape Douglas	c	20120715	45	-0.40			no
8/3/12	Cape Douglas	c	20120716	24	-0.40			no
8/3/12	Cape Douglas	c	20120717	53	1.00	*		possible
6/16/11	Cape Douglas	c	20110315	16	-0.33			no
6/16/11	Kiukpalik Is.	c	20110317	54	-0.03			no
6/16/11	Kiukpalik Is.	c	20110318	28	-0.33			no
6/16/11	Kiukpalik Is.	c	20110319	2	-0.03			no
6/16/11	Kiukpalik Is.	c	20110320	18	-0.33			no
8/4/12	Kiukpalik Is.	c	20120733	20	-0.03			no
8/4/12	Kiukpalik Is.	c	20120734	15	-0.03			no
8/4/12	Kiukpalik Is.	c	20120735	24	-0.03			no
8/4/12	Kiukpalik Is.	c	20120736	17	-0.03			no
6/16/11	Cape Douglas		20110305	93	0.67	*	*	yes
6/16/11	Cape Douglas		20110306	129	0.57	*	*	yes
6/16/11	Cape Douglas		20110307	154	1.00	*	*	yes
6/16/11	Cape Douglas		20110308	93	1.00	*	*	yes
6/16/11	Cape Douglas		20110309	184	1.00	*	*	yes
6/16/11	Cape Douglas		20110310	72	0.67	*		possible
6/16/11	Cape Douglas		20110311	77	0.33			no
6/16/11	Cape Douglas		20110312	86	0.63	*		possible
6/16/11	Cape Douglas		20110313	37	-0.03			no

6/16/11	Cape Douglas	20110314	12	-0.33			no
8/3/12	Cape Douglas	20120704	84	1.00	*	*	yes
8/3/12	Cape Douglas	20120705	521	1.00	*	*	yes
8/3/12	Cape Douglas	20120706	282	1.00	*	*	yes
8/3/12	Cape Douglas	20120707	410	1.00	*	*	yes
8/3/12	Cape Douglas	20120708	1225	1.00	*	*	yes
8/3/12	Cape Douglas	20120709	698	1.00	*	*	yes
8/3/12	Cape Douglas	20120710	93	0.33		*	no
8/3/12	Cape Douglas	20120711	81	0.33			no
8/3/12	Cape Douglas	20120712	282	1.00	*	*	yes
8/3/12	Cape Douglas	20120713	159	0.33		*	no
6/16/11	Kiukpalik Is.	20110322	526	-0.40			no
6/16/11	Kiukpalik Is.	20110323	784	-0.40			no
6/16/11	Kiukpalik Is.	20110324	806	-0.40			no
6/16/11	Kiukpalik Is.	20110325	72	-0.03			no
6/16/11	Kiukpalik Is.	20110326	1528	0.03			no
6/16/11	Kiukpalik Is.	20110327	780	-0.03			no
6/16/11	Kiukpalik Is.	20110328	290	0.27			no
6/16/11	Kiukpalik Is.	20110329	236	0.27			no
6/16/11	Kiukpalik Is.	20110330	977	0.70	*		possible
8/4/12	Kiukpalik Is.	20120723	283	1.00	*	*	yes

8/4/12	Kiukpalik Is.	20120724	330	1.00	*	*	yes
8/4/12	Kiukpalik Is.	20120725	231	1.00	*	*	yes
8/4/12	Kiukpalik Is.	20120726	324	1.00	*	*	yes
8/4/12	Kiukpalik Is.	20120727	1323	1.00	*	*	yes
8/4/12	Kiukpalik Is.	20120728	484	1.00	*	*	yes
8/4/12	Kiukpalik Is.	20120729	438	1.00	*	*	yes
8/4/12	Kiukpalik Is.	20120730	165	0.70	*	*	yes
8/4/12	Kiukpalik Is.	20120731	377	1.00	*	*	yes

Table 6. Hydrocarbon concentrations and model results in mussel tissue. Total PAH and total calibrated alkane (cAlkanes) concentrations (ng / g wet weight) were adjusted by method detection limit (MDL); analyte concentrations below MDL were set to zero. PAH, alkane, and odd models are explained in Methods. UCM is the unresolved complex mixture. SIN is sample identification number.

Date	**Location**	**SIN**	**TPAH**				**Odd**	**UCM**
			ng/g	**model**	**ng/g**	**model**		**ng/g**
6/16/2011	Cape Douglas	20110332	3	-0.03	658	0.90		0.00
5/18/2011	Kiukpalik Is.	20110334	3	-0.08	1672	0.94		0.00
5/18/2011	Kiukpalik Is.	20110335	3	0.13	1352	0.94		0.00
8/3/2012	Cape Douglas	20120721	10	-0.12	379	0.00	-1.00	0.00
8/4/2012	Kiukpalik Is.	20120740	8	-0.03	431	0.00	-1.00	0.00

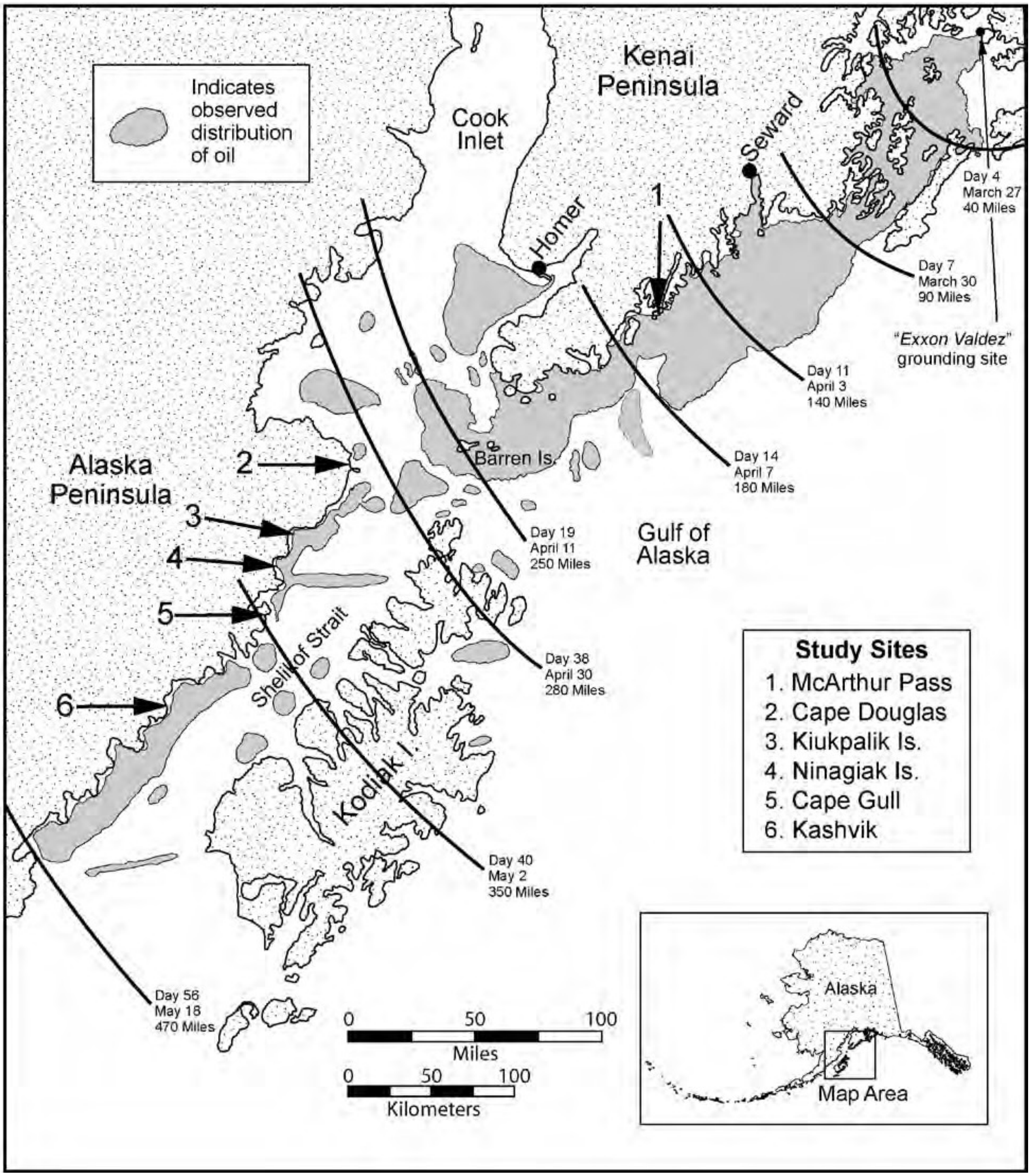

Figure 1. The spread of oil along the Alaska coastline following the 1989 *Exxon Valdez* spill, with date and distance of the oil's extent. The oil distribution map is courtesy of the State of Alaska, Department of Environmental Conservation. Arrows point to the long-term monitoring sites discussed in this study. Site 1 is in Kenai Fjords National Park and Preserve, and Sites 2-6 are in Katmai National Park and Preserve.

Figure 2. A well-integrated boulder armor near the Cape Douglas site. The stocking hat measures 22 cm across. The dark color on the flanks and protected surfaces of these boulders is lichen of the genus *Verrucaria.* The presence of the lichen is further evidence that boulders in this armor are relatively stable.

Figure 3. Top photo shows oil mousse ringing a hole where a dip stone was removed (right-hand side of image) and oil sheen on small pool to the left, from disturbance. The asphaltic surface of undisturbed oil is also apparent (Kiukpalik Island, 2012). Lower right photo is of a dip stone with mousse after being dislodged and removed from between boulders at Cape Douglas in 2012. Oil extends to the bottom of the dip stone. Ruler is not in the orientation used to measure depth of oil.

.

Figure 4. A passive sampler (PEMD) in a metal housing (11 cm diameter) bolted to a boulder at the Kiukpalik Island site in 2012. The sampler is deployed above a patch of remnant *Exxon Valdez* oil which has a surficial asphaltic layer covering little-weathered oil mousse. The passive sampler's purpose is to detect if oil constituents are being released into the water column.

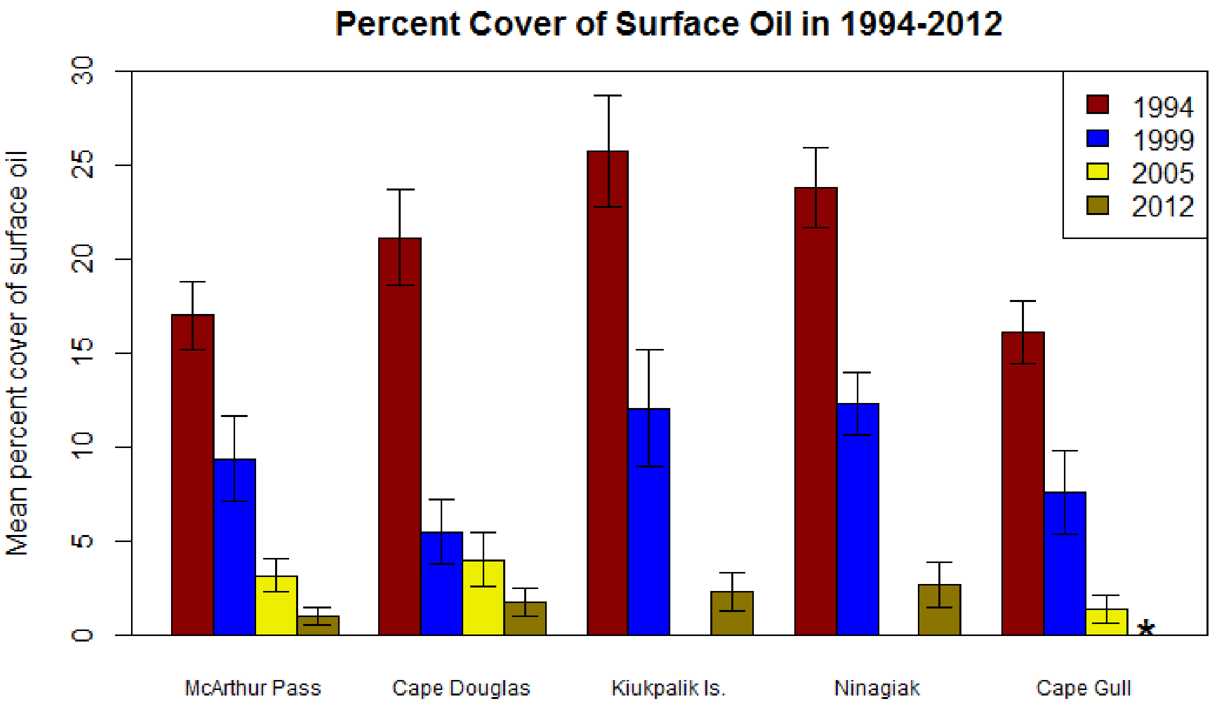

Figure 5. Mean percent cover surface oil at study sites in 1994, 1999, 2006, and 2012. Error bars represent ±1 standard error. No 2005 data for Kiukpalik and Ninagiak are presented since most quadrats could not be assessed. The '*' for Cape Gull indicates that the site was assessed in 2012, however, no (0%) surface oil was found in the quadrats. A Regional Kendall test suggests that all sites have had a significant ($p < 0.001$) and continued decrease in the percent cover of surface oil from 1994 to 2012.

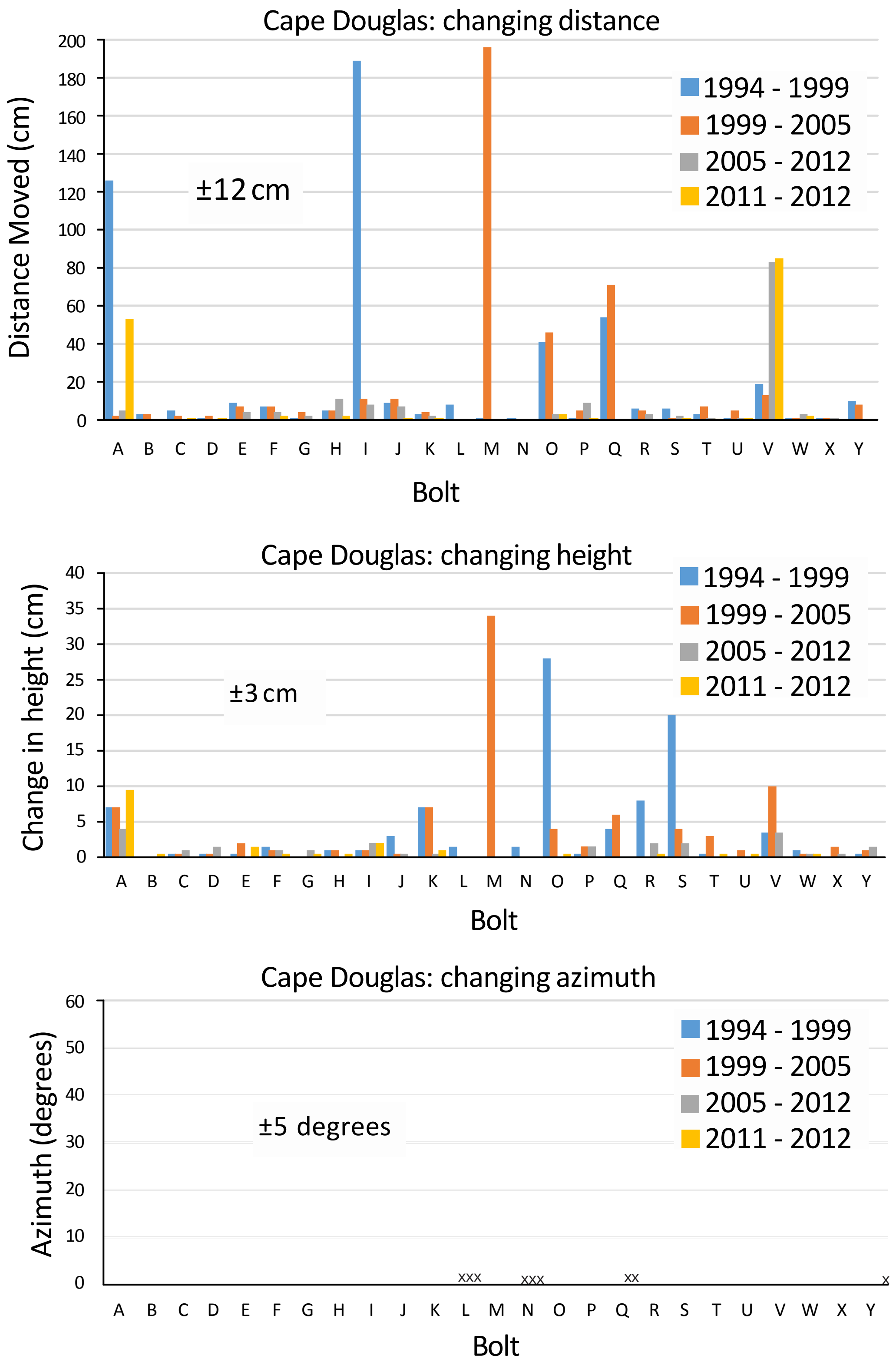

Figure 6. Movements of bolts affixed to boulders at the Cape Douglas site. "Xs" in lower panel indicate bolts not re-located in that year's survey.

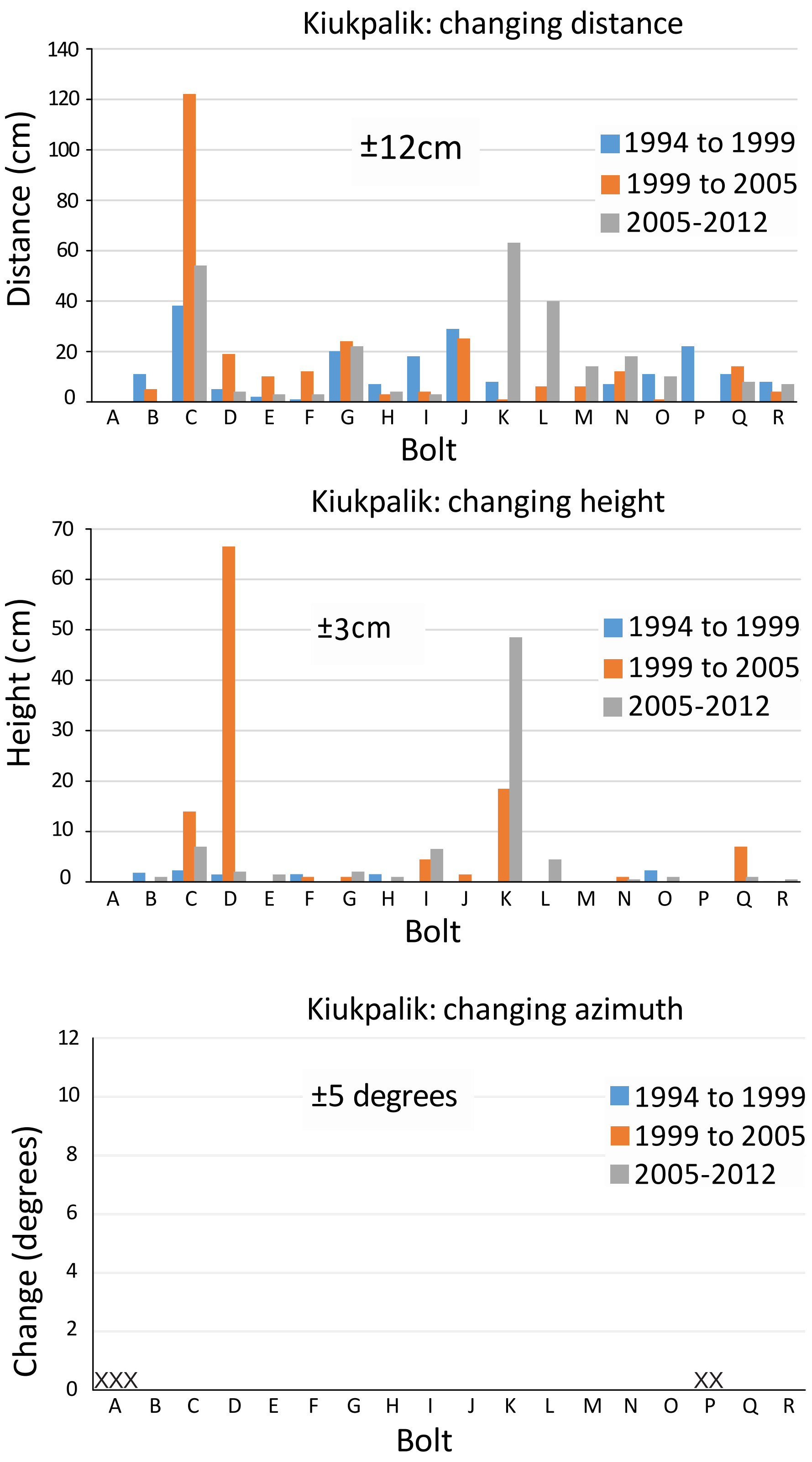

Figure 7. Movements of bolts affixed to boulders at the Kiukpalik Island site. "Xs" in lower panel indicate bolts not re-located in that year's survey.

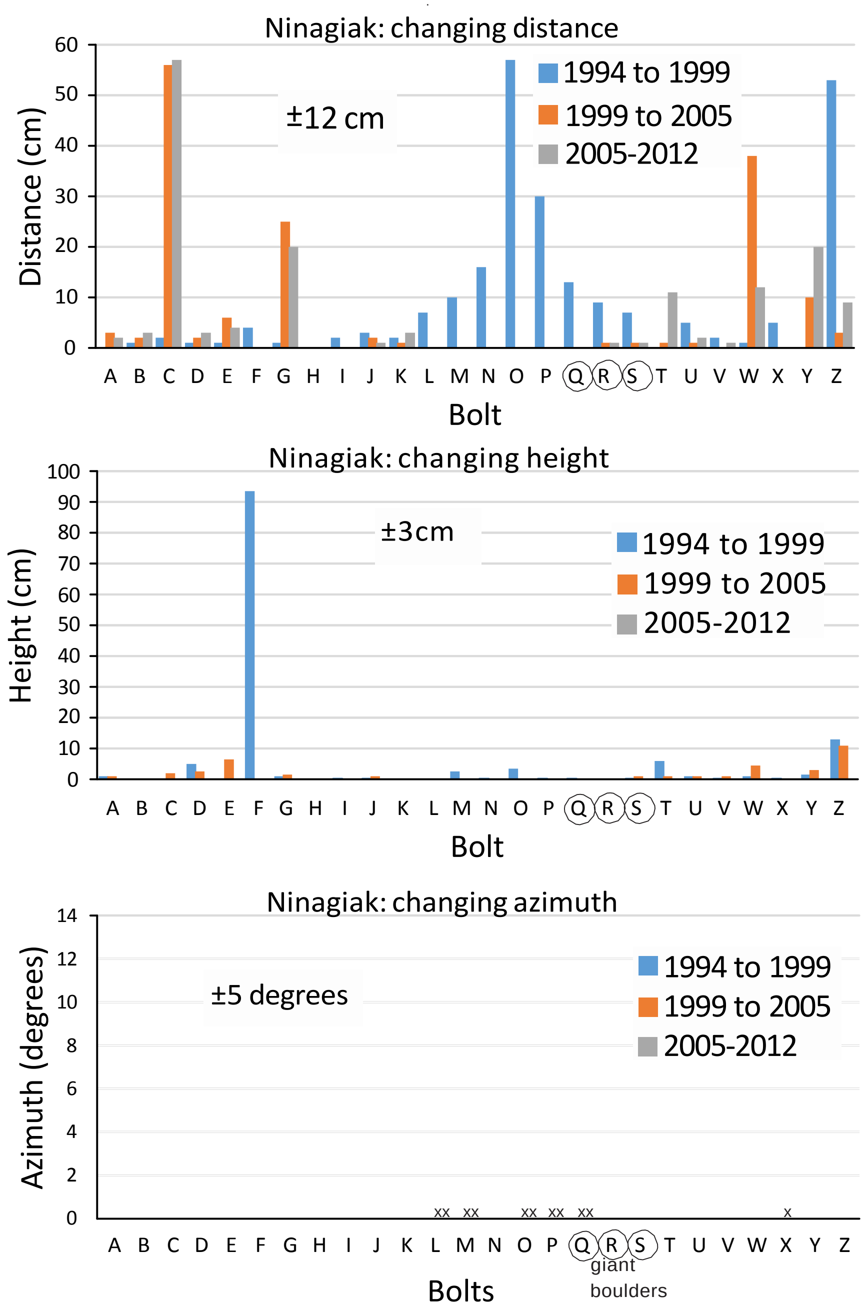

Figure 8. Movements of bolts affixed to boulders at the Ninagiak Island site. This site was largely buried by pebbles and cobbles between 1999 and 2005 and then mostly re-exposed before 2009. "Xs" in lowest panel indicate bolts that not re-located in that year's re-survey. Bolts Q, R, and S were placed in boulders too large to be moved by waves.

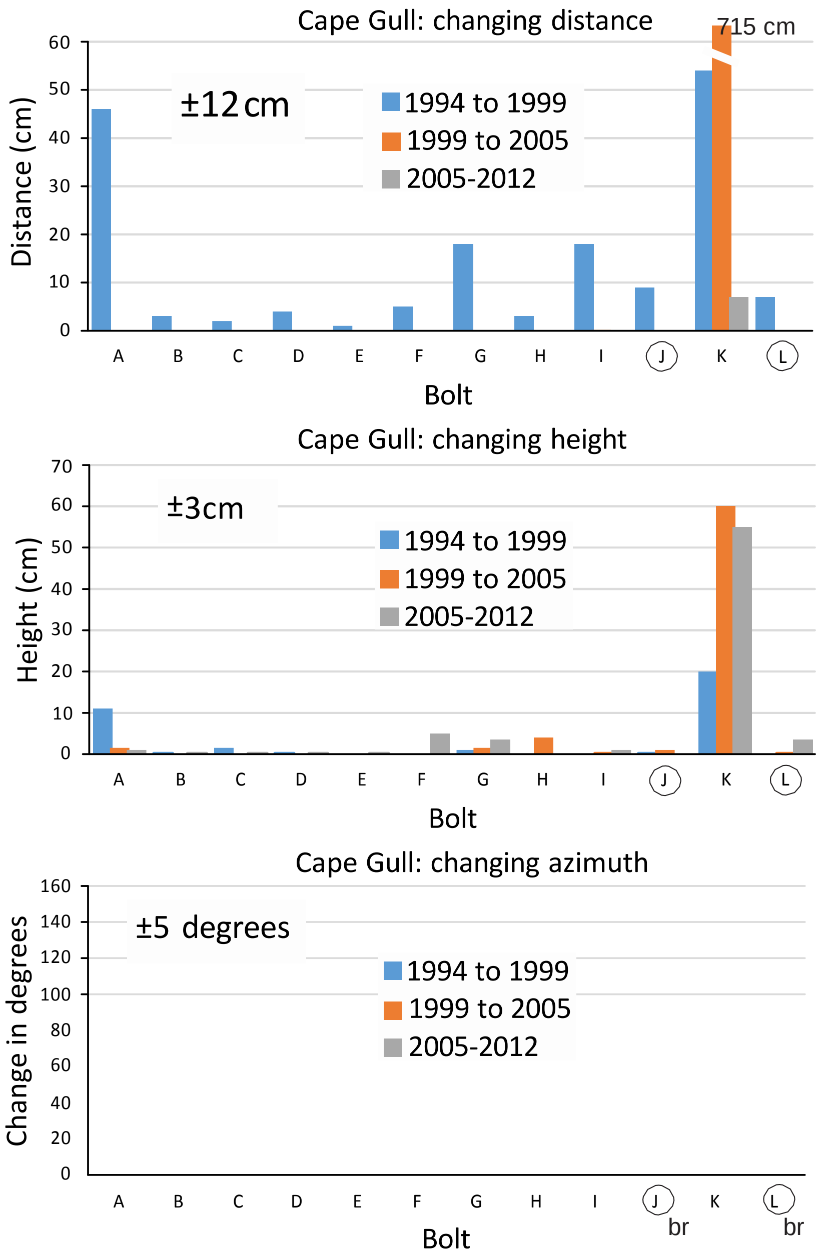

Figure 9. Movements of bolts affixed to boulders at Cape Gull site. Bolts J and L were placed in bedrock.

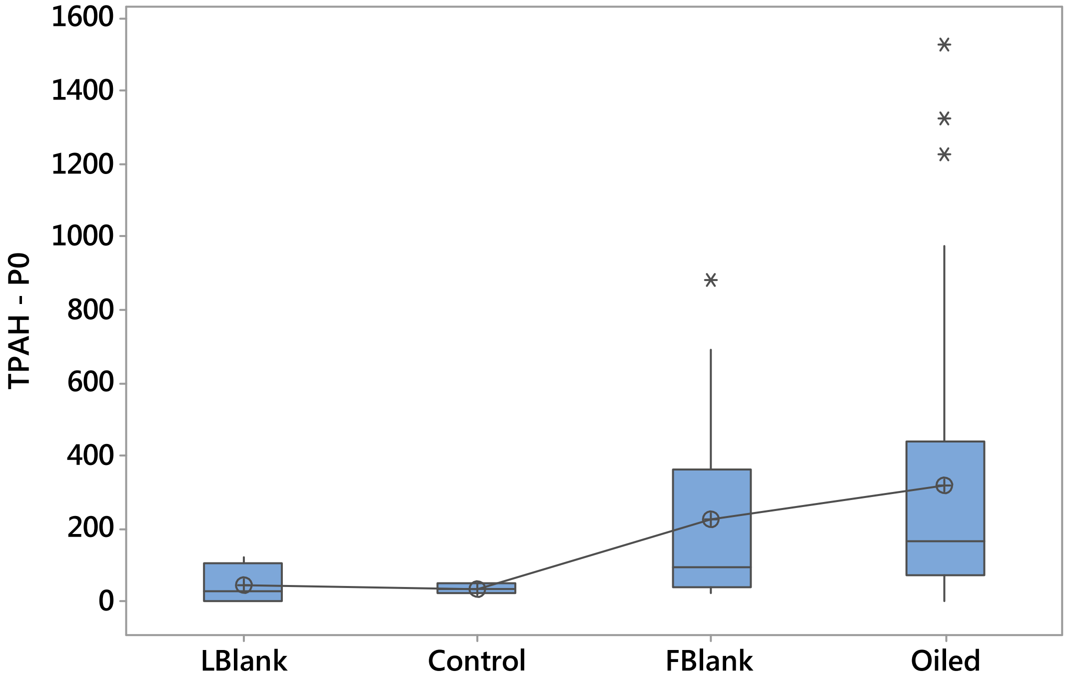

Figure 10. Comparison of TPAH (ng/g device, top panel) in PEMDs among laboratory blanks (LBlank), site controls, field blanks (FBlank), and those deployed at oiled sites. Geographic location and year were not considered in this analysis.

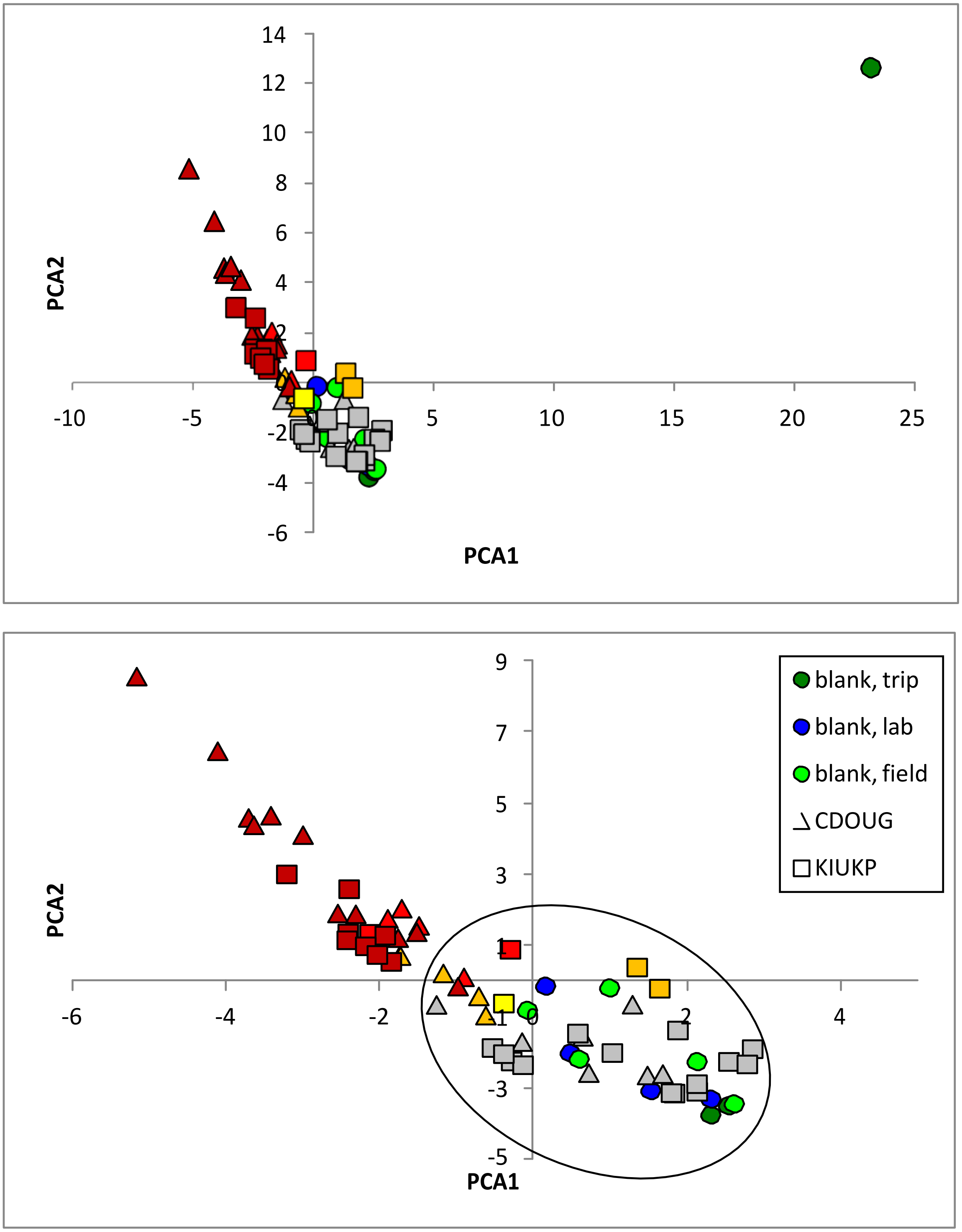

Figure 11. Principal components analysis (PCA) of normalized PAH in the PEMDs. Sample locations are Cape Douglas (CDOUG) and Kiukpalik Island (KIUK). The bottom panel enlarges the primary point cloud. The field samples are color-coded by the PAH source model; gray (<0), yellow (0 – 0.25), orange (0.25 – 0.5), red (0.5 – 0.75), dark red (0.75 – 1.0). Axes are principal component 1 (PCA1, x-axis) and principal component 2 (PCA2, y-axis).

Figure 12. An example PAH composition in mussel tissue. The top panel is representative of composition in 2011; the bottom panel is representative of PAH composition in 2012. See Table 1 for compound abbreviations; y-axis is PAH concentration (ng / g wet weight).

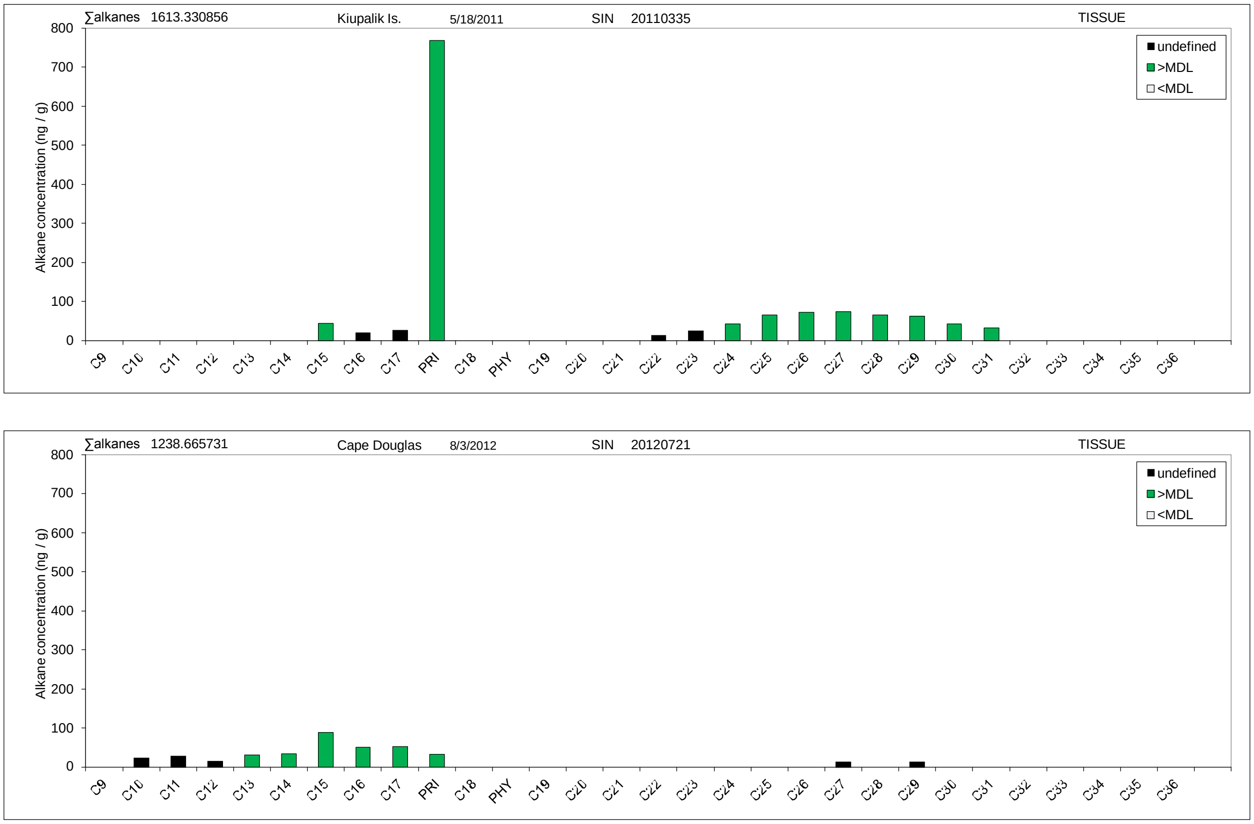

Figure 13. Example of alkane composition in mussels. The top panel is representative of composition in 2011; the bottom panel is representative in 2012. See Table 2 for compound abbreviations; y-axis is alkane concentration (ng / g wet weight).

Chapter 2

Exxon Valdez oil persists on Gulf of Alaska beaches after 23 years: Using new methods to look at old stranded oil

Gail V. Irvine,[1] Christoph Aeppli,[2] Mark Carls,[3] Robert K. Nelson[4] Larry Holland,[3] Christopher M. Reddy,[4] Daniel H. Mann[5]

[1] U.S. Geological Survey Alaska Science Center, Anchorage AK
[2] Bigelow Laboratory for Ocean Sciences, East Boothbay ME
[3] NOAA, Auke Bay Laboratories, Juneau, AK
[4] Department of Marine Chemistry and Geochemistry, Woods Hole Oceanographic Institution, Woods Hole MA
[5] University of Alaska, Fairbanks, AK

Abstract

The *Exxon Valdez* spill stranded oil on rocky beaches in the Gulf of Alaska in 1989. Twenty-three years later, some oil still persists on long-term monitoring sites 240 – 650 km away from the spill origin. We investigated the extent of weathering in oiled sediment collected beneath stable boulder armors or in bedrock crevices from six locations in 2012. Sample extracts were analyzed with traditional gas chromatography, comprehensive two-dimensional gas chromatography (GC×GC), as well as thin layer chromatography (TLC) to chemically describe the oil on a molecular and bulk level. To confirm that the oil residues were indeed from the *Exxon Valdez* cargo, hopane and sterane biomarkers were employed. Surprisingly, stranded oil at two shoreline sites could not be confidently matched to *Exxon Valdez* oil, but instead indicated another oil source (e.g., secondary contamination) and/or the occurrence of substantial biomarker alteration. Chemical analyses suggest that evaporation has been the main weathering process and reveal only minor amounts of biodegradation of the stranded *Exxon Valdez* oil at the other four sites, even though the oil has been in the environment for 23 years. In line with the absence of advanced oil degradation, no major increase of oil degradation products was found. Such compounds were found to form a recalcitrant polar oil fraction after the *Deepwater Horizon* disaster. We conclude that weathering of the oil at most of our Gulf of Alaska monitoring sites has been very slow. We suspect that this was primarily due to the formation of oil mousse within days after the spill, prior to the long-distance transport of the oil. The stranding of the oil on stable, boulder-armored shores or on a low-energy bedrock/boulder beach further protected the oil and slowed oil degradation processes.

Introduction

The reliance of the modern world on fossil fuels continues, and oil spills occur during exploration, production, recovery, storage and transport operations (Hayes and Gundlach 1979; Jackson et al. 1989; Wolfe et al. 1994; National Research Council 2003). The aftermath of every oil spill provides an opportunity to examine how various ecosystems respond to the point releases of different types of hydrocarbons. When studied across decadal time scales, the changing properties of the spilled oil provide valuable insights into the physical, chemical and biological processes governing the fate and persistence of different types of oil released under different conditions, and in different locations (Corredor et al. 1990; Baker et al. 1993; Burns et al. 1994; Vandermeulen and Singh 1994; Wang et al. 1994; Dauvin 1998; Mille et al. 1998; Wang et al. 2001; Reddy et al. 2002; Peterson et al. 2003; Peacock et al. 2005; Irvine et al. 2006; Peacock et al. 2007; Short et al. 2007). As oil exploration in the Arctic is likely to expand in the future, knowledge on how oil behaves in cold regions is needed in order to make the most well-informed decisions about response activities after spills and restoration of impacted areas.

The *Exxon Valdez* Oil Spill (EVOS)

The *Exxon Valdez* spill provides an ideal opportunity to learn more about how oil weathers on high latitude shorelines. Briefly, the T/V *Exxon Valdez* struck a reef in Prince William Sound (PWS), Alaska (Figure 1) in March 1989 and spilled ~35,000 metric tons of Alaska North Slope (ANS) crude oil (Leschine et al. 1993). Over the course of the next two months , the oil was transported by winds and currents in a largely counterclockwise direction by the Alaska Coastal Current (Royer et al. 1990), contaminating over 2000 km of coastline with 20,000 metric tons of oil. In the Gulf of Alaska, more than 750 km of coast experienced sporadic contamination and ultimately only 2-4% of the total *Exxon Valdez* spill stranded on the more distal coastlines of the Shelikof Strait (Wolfe et al. 1994) (Figure 1).

Spilled oil was immediately subjected to a variety of weathering processes. In PWS ten days after the spill, the physical state of the oil was highly variable, ranging from extremely fluid oil to more emulsified oil and mousse (Payne et al. 1991). This led to the stranding of variable oil forms within PWS. However, by the time the spilled oil exited PWS and started beaching along Gulf of Alaska (GOA) shorelines, it was almost entirely mousse, a viscous water-in-oil emulsion. Oil mousse has been shown to be less susceptible to chemical weathering than fluid oil (Payne and Phillips 1985; Baker et al. 1993; Short and Heintz 1997; Irvine et al. 1999; Irvine et al. 2006; Irvine et al. 2007; Short et al. 2007). In 1992, six long-term GOA monitoring sites were established on national park beaches known to have been contaminated by *Exxon Valdez* oil (EVO) (Figure 1) (Schoch 1993). These sites, arrayed from 240 – 640 km from the spill origin, have been studied at periodic intervals of approximately five to six years through 2012 (Irvine et al. 1999; Irvine et al. 2006; Irvine et al. 2007; Short et al. 2007).

Recent Advances in Chemical Characterization of Hydrocarbons

Crude oils are chemically complex substances composed of many constituents. Traditionally, analysis focuses on *n*-alkanes, other select branched and cyclic saturates, polycyclic aromatic hydrocarbons (PAH) as well as hopane and sterane biomarkers using gas chromatography (GC) with flame ionization detection (FID) or with mass spectrometry (MS) (Stout and Wang 2007). While GC-FID and GC-MS are powerful techniques, they have limitations when it comes to chromatographically resolving compounds classes beyond *n*-alkanes and PAHs, two compound classes that can be degraded relatively rapidly in the environment. Recently, comprehensive two-dimensional gas chromatography (GC×GC) has evolved as a technique very suitable for oil analysis. This is due to its ability for high chromatographic resolution, which allows for discrimination of thousands of oil components (Gaines et al. 2007). Previous work has demonstrated the effectiveness of GC×GC for capturing and disentangling the combined processes of evaporation and dissolution weathering (Arey et al. 2007; Wardlaw et al. 2008).

GC×GC relies on compound separation based on the molecular interactions (dipole-dipole electrostatic attraction, hydrogen bonding, and Van der Waals forces) between individual compounds and the stationary phase within the column. Petroleum compounds with relatively higher polarities will have greater elution times in the second dimension and appear towards the top of the chromatogram, whereas larger compounds have greater elution times in the first dimension, resulting in an increase in molecular size from left to right across the chromatogram. This results in compounds ordered by carbon number along the *x*-axis and chemical class (alkanes, cycloalkanes and one- two- and multi-ring aromatics and their alkylated homologues) along the *y*-axis (Nelson et al. 2006; Ventura et al. 2010). Because compound volatility and polarity are related to a compound’s propensity to evaporate or dissolve, GC×GC can provide quantitative and visual information on compounds lost due to these weathering processes. In addition, GC×GC allows for a highly accurate analysis of petroleum biomarkers (Eiserbeck et al. 2012), which are recalcitrant oil compounds that are highly characteristic for different types and origins of oil (Peters et al. 2005). Use of GCxGC analysis of oil and sediment samples collected more than 20-years after the EVOS should therefore allow for enhanced capability to differentiate constituents of oil present in sediments and compare those to the original composition of the oil.

Not all petroleum constituents can be analyzed by GC. Examples of such non-GC amenable compounds are heteroatom-containing resins and asphaltenes, which are native oil compounds. Furthermore, this non-GC amenable fraction can increase during oil weathering due to photooxidation or biodegradation; these processes oxygenate petroleum hydrocarbons (Charrie-Duhaut et al. 2000; Aeppli et al. 2012). To quantify this non-GC amenable fraction, thin layer chromatography-FID (TLC-FID) has been employed. TLC-FID separates bulk fractions according to polarity, in a saturated, an aromatic, and two fractions that are more polar than the saturated and aromatic fractions. These four fractions are operationally defined, and are dependent on the employed solvent system (Charrie-Duhaut et al. 2000). The two polar fractions are often referred as “resins” and “asphaltenes” if the sample is crude oil, or more generally as “oxygenated hydrocarbons” (OxHC) if the sample is a weathered oil sample.

In 2012, we resampled our long-term oil monitoring sites in the GOA. Oil at these same sites had also been sampled in 1992, 1994, 1999 and 2005. In Chapter 1, Irvine et al. (2014) quantify the persistence of surface and subsurface oiling, the dynamics of the boulder armors, and examine whether oil constituents are being released from these sites. In this chapter, we report the results of chemical analyses by GC-MS, GC×GC, and TLC-FID of oil/sediment samples collected in 2012. Our goal here is to: (*i*) identify the source of the oil contamination at each site and (*ii*) describe how the oil has weathered over the 23 years since release from the *T/V Exxon Valdez*. To do this, we compare 2012 oil samples taken from the monitoring sites to EVO, as well as to field samples taken in the past. This allows us to assess changes in the extent of weathering over time. We analyzed 24 oil/sediment samples from the 6 long-term monitoring sites in the GOA and one source oil sample to determine the complex chemical state of the oil and its weathering status 23 years after the EVOS.

Material and Methods

Field sites and samples. Duplicate sets of 18 samples (consisting of 12 oil/sediment samples and six field blanks) from a total of six study sites were collected in Aug 2012. One set was sent to Woods Hole Oceanographic Institution (WHOI) and one to the National Oceanic and Atmospheric Administration (NOAA) Auke Bay Laboratories (ABL) in Juneau, Alaska (Table 1). At five of the six study sites, duplicate oil/sediment samples were collected from two different locations per site. Only at the Cape Gull site was duplicate sampling restricted by the limited amount of remaining subsurface oil; duplicate samples were collected at one sampling location, but the other samples were collected from separate locations (Table 1). At most locations, the samples were of mousse-like oil; only at Kashvik were the samples predominantly sediment, as no oil was observed at this site. Oil/sediment samples were taken from depths of ~1-9 cm. Samples were sent for analysis by GC-MS (NOAA) or by GC×GC and TLC-FID (WHOI). For analytical quality control reasons we collected duplicate field blanks at each site, one for each lab. A field blank was a jar opened during collection of a sediment/oil sample, usually placed on a nearby rock, and capped when oil/sediment collection was completed. The EVO cargo sample was obtained from ABL. The *T/V Exxon Valdez* carried only a single mixture of Alaska North Slope crude oils.

Sample extraction and total PAH mass. Sediment samples were shipped for sample extraction and analysis to ABL and WHOI. The extraction procedure at ABL was as follows: For 10 out of 12 samples, minimal sediment was present and the sample consisted mostly of oil. These samples were dissolved with dichloromethane (DCM); a subsample was exchanged with hexane over steam and separated into aliphatic and aromatic fractions by column chromatography (10 g of 2% deactivated alumina over 20 g of 5% deactivated silica gel). The PAHs were eluted with 50 mL of 1:1 (v/v) pentane:DCM and exchanged into 1 mL of hexane over steam. DCM was evaporated from the remaining extract to determine the total mass of extracted oil and reported units are ng PAH g^{-1} oil. The remaining two oiled sediment samples were processed as sediment; about 20 g were extracted and the divisor was the total sample weight to yield ng PAH g^{-1} sediment.

At WHOI, 0.5 to 150 g sediment samples were extracted with 30 to 200 mL DCM/hexane (1/1 v/v). The extracts were dried (Na_2SO_4) and the solvent volume reduced to 4 mL using a rotary evaporator. The final concentration of oil in the samples was approximately 2 mg mL^{-1}.

Analytical methods. GC-MS analysis was performed at ABL. The method details have been described elsewhere (Short et al. 1996; Carls 2006). Aromatic fractions were analyzed for PAHs by a gas chromatograph equipped with a mass selective detector. The data were acquired in selected ion monitoring (SIM) mode, and concentrations were determined by the internal standard method (Carls et al. 2004). Experimentally determined method detection limits were generally < 1 ng/g in sediment. The accuracy of the PAH analyses was about ± 15% based on comparison with National Institute of Standards and Technology values (SRM1944), and precision expressed as coefficient of variation was usually less than about 20%, depending on the PAH. Surrogate recoveries averaged 88%. Total PAH (TPAH) concentrations were calculated by summing concentrations of individual PAH (Chapter 1, Table 1). Relative PAH concentrations were calculated as the ratio of PAH_i / TPAH.

Aliphatic fractions were analyzed for *n*-alkanes by GC-FID at ABL. Analyte concentrations were determined by the internal standard method. Experimentally determined method detection limits were generally < 1 ng/g in sediment. The accuracy of the alkane analyses was ± 15% based on a spiked blank processed with each set of samples, and precision expressed as coefficient of variation was usually less than about 20%. Surrogate recoveries averaged 72 and 74% in tissue and sediment, respectively. Total calibrated alkane concentrations (cAlk) were calculated by summing concentrations of individual calibrated alkanes (Chapter 1, Table 2). Relative alkane concentrations were calculated as the ratio of $alkane_i$ / total alkanes.

Aliphatic fractions of sediments were analyzed for biomarkers by GC-MS at ABL. The data were acquired in SIM mode, and concentrations were determined by the internal standard method with response factors (RF) based on two representative compounds, 17α (H),21β(H)-hopane (H30) and 5α(H),14α(H),17α(H)-cholestane. The accuracy of the biomarker analyses was about ± 15% based on a spiked blank processed with each set of samples, and precision expressed as coefficient of variation was about 20%, depending on the biomarker. Biomarker concentrations were not corrected for recovery; surrogate recovery averaged 93% (range 59 to 125%).

Comprehensive two-dimensional gas chromatography coupled to a flame ionization detector (GC×GC-FID) was performed at WHOI using a GC×GC-FID from Leco (St. Joseph, MI). The method was optimized towards maximizing chromatographic peak resolution throughout the range of GC-amenable components found in Alaska North Slope crude oil. The first-dimension column was a Restek Rtx-1 column (60 m, 0.25mm ID, 0.25μm film thickness). The second-dimension column was an SGE BPX-50 (1.25 meters, 0.10mm ID, 0.10μm film thickness). The inlet temperature was held at 300 ºC. The injection mode was splitless and the carrier gas was hydrogen at a constant flow rate of 0.8 mL min^{-1}. The first oven was programmed as follows: isothermal at 50 ºC for 5.0 min., 50 to 333 ºC at 2 ºC min^{-1}, isothermal at 333 ºC for 2 min. The second oven was programmed as follows: isothermal at 57 ºC for 2.0 min., 57 to 340 ºC at 2 ºC min^{-1}, isothermal at 340 ºC for 2 min. The modulation period was 6 seconds.

Thin layer chromatography-FID (TLC-FID) was performed according to a previous study (Aeppli et al. 2012). Briefly, 1 to 5 µL of sample extracts were spotted on the base of a silica-gel sintered glass rod and successively developed in hexane (26-min development time), toluene (12 min), and DCM/methanol 97/3 (5 min). The rods were analyzed in the TLC-FID analyzer (Iatroscan MK-5). In this report we use the terms saturated fraction, aromatic fraction, resins and asphaltenes for the four peaks obtained by TLC-FID (see, e.g., Figure 6). Note that the resin and asphaltene fraction can also contain oxygenated hydrocarbons formed due to oil weathering (Aeppli et al. 2012). While the EVO does contain operationally defined resins and asphaltenes using this technique, any weathering processes that would produce oxygenated products would also be captured in these fractions.

Nonparametric identification of EVO. To understand if samples were oiled and by what, observed concentrations and composition of alkanes and PAHs were considered. These considerations were codified and summarized numerically, and in some cases modeled, as follows: (*i*) TPAH Scores: Elevated total PAH (TPAH) was considered indicative of contamination; if TPAH (ng/g) > 10,000, the score (s) = 1; > 1000, s = 0.85; > 500, s = 0.75; > 200, s = 0.6; and >100, s = 0.5; else 0. Scaling was different for samples analyzed as oil (masses were relatively small, roughly 0.01 g) so to achieve comparable scoring, the scoring algorithm was adjusted; if TPAH (ng/g) > 1,000,000, s =1; > 500,000, s = 0.85; > 200,000, s = 0.75; > 100,000, s = 0.6; and >50,000, s = 0.5; else 0). (*ii*) Alkane Scores: Calibrated alkane concentrations (ng/g) were scored on the same scales as TPAH concentrations. (*iii*) Petrogenic/Pyrogenic: Composition of PAH was modeled to characterize source attributes (petrogenic or pyrogenic) using revised methods of Short et al. (1996) and Carls (2006); values ranged from -1 (pyrogenic) to +1 (petrogenic). (*iv*) Perylene Scores: Perylene was examined as a special case; it can be produced by contemporary microbial sources (Venkatesan 1988).The fraction of perylene (of TPAH) was scored as follows: if ≥ 0.5, score = -1; if ≥ 0.3 then -0.75; if ≥ 0.2 then -0.5; and if ≥ 0.10 then -0.25. (*v*) Odd/Even Scores: normal alkane composition was modeled to identify the presence or absence of oil. The first step was to determine whether oil was present or not. To that end, n-C_{12} through n-C_{36} were examined; if concentration for each individual *n*-alkane was > 0 then it received a score of 1, else 0. These scores were summed and divided by the number of observations. If this value was > 0.6, then a petrogenic signal might be present and F = 1 (else 0). The second step was to determine if concentration patterns were consistent with source oil. Even pairs and odd pairs were compared in the range n-C_{26} to n-C_{36}. Even-even and odd-odd comparisons were chosen to mitigate possible interference from *n*-alkanes produced by plants (Wang and Fingas 2003). For each pair, if the concentration of the larger compound was greater, the pair was assigned a score of -1; if it was less, 1; else 0. These scores were summed and divided by the number of pairs; if this value was > 0.6 then concentration declined with molecular weight and H = 1 (else 0). Alkane concentration potentially associated with oil droplets was estimated as $C = \sum (Alk_i - Alk_{max\ control})$ and the fraction of alkanes associated with droplets, D, was $F \cdot H \cdot (C / cAlk)$, where Alk is the ith alkane concentration and cAlk is total calibrated alkane concentration. Values for D ranged from 0 to 1. Alkane composition was also examined for the presence of prominent odd-numbered compounds indicative of a contemporary plant source. The fraction of odd alkanes was $Z = \sum (C_{21} + C_{23} + \ldots C_{35}) / \sum (C_{21} + C_{22} + \ldots C_{36})$. Odd scores were assigned as -1 if $Z \geq 0.9$, -0.75 if $Z \geq 0.85$, and -0.5 if $Z \geq 0.8$. (*vi*) UCM Scores: An unresolved complex mixture (UCM) score was set equal to 1 if the UCM ≥ 100,000, 0.75 if UCM ≥ 50,000, and 0.5 if UCM ≥ 10,000. A subset of these scores (UCM and perylene) was used to determine if composition was biogenic. Samples with mean scores (UCM and perylene) ≤ -0.5 were considered biogenic. Samples were considered consistent with background concentrations when concentrations < 100 ng/g. (*vii*) Hopane/Triterpane/Sterane Scores: Based on the long-term stability of hopanoid and sterane biomarkers in the environment the following method was used to identify source oil in oiled samples. For example, hopanes from specific sources have specific composition patterns (Wang et al. 2007). Samples from unknown sources can be compared to see if the patterns match (or not). EVO was chosen as the source oil and samples in this study were compared to it. Source oil bounds were set at mean ± 20%, expressed in proportional units ($H_i / \sum H$), where H_i is the i^{th} hopane concentration and $\sum H$ is the total hopanoid concentration. The fraction of H_i in the unknown sample within each of the source oil bounds was calculated. The probability that an unknown sample would match EVO composition was assessed by reference to results of randomly permuting the source oil data set 10,000 times. The probability of randomly encountering a match >0.55 is <0.0001 (determined by randomly permuting the sample 10,000 times), thus any score > 0.55 was consistent with EVO. Triterpanes and steranes were similarly modeled. All scores from each set of information were averaged; samples with estimates $s > 0.65$ (65%) were considered oiled.

Principal component analysis (PCA) for EVO identification. In addition to the previously described method, MDL-filtered data were analyzed by PCA, thus providing independent insight into the presence (or absence) of oil and weathering. Concentration data were normalized before analysis (PAH_i / TPAH or $alkane_i / \sum alkanes$) to understand composition similarities and differences. Only those analytes in common throughout the historical data set were included in analysis; F4, D4, and FP2-FP4 were not analyzed in early years, thus were not included (Chapter 1, Table 1). Similarly, n-C_9-, n-C_{31}-, n-C_{33}-, n-C_{35}-, and n-C_{36}-normal-alkanes were not measured in all years and were not included (Chapter 2, Table 2). Independent PCAs for normalized PAHs and alkanes were completed with Minitab, using correlation matrices. .

Nordtest biomarker analysis for EVO identification. The Nordtest (Daling et al. 2002) provides an alternative approach to evaluate biomarker matching between oil samples. The biomarker ratios (Daling et al. 2002) for mean EVO were plotted against the same ratios for each individual sediment sample. The ratios estimated with our data were %27Ts, %28ab, %25nor30αβ, %29Ts, %30o, %30g, %29αβ, %32αβS, %27dia, %29ααS, %29ββ, %27ββSTER, %28ββSTER, and %29ββSTER as defined by (Daling et al. 2002) (Chapter 2, Appendix). Residuals, $\sum|\text{ratio}_{\text{EVO}} - \text{ratio}_{\text{sample}}|$ were calculated for each comparison as a method of deciding among possible interpretations given by the authors (positive match, probable match, inconclusive or non-match).

GC×GC-FID biomarker analysis for EVO identification. Using GC×GC-FID, sterane and hopane biomarkers were chromatographically separated and plotted on the two-dimensional GC space (Gaines et al. 2007). The biomarker range of the chromatograms was used for visual comparison of the samples with EVO.

Weathering values from GC-MS. A weathering model based on first-order loss-rate kinetics for PAHs was applied to both historical oil samples from these GOA sites and the 2012 samples to estimate their weathering and match with EVO (Short and Heintz 1997). Parameters of the weathering model include the PAH proportions of unweathered EVO, relative first-order loss-rate constants for 14 selected PAH (Chapter 1, Table 1), and a parameter w for the extent of weathering. This latter parameter increases from near 0 for unweathered EVO, <2 for slightly weathered and >7 for severely weathered EVO (Short and Heintz 1997).

The goodness-of-fit between the relative PAH distribution patterns of modeled versus measured PAH in a sample is described by a mean-square-error (MSE) term, where MSE values of zero correspond to a perfect match, and increasingly positive values indicate progressively larger discrepancies between modeled vs. measured relative PAH abundances. An MSE value of 0.57 corresponds with a type I error of 0.05, indicating that a lack of fit between modeled and measured PAH of this magnitude occurs at a frequency of 5% from random effects when EVO actually is the sole source of the PAH. The median MSE value of samples known to contain EVO as the dominant hydrocarbon source is 0.15 (Short and Heintz 1997).

Results and Discussion

Fingerprinting of samples as EVO using non-parametric methods. Using the non-parametric score-approach**,** 8 of 12 oiled sediment samples were identifiable as EVO (Table 2). Samples from Cape Douglas, Kiukpalik Island, Ninagiak Island, and McArthur Pass had mean scores of 0.95±0.03. Matches at Cape Gull were weaker than at the other sites (mean scores of 0.63); only the hopane distribution was consistent with EVO (Table 2, Figure 2d). Oil was not detected in Kashvik samples; oil was not evident in either PAHs or alkanes and concentrations of these compounds were consistent with background levels. Only the hopane distribution in one of the two Kashvik samples was similar to EVO, albeit with a rather low score of 0.65 (compared to 0.9 to 1.0 for the other samples (Table 2 and Figure 2b). Interestingly, EVO was present at all these locations in previous years (Irvine et al. 1999; Irvine et al. 2006; Irvine et al. 2007; Short et al. 2007); however in 2005 it was not possible to sample oil at Kiukpalik Island and Kashvik (Irvine et al. 2007).

Biomarker fingerprinting using GC-MS derived PAH and alkane data. For these analyses we also included historical data from samples collected from 1989 to 2005 (see Table 3 for samples). The PAHs in the majority of GOA sediment samples grouped closely together in PCA space (Figure 3a). The samples from the Cape Gull site were an exception. Only two of 11 Cape Gull samples clustered closely with the majority; one of these was a sample collected in 1989, the other in 1994[2]. A closer inspection into the cause for this variability showed that proportions of chrysenes and higher molecular weight PAHs were unusually high in the Cape Gull samples compared to the other samples. This was evident in PCA space because PCA1 correlated with the sum of higher

---

[2] These same two samples were the only two Cape Gull samples identified as oiled by the alternative source model and decision matrix approach (Table 2).

molecular weight PAHs ($r = 0.962$; $P < 0.001$; $n = 60$). Also distinctly different from the majority were two out of eight Kashvik samples. These two samples, both collected in 2012, were inconsistent with oil.

The tight clustering of the PAH composition suggests that the PAHs in the majority of sediment samples have undergone very little chemical weathering. Weathering is typically evident in PCA space and the first principal component often correlates with measures that indicate weathering, such as percent chrysenes (M. Carls, pers. obs.). In contrast, the first component in this analysis correlated strongly with chrysenes ($r = 0.946$) in addition to correlation with the high molecular weight (HWM) PAHs (see previous paragraph), but the majority of samples were not distinguishable along this axis. The second axis was not a function of weathering ($r = 0.155$, $P = 0.119$ for chrysenes), thus weathering was not apparent in the PCA[3].

In most of the GOA sediment samples, alkanes grouped closely together in PCA space, except for samples from Cape Gull (Figure 3b). Only three of 11 Cape Gull samples clustered with the majority of samples; these were collected in 1989, 1992, and 1994. Samples from Cape Gull generally had relatively fewer alkanes in the n-C_{16} to n-C_{22} range and relatively more in the n-C_{28} to n-C_{34} range than other samples. Similar to the PAH results, two of eight Kashvik Bay samples, those collected in 2012 were inconsistent with whole oil[4]; one of these had unusual quantities of n-C_{10}- to n-C_{13}-alkanes and both had unusual odd-chain concentrations in the n-C_{25}- to n-C_{31}-alkane range. Alkanes in PWS samples were distinct from GOA samples because they were less weathered. There were proportionately more of the smallest, most environmentally labile n-alkanes (n-C_{10} to n-C_{15}, median 0.27, $n = 3$) in PWS than in GOA samples (median 0.05, $n = 55$; $P = 0.017$, Kruskal-Wallis one-way ANOVA on ranks). The exception was the proportion of small alkanes in one KASHB sample, 0.38; this sample did not contain EVO (SIN 20120746, Table 2) and was not included in the alkane weathering analysis.

---

[3] Lack of weathering was also evident by analysis of w versus time (Short and Heintz (1997) model; $r = 0.036$, $n = 55$) and percent chrysenes versus time ($r = 0.120$, $n = 61$) for data from all sites, and increased weathering was not observed on a site-by-site basis.

[4] Multiple approaches identify these two samples as not oiled.

Biomarker fingerprinting using GC-MS derived data. We used the Nordtest protocol (Daling et al. 2002) to evaluate biomarker concentrations determined by GC-MS. The biomarker ratios were consistent with *Exxon Valdez* oil at all sites except Cape Gull and Kashvik Bay (Figure 4). Matches to EVO were probable at Cape Douglas, Kiukpalik Island, Ninagiak Island, and McArthur Pass ($0.27 \leq |\text{residual}| \leq 0.41$). In contrast, Kashvik Bay sediment samples ($0.77 \leq |\text{residual}| \leq 0.97$) and Cape Gull oiled sediment samples ($0.85 \leq |\text{residual}| \leq 0.99$) did not match EVO. These results are in line with the results obtained from non-parametric oil identification and PCA.

Biomarker fingerprinting using GC×GC derived data. GC×GC-FID biomarker analysis was used to compare oil samples from the GOA monitoring sites with EVO. In contrast to GC-MS, GC×GC analysis allows for chromatographic separation of biomarker compounds, which leads to more detailed oil fingerprinting than GC-MS (Eiserbeck et al. 2012). In line with the GC-MS based models described above, the samples from Cape Douglas, Kiukpalik Is, Ninagiak Is and McArthur Pass clearly matched EVO (Figure 5). The relative distribution of hopanoids, steranes, diasteranes, and triaromatic steranes match EVO on visual inspection. On close inspection, it appears that the steranes and diasteranes are slightly less abundant in the field samples from 2012 than they were in the fresh (neat) EVO. This might be explained by the published observation that diasteranes and C_{27}-steranes can be less recalcitrant than hopanoids in the environment (Munoz et al. 1997; Wang et al. 2001; Prince et al. 2002). However, sterane and hopanoid biomarkers are generally assumed to be more recalcitrant than *n*-alkanes, which still can be found in many of the field samples collected in 2012.

The sample from Cape Gull differed somewhat from those of the EVO-like samples, consistent with the lower scores based on GC-MS analysis for these samples (see Table 2). In the Cape Gull samples, the relative distribution of triaromatic steranes is different from EVO, with a higher abundance of the C_{26}-triaromatic steranes relative to the C_{27}- and C_{28}-triaromatic steranes. Furthermore, the diasteranes and steranes are present in greater abundance compared to hopanes (Figure 5). This could be for two reasons. First, the sampled oil might not be EVO. As previous studies showed the presence of EVO at these sites (Irvine et al. 1999), this hypothesized non-EVO oil must be a more recent contamination. Second, oil weathering might have altered the biomarker ratios. As stated above, steranes and diasteranes have been shown to be less stable than hopanoids in the environment. While the Cape Gull samples appear to be more weathered than the other samples (see discussion below), they have a higher abundance of steranes and diasteranes than the EVO-matching samples. Because these compounds are known to be more susceptible to biodegradation than hopanes (Wang et al. 1994; Munoz et al. 1997; Wang et al. 2001), the scenario of biomarker degradation would therefore suggest so-far unknown degradation processes that lead to faster disappearance of hopanes than steranes and diasteranes.

Based on the GC-FID (Figure 6) and GC×GC-FID chromatograms (Figure 7), the 2012 sediment samples from Kashvik did not contain crude oil but instead a mid-range distillate such as diesel or jet fuel within the boiling range of n-C_{12} to n-C_{18} (see discussion below). Furthermore, the sample contained only trace levels of hopanoids (Figure 5), and no homohopanes or norhopane, which are typically found in petroleum. We therefore conclude that the Kashvik sediment did not contain detectable amount of EVO (relative to the detected mid-distillate oil), but instead was contaminated by diesel or jet-fuel oil prior to sampling in 2012. Note that in previous years of sampling, EVO was found at Kashvik (Irvine et al. 1999; Irvine et al. 2006; Irvine et al. 2007; Short et al. 2007). We hypothesize that at this location, EVO was completely degraded over the observed time scale of 23 years.

General Weathering Characteristics. We used GC-FID and GC×GC to investigate how oil weathered on shorelines over the 23 years since the EVOS. In samples from Cape Douglas, Kiukpalik Island, and Ninagiak Island only slight weathering occurred compared to EVO (Figure 6). The main weathering process at these three sites, where subsurface oil depths have not changed since 1994, has been evaporation, as can be seen by the removal of most compounds with carbon number $< C_{16}$ in GC-FID. For compounds $> C_{16}$, the alkane distribution is still similar to EVO, though slightly decreased (as can be seen by the relative increase of the unresolved complex mixtures, UCM). The samples from McArthur Pass show a similar behavior, though removal of n-alkanes is also apparent, most probably due to some degree of microbial degradation

(Figure 6e). Similar observations can be made by GC×GC (Figure 5). These observations suggest that oil-removing processes (such as biodegradation) were not effective during the 23 years the oil has been exposed to environmental conditions. In comparison, 18 months after the *Deepwater Horizon* oil spill, all samples found on beaches were severely weathered (Aeppli et al. 2012). This shows the importance of the environmental conditions (Gulf of Mexico *vs* Gulf of Alaska) as well as of the source oil (light sweet crude *vs* a medium sour crude), transformation of the oil (e.g., the conversion of EVO into mousse (Payne et al. 1991; Irvine et al. 1999)), and sheltering (EVO) in affecting the efficiency of oil-removing processes.

The Cape Gull samples are distinct from the above-discussed samples because that oil mostly consists of the UCM, with almost no resolvable alkane peaks visible in GC-FID (Figure 6f). The UCM at the Cape Gull site consists of cyclic alkanes (Figure 7). Biodegradation removes the straight and branched alkanes (Gros et al. 2013), leaving behind the cyclic alkanes that are more difficult to degrade. The oil residue at Cape Gull oil is therefore highly biodegraded. Note, however, that the biomarker analysis left open the possibility that a secondary contamination occurred rather than that EVO was not the source oil at Cape Gull.

GC-FID and GC×GC analysis of Kashvik Bay samples showed the presence of a mid-range distillate in the range of C_{12}-C_{18}, which is typical for a diesel or jet fuel oil but not for crude oil. While it is possible that the distillate is a secondary contamination and that EVO is mixed in the sample, it is not possible to disentangle the contributions of the distillate *vs* EVO in these samples.

Formation of Polar Oil Degradation Products. In previous studies investigating oil from the *Deepwater Horizon* spill, we found formation of a relatively recalcitrant non-GC amenable fraction during oil weathering (Aeppli et al. 2012; Hall et al. 2013). This fraction elutes in the resins and asphaltenes range on TLC-FID. Here we investigated the changes in these fractions for environmentally weathered EVO (Figure 8). For the samples from Cape Douglas, Kiukpalik Island, and Ninagiak Island that have mainly been weathered by evaporation rather than biodegradation, we did not see a major increase of the resins and asphaltenes fractions compared to EVO. Although the samples from McArthur Pass show an early degree of biodegradation (Figure 6e), we observed no significant increase in the resin or asphaltene fraction.

In contrast, we observed an increase in the resin and asphaltene fractions in the two samples from Cape Gull, where we hypothesized biodegradation. Note, however, that the evaluation of the biomarkers did not lead to a match with EVO for Cape Gull. As expected for a mid-range distillate (such as diesel or jet fuel oil), the Kashvik Bay samples have a very different resin and asphaltene profile than crude oil.

Comparison with Historical Data from these Sites. Most of the samples from 2012 and previous years had weathered very little beyond the initial evaporative weathering that occurred immediately following the *Exxon Valdez* oil spill (Table 3). Note that no samples could be collected from Kashvik or Kiukpalik Island in 2005. Volatility losses of benzene, toluene, ethylene, xylene, and the lower molecular mass aliphatic hydrocarbons resulted in losses of about 20% of the mass of the oil and increased the concentrations of most of the hydrocarbons remaining, including the PAH. Samples of EVO collected as mousse from the sea-surface of Prince William Sound 11 days following the oil spill (Short et al. 2007) contained substantial proportions of naphthalenes and of the less-substituted alkyl-homologues of dibenzothiophene and other PAH. This 11-day old sample was the first sample of the spilled oil collected from the sea surface that showed evaporative weathering changes and was properly documented, making it the most appropriate reference for initial composition of the oil as it impacted beaches in the Gulf of Alaska, as opposed to when it first entered the sea at Bligh Reef. Prior to 2012, proportions of PAH in all of the armored-beach samples, except for the Cape Gull samples, were similar. This indicates little additional weathering for these samples compared with the 11-day old sea-surface EVO samples. However, by 2005, the Cape Gull oil samples were so weathered that little of the initial complement of PAH was left, with the remaining PAH consisting mostly of 4-ring homologues. This weathering might have continued, leading to the observed biomarker pattern for the Cape Gull sample in 2012. The additional information provided by analyses of biomarkers for 2012 samples provides alternative hypotheses for the differences observed in weathering of the Cape Gull oil. The lack of observable oil at Kashvik in 2012, coupled with the lack of 2005 samples, means that we have a coarse view of the loss of EVO at that site. Planned analyses of historical samples by newer methods used in this chapter should allow us to more clearly define the changes in oil chemistry over this 23-year period after the spill.

Conclusions

In contrast to other oil spills, the oil at most of these shoreline sites in the Gulf of Alaska has persisted in a slightly weathered state for 23 years. It is compositionally similar to 11-day old oil from Prince William Sound, with similar PAHs but more loss of smaller *n*-alkanes. Besides evaporation, no major oil weathering was observed at four of the sites (Cape Douglas, Kiukpalik Island, Ninagiak Island, and McArthur Pass). Among those sites, only at McArthur Pass was some biodegradation evident. At the two remaining sites, more complex pictures of oil chemistry and loss have been revealed by the use of both GC-MS and newer chemical methods such as GCxGC and TLC-FID. At Cape Gull, more advanced oil degradation may have occurred; however, more in-depth biomarker analysis is necessary to confirm or exclude EVO as the source of oil there in years after 1989. For the Kashvik Bay site, where no oil was observed in 2012 for the first time since 1989, the hydrocarbon signature measured from sediments seems to be derived largely from secondary contamination by diesel or jet fuel oil. Overall, these results further our understanding of the chemical state and long-term weathering of stranded crude oil in sub-arctic environments.

Acknowledgments

We appreciate and acknowledge the initial work by Carl Schoch and Joel Cusick (National Park Service), the previous involvement in our studies of Jeffrey W. Short, and the support of T. Scott Smeltz, Carson Baughman, Carissa Turner, Erica Madison, Yvette Gillies, Sharon Kim, Jeff Mondragon, Jennifer Mondragon, Johnny Zutz, Marie Larsen, Jeep Rice, Billy Choate, Collette Choate, Bill Albrecht, John Rogers, Mike Yourkowski, Michael Parks, and Lydia Rabottini. Helicopter support was provided by Pathfinder Aviation and Maritime Helicopters. Funding was provided primarily by the *Exxon Valdez* Oil Spill Trustee Council, with additional support from the U.S. Geological Survey

(Alaska Science Center), the National Oceanic and Atmospheric Agency (Auke Bay Laboratories), the National Park Service and the DEEP-C consortium. The findings and conclusions are those of the authors and do not necessarily reflect the views or position of the *Exxon Valdez* Oil Spill Trustee Council. Any mention of trade names is for descriptive purposes only and does not represent endorsement by the U.S. government.

References

Aeppli, C., C. A. Carmichael, R. K. Nelson, K. L. Lemkau, W. M. Graham, M. C. Redmond, . . . C. M. Reddy (2012). "Oil weathering after the Deepwater Horizon disaster led to the formation of oxygenated residues." Environmental Science & Technology **46**(16): 8799-8807.

Arey, J. S., R. K. Nelson and C. M. Reddy (2007). "Disentangling oil weathering using GCxGC. 1. Chromatogram analysis." Environmental Science & Technology **41**(16): 5738-5746.

Baker, J. M., G. M. Leonardo and P. D. Bartlett (1993). "Long-term fate and effects of untreated thick oil deposits on salt marshes." Proceedings of the International Oil Spill Conference **1993**(No. 1): 395-399.

Burns, K. A., S. D. Garrity, D. Jorissen, J. MacPherson, M. Stoelting, J. Tierney and L. Yellesimmons (1994). "The Galeta oil spill. 2.Unexpected persistence of oil trapped in mangrove sediments." Estuarine Coastal And Shelf Science **38**(4): 349-364.

Carls, M. G. (2006). "Nonparametric identification of petrogenic and pyrogenic hydrocarbons in aquatic ecosystems." Environmental Science & Technology **40**(13): 4233-4239.

Carls, M. G., L. G. Holland, J. W. Short, R. A. Heintz and S. D. Rice (2004). "Monitoring polynuclear aromatic hydrocarbons in aqueous environments with passive low-density polyethylene membrane devices." Environmental Toxicology and Chemistry **23**(6): 1416-1424.

Charrie-Duhaut, A., S. Lemoine, P. Adam, J. Connan and P. Albrecht (2000). "Abiotic oxidation of petroleum bitumens under natural conditions." Organic Geochemistry **31**(10): 977-1003.

Corredor, J. E., J. M. Morell and C. E. Del Castillo (1990). "Persistence of spilled crude oil in a tropical intertidal environment." Marine Pollution Bulletin **21**(8): 385-388.

Daling, P. S., L.-G. Faksness, A. B. Hansen and S. A. Stout (2002). "Improved and standardized methodology for oil spill fingerprinting." Environmental Forensics **3**: 263-278.

Dauvin, J. C. (1998). "The fine sand Abra alba community of the Bay of Morlaix twenty years after the Amoco Cadiz oil spill." Marine Pollution Bulletin **36**(9): 669-676.

Eiserbeck, C., R. K. Nelson, K. Grice, J. Curiale and C. M. Reddy (2012). "Comparison of GC–MS, GC–MRM-MS, and GC×GC to characterise higher plant biomarkers in Tertiary oils and rock extracts." Geochimica Et Cosmochimica Acta **87**: 299-322.

Gaines, R. B., G. S. Frysinger, C. M. Reddy and R. K. Nelson (2007). Oil Spill Source Identification by Comprehensive Two-Dimensional Gas Chromatography (GC x GC). Oil Spill Environmental Forensics - Fingerprinting And Source Identification, Academic Press**:** 169-206.

Gros, J., C. M. Reddy, C. Aeppli, R. K. Nelson, C. A. Carmichael and J. S. Arey (2013). "A new biodegradation index for weathered oils based on saturated hydrocarbons: Insights from the Deepwater Horizon disaster." Environmental Science & Technology: in press.

Hall, G. J., G. S. Frysinger, C. Aeppli, C. A. Carmichael, J. Gros, K. L. Lemkau, . . . C. M. Reddy (2013). "Oxygenated weathering products of Deepwater Horizon oil come from surprising precursors." Marine Pollution Bulletin **75**(1-2): 140-149.

Hayes, M. O. and E. R. Gundlach (1979). "Role Of Dynamic Coastal Processes In The Impact And Dispersal Of The Amoco Cadiz Oil Spill (March 1978) Brittany, France." International Oil Spill Conference Proceedings **1979**(No. 1): 193-198.

Irvine, G. V., D. H. Mann and J. W. Short (1999). "Multi-year persistence of oil mousse on high energy beaches distant from the Exxon Valdez spill origin." Marine Pollution Bulletin **38**(7): 572-584.

Irvine, G. V., D. H. Mann and J. W. Short (2006). "Persistence of 10-year old *Exxon Valdez* oil on Gulf of Alaska beaches: the importance of boulder-armoring." Marine Pollution Bulletin **52**(9): 1011-1022.

Irvine, G. V., D. H. Mann and J. W. Short (2007). Monitoring lingering oil from the *Exxon Valdez* spill on Gulf of Alaska armored beaches and mussel beds sixteen years post-spill. *Exxon Valdez* Oil Spill Restoration Project Final Report (Restoration Project 040708). Anchorage, Alaska, U.S. Geological Survey, Alaska Science Center: 1-81.

Jackson, J. B. C., J. D. Cubit, B. D. Keller, V. Batista, K. Burns, H. M. Caffey, . . . E. Weil (1989). "Ecological effects of a major oil spill on Panamanian coastal marine communities." Science **243**(4887): 37-44.

Larsen, M. L., L. Holland, D. Fremgen, J. Lunasin, M. Wells and J. Short (2008). Standard operating procedures for the analysis of petroleum hydrocarbons in seawater, marine sediments, and marine faunal tissue at the Auke Bay Laboratory. Juneau, AK, NOAA, NMFS, Alaska Science Center, Auke Bay Laboratories: 81.

Leschine, T. M., J. McGee, R. Gaunt, A. van Emmerik, D. M. McGuire, R. Travis and R. McCready (1993). T/V Exxon Valdez oil spill : Federal On Scene Coordinator's Report, Washington, D.C. : U.S. Coast Guard : Dept. of Transportation.

Mille, G., D. Munoz, F. Jacquot, L. Rivet and J. C. Bertrand (1998). "The Amoco Cadiz oil spill: Evolution of petroleum hydrocarbons in the Ile Grande salt marshes (Brittany) after a 13-year period." Estuarine Coastal And Shelf Science **47**(5): 547-559.

Munoz, D., M. Guiliano, P. Doumenq, F. Jacquot, P. Scherrer and G. Mille (1997). "Long term evolution of petroleum biomarkers in mangrove soil (Guadeloupe)." Marine Pollution Bulletin **34**(11): 868-874.

National Research Council (2003). Oil in the Sea III:Inputs, Fates, and Effects, The National Academies Press.

Nelson, R. K., B. M. Kile, D. L. Plata and S. P. Sylva (2006). "Tracking the weathering of an oil spill with comprehensive two-dimensional gas chromatography." Environmental Forensics **7**: 33-44.

Payne, J. R., J. R. Clayton Jr, J. G. Daniel McNabb and B. E. Kirstein (1991). "*Exxon Valdez* oil weathering fate and behavior: Model predictions and field observations." Proceedings of the International Oil Spill Conference **1991**(No. 1): 641-654.

Payne, J. R. and C. R. Phillips (1985). Petroleum spills in the marine environment: The chemistry and formation of water-in-oil emulsions and tar balls. Chelsea, MI., Lewis Publishers.

Peacock, E. E., G. R. Hampson, R. K. Nelson, L. Xu, G. S. Frysinger, R. B. Gaines, . . . C. M. Reddy (2007). "The 1974 spill of the Bouchard 65 oil barge: Petroleum hydrocarbons persist in Winsor Cove salt marsh sediments." Marine Pollution Bulletin **54**(2): 214-225.

Peacock, E. E., R. K. Nelson, A. R. Solow, J. D. Warren, J. L. Baker and C. M. Reddy (2005). "The West Falmouth oil spill: ~100 kg of oil found to persist decades later." Environmental Forensics **6**(3): 273-281.

Peters, K. E., C. C. Walters and J. M. Moldowan (2005). The Biomarker Guide: Biomarkers and isotopes in the environment and human history, Cambridge University Press.

Peterson, C. H., S. D. Rice, J. W. Short, D. Esler, J. L. Bodkin, B. E. Ballachey and D. B. Irons (2003). "Long-Term Ecosystem Response to the Exxon Valdez Oil Spill." Science **302**(5653): 2082-2086.

Prince, R. C., E. H. Owens and G. A. Sergy (2002). "Weathering of an Arctic oil spill over 20 years: the BIOS experiment revisited." Marine Pollution Bulletin **44**(11): 1236-1242.

Reddy, C. M., T. I. Eglinton, A. Hounshell, H. K. White, L. Xu, R. B. Gaines and G. S. Frysinger (2002). "The West Falmouth oil spill after thirty years: The persistence of petroleum hydrocarbons in marsh sediments." Environmental Science & Technology **36**(22): 4754-4760.

Royer, T. C., J. A. Vermersch, T. J. Weingartner and H. J. Niebauer (1990). "Ocean circulation influencing the Exxon Valdez oil spill." Oceanography **3**(2): 3-10.

Schoch, G. C. (1993). 1992 Stranded Oil Persistence Study on Kenai Fjords National Park and Katmai National Park and Preserve. Coastal Program Division, National Park Service, Anchorage, Alaska.

Short, J. W. and R. A. Heintz (1997). "Identification of Exxon Valdez oil in sediments and tissues from Prince William Sound and the Northwestern Gulf of Alaska based on a PAH weathering model." Environmental Science & Technology **31**(8): 2375-2384.

Short, J. W., G. V. Irvine, D. H. Mann, J. M. Maselko, J. J. Pella, M. R. Lindeberg, . . . S. D. Rice (2007). "Slightly weathered *Exxon Valdez* oil persists in Gulf of Alaska beach sediments after 16 years." Environmental Science & Technology **41**(4): 1245-1250.

Short, J. W., T. J. Jackson, M. L. Larsen and T. L. Wade (1996). "Analytical methods used for the analysis of hydrocarbons in crude oil, tissues, sediments, and seawater collected for the natural resources damage of the Exxon Valdez oil spill." American Fisheries Society Symposium.

Short, J. W., T. L. Jackson, M. L. Larsen and T. L. Wade (1996). "Analytical methods used for the analysis of hydrocarbons in crude oil, tissues, sediments, and seawater collected for the natural resources damage assessment of the *Exxon Valdez* oil spill." American Fisheries Society Symposium **18**: 140-148.

Stout, S. A. and Z. Wang (2007). Chemical Fingerprinting of Spilled or Discharged Petroleum — Methods and Factors Affecting Petroleum Fingerprints in the Environment. Oil Spill Environmental Forensics - Fingerprinting And Source Identification, Academic Press**:** 1-53.

Vandermeulen, J. H. and J. G. Singh (1994). "Arrow oil spill, 1970-90: Persistence of 20-yr weathered bunker C fuel oil." Canadian Journal of Fisheries and Aquatic Sciences **51**(4): 845-855.

Venkatesan, M. I. (1988). "Occurrence and possible sources of perylene in marine sediments - a review." Marine Chemistry **25**: 1-27.

Ventura, G. T., B. Raghuraman, R. K. Nelson, O. C. Mullins and C. M. Reddy (2010). "Compound class oil fingerprinting techniques using comprehensive two-dimensional gas chromatography (GC × GC)." Organic Geochemistry **41**(9): 1026-1035.

Wang, Z., M. Fingas and G. Sergy (1994). "Study of 22-Year-Old Arrow Oil Samples Using Biomarker Compounds by GC/MS." Environmental Science & Technology **28**(9): 1733-1746.

Wang, Z. and M. F. Fingas (2003). "Development of oil hydrocarbon fingerprinting and identification techniques." Marine Pollution Bulletin **47**(9-12): 423-452.

Wang, Z., C. Yang, M. Fingas, B. Hollebone, U. H. Yim and J. R. Oh (2007). Petroleum Biomarker Fingerprinting for Oil Spill Characterization and Source Identification. Oil Spill Environmental Forensics - Fingerprinting And Source Identification, Academic Press**:** 73-146.

Wang, Z. D., M. Fingas, E. H. Owens, L. Sigouin and C. E. Brown (2001). "Long-term fate and persistence of the spilled Metula oil in a marine salt marsh environment - Degradation of petroleum biomarkers." Journal Of Chromatography A **926**(2): 275-290.

Wang, Z. D. and M. F. Fingas (2003). "Development of oil hydrocarbon fingerprinting and identification techniques." Marine Pollution Bulletin **47**(9-12): 423-452.

Wardlaw, G. D., J. S. Arey, C. M. Reddy, R. K. Nelson, G. T. Ventura and D. L. Valentine (2008). "Disentangling oil weathering at a marine seep using GCxGC: Broad metabolic specificity accompanies subsurface petroleum biodegradation." Environmental Science & Technology **42**(19): 7166-7173.

Wolfe, D. A., M. J. Hameedi, J. A. Galt, G. Watabayashi, J. Short, C. O'Claire, . . . D. Sale (1994). "The fate of the oil spilled from the Exxon Valdez." Environmental Science & Technology **28**(13): 560A-568A.

Table 1. Sampling location, date, and identifier (ABL sample identification number SIN, and WHOI sample identification) of samples investigated for this study.

SIN	WHOI ID	Date	Matrix	Location (site ID)	Lat / Long	Collection Method
	EVO		Crude oil	Exxon Valdez		
20120718	USGS-2012-001	3-Aug-12	Oiled sediment	Cape Douglas (2)	N 58°52.705'; W 153°17.679'	spoon
20120719	USGS-2012-002	3-Aug-12	Field blank	Cape Douglas (2)	N 58°52.705'; W 153°17.679'	
20120720	USGS-2012-003	3-Aug-12	Oiled sediment	Cape Douglas (2)	N 58°52.705'; W 153°17.679'	spoon
20120737	USGS-2012-004	4-Aug-12	Oiled sediment	Kiukpalik Island (3)	N 58°35.810'; W 153°33.187'	spoon
20120738	USGS-2012-005	4-Aug-12	Field blank	Kiukpalik Island (3)	N 58°35.810'; W 153°33.187'	
20120739	USGS-2012-006	4-Aug-12	Oiled sediment	Kiukpalik Island (3)	N 58°35.810'; W 153°33.187'	spoon
20120742	USGS-2012-007	5-Aug-12	Oiled sediment	Ninagiak Island (4)	N 58°27.31'; W 153°59.94'	spoon
20120743	USGS-2012-008	5-Aug-12	Oiled sediment	Ninagiak Island (4)	N 58°27.31'; W 153°59.94'	spoon
20120744	USGS-2012-009	5-Aug-12	Field blank	Ninagiak Island (4)	N 58°27.31'; W 153°59.94'	
20120745	USGS-2012-010	6-Aug-12	Oiled sediment	Kashvik (6)	N 57°54.45'; W 155°4.24'	spoon
20120746	USGS-2012-011	6-Aug-12	Oiled sediment	Kashvik (6)	N 57°54.45'; W 155°4.24'	spoon
20120747	USGS-2012-012	6-Aug-12	Field blank	Kashvik (6)	N 57°54.45'; W 155°4.24'	
20120748		7-Aug-12	Oiled sediment	Cape Gull (5)	N 58°14.12'; W 154°9.25'	spoon
	USGS-2012-013	7-Aug-12	Oiled sediment	Cape Gull (5)	N 58°14.12'; W 154°9.25'	spoon
20120749	USGS-2012-014	7-Aug-12	Field blank	Cape Gull (5)	N 58°14.12'; W 154°9.25'	
20120750	USGS-2012-015	7-Aug-12	Oiled sediment	Cape Gull (5)	N 58°14.12'; W 154°9.25'	spoon
20120751	USGS-2012-016	9-Aug-12	Oiled sediment	McArthur Pass (1)	N 59°28'; W 150°22.3'	spoon
20120752	USGS-2012-017	9-Aug-12	Oiled sediment	McArthur Pass (1)	N 59°28'; W 150°22.3'	spoon
20120753	USGS-2012-018	9-Aug-12	Field blank	McArthur Pass (1)	N 59°28'; W 150°22.3'	

Table 2. Model score matrix. Location is collection location; SIN is sample identification number; visible scores (‘vis’) denote visual presence (1) or absence (0) of oil; and scores are as described in methods. ‘Conc’ indicates concentration was the basis of the score, ‘comp’ indicates composition was the basis of the score. The mean is mean score and these were interpreted as oil (marked with one or more asterisks) or no oil (no). Biomarkers were examined in sediment to determine if the source was EVO. Samples were also assessed to determine if they were consistent with biogenic composition (Biog.) and background (Bg) (see Methods).

		Scores															
Location	**SIN**	vis	TPAH conc	TPAH comp	cAlk conc	cAlk comp	Odd comp	UCM conc	Triterp comp	Hopane comp	Sterane comp	mean	**Oil**	**EVO**	**Biogenic**		**Bg**
C. Douglas	20120718	1	1	1	0.85	0.89		1	0.89	0.95	0.93	0.95	**	yes	0	no	no
C. Douglas	20120720	1	1	1	0.85	0.82		1	1	1	1	0.96	***	yes	0	no	no
Kiukpalik Is	20120737	1	1	1	0.85	0.86		1	1	0.95	0.93	0.96	***	yes	0	no	no
Kiukpalik Is	20120739	1	1	1	0.85	0.89		1	1	0.95	0.93	0.96	***	yes	0	no	no
Ninagiak Is	20120742	1	1	1	0.85	0.84		1	1	0.95	0.93	0.95	***	yes	0	no	no
Ninagiak Is	20120743	1	0.75	1	0.85	0.72		1	0.89	1	1	0.91	**	yes	0	no	no
Kashvik	20120745	0	0	-0.67	0	0	-1		0.22	0	0.2	-0.14	no	no	-0.5	yes	yes
Kashvik	20120746	0	0	-0.67	0	0	-1		0.44	0.65	0.33	−0.03	no	no	-0.5	yes	yes
Cape Gull	20120748	1	0.75	0.92	0.75	0		1	0.44	0.9	0.2	0.66	*	no	0	no	no
Cape Gull	20120750	1	0.5	0.83	0.6	0			0.44	0.9	0.53	0.60	no	no	0	no	no
McArthur P.	20120751	1	0.75	1	0.85	0		1	1	1	0.93	0.84	*	yes	0	no	no
McArthur P.	20120752	1	1	1	0.85	0.79		1	0.89	0.95	0.93	0.94	**	yes	0	no	no

Table 3. Total polycyclic aromatic hydrocarbon (TPAH) concentrations and weathering parameter (*w*) with mean standard error (MSE) for samples collected from Gulf of Alaska Beaches between 1999 and 2012.

Location	**1989**			**1992**			**1994**			**1999**			**2005**			**2012**		
	TPAH (a) (mg/g)	w (b)	MSE	TPAH (mg/g)	w	MSE	TPAH (mg/g)	w	MSE	TPAH (mg/g)	w	MSE	TPAH (mg/g)	w	MSE	TPAH (mg/g)	w	MSE
McArthur Pass							0.51	2.45	0.14	0.31	1.65	0.25	0.50	3.43	0.16	0.46	1.30	0.144
McArthur Pass							1.99	2.67	0.35	1.23	1.21	0.11	0.51	1.72	0.14	2.56	-0.06	0.211
Cape Douglas				0.52	1.44	0.16	3.52	1.82	0.15	1.81	0.28	0.14	3.37	1.04	0.10	3.26	-0.96	0.367
Cape Douglas				0.83	1.05	0.15	3.43	2.03	0.16	0.31	0.58	0.24	2.50	0.97	0.09	1.02	0.07	0.247
Kiukpalik Is				1.24	0.74	0.14	2.84	1.49	0.13	1.70	-0.06	0.12				1.54	-0.59	0.263
Kiukpalik Is				2.80	0.46	0.18	2.75	1.53	0.10	1.21	0.45	0.10				2.68	-0.97	0.295
Ninagiak Is	3.00	1.58	0.16	1.10	1.42	0.12	2.12	1.39	0.28	1.18	1.47	0.07	1.64	1.76	0.10	1.29	-0.48	0.297
Ninagiak Is				2.21	0.64	0.20	2.37	0.82	0.17	0.40	1.83	0.13	1.03	3.87	0.09	0.37	1.32	0.083
Ninagiak Is													1.54	1.89	0.13			
Cape Gull	3.20	0.11	0.23	0.26	5.90	0.30	0.34	2.02	0.06	0.01	>30.00 (c)		ND (e)			0.266 (d)	9.45	0.720
Cape Gull				0.29	7.86	0.45	0.36	5.56	0.07	0.08	10.90 (c)		0.01	>30.00 (c)		0.082	8.94	0.797
Kashvik				0.58	1.12	0.11	1.81	0.84	0.22	0.63	0.04	0.08				0.00		0.144
Kashvik				4.00	0.49	0.14	3.09	0.47	0.20	0.78	0.10	0.16				0.00		0.211
Cp. Kubugakli	2.83	1.93	0.33															
Smith Island	10.85	0.87	0.09															
Snug Harbor	15.06	0.88	0.09															
Bay of Isles	17.48	0.23	0.13															

(a) Concentrations for TPAH are given as mg TPAH/g dry sample weight. (b) Weathering parameter *w* values are dimensionless (Short and Heintz 1997), with increasing values corresponding to greater weathering. (c) Values were estimated because of sample over-dilution. (d) Cape Gull sample taken slightly out of site area. (e) ND = not detected.

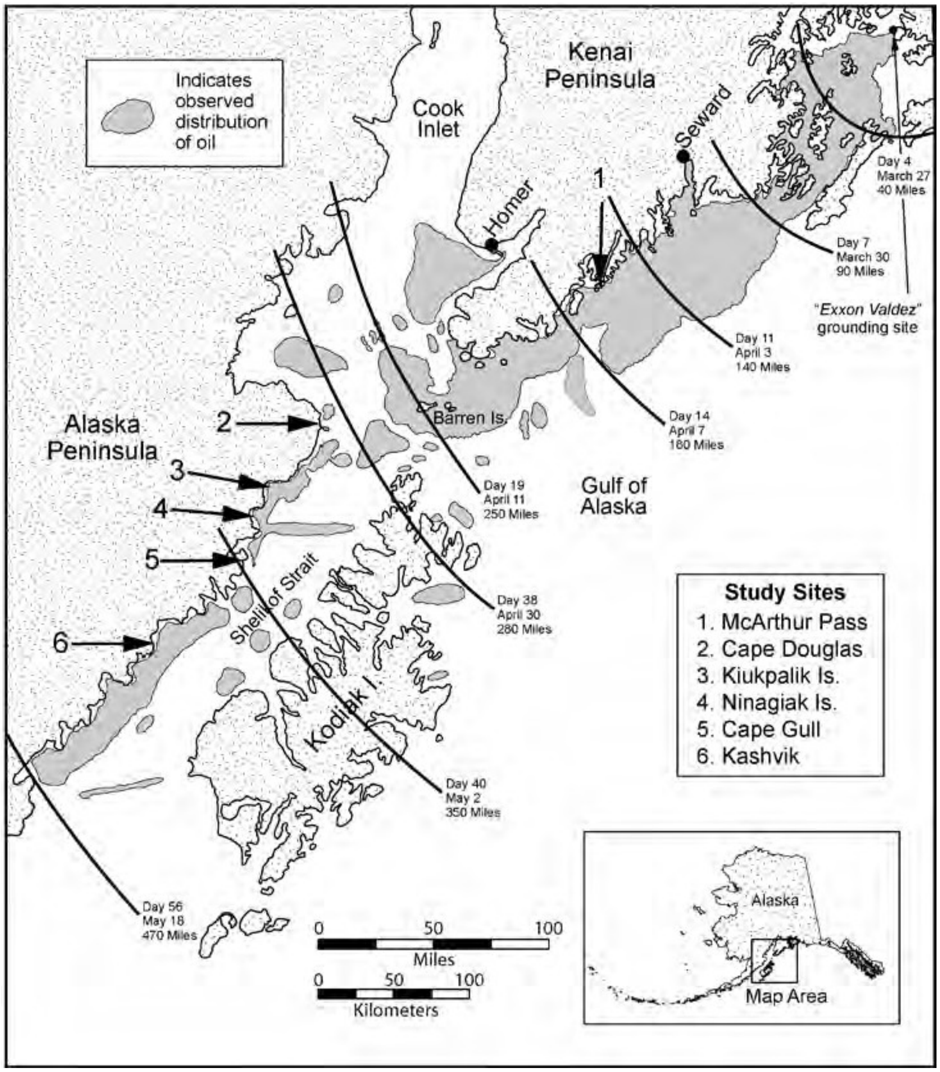

Figure 1. Map detailing location of study sites and the geographical distribution of oil through time following the 1989 *Exxon Valdez* spill. The oil distribution map is courtesy of the State of Alaska, Department of Environmental Conservation. Arrows point to the long-term monitoring sites discussed in this study: Site 1 is in Kenai Fjords National Park and Preserve (NP&P), and Sites 2-6 are in Katmai NP&P.

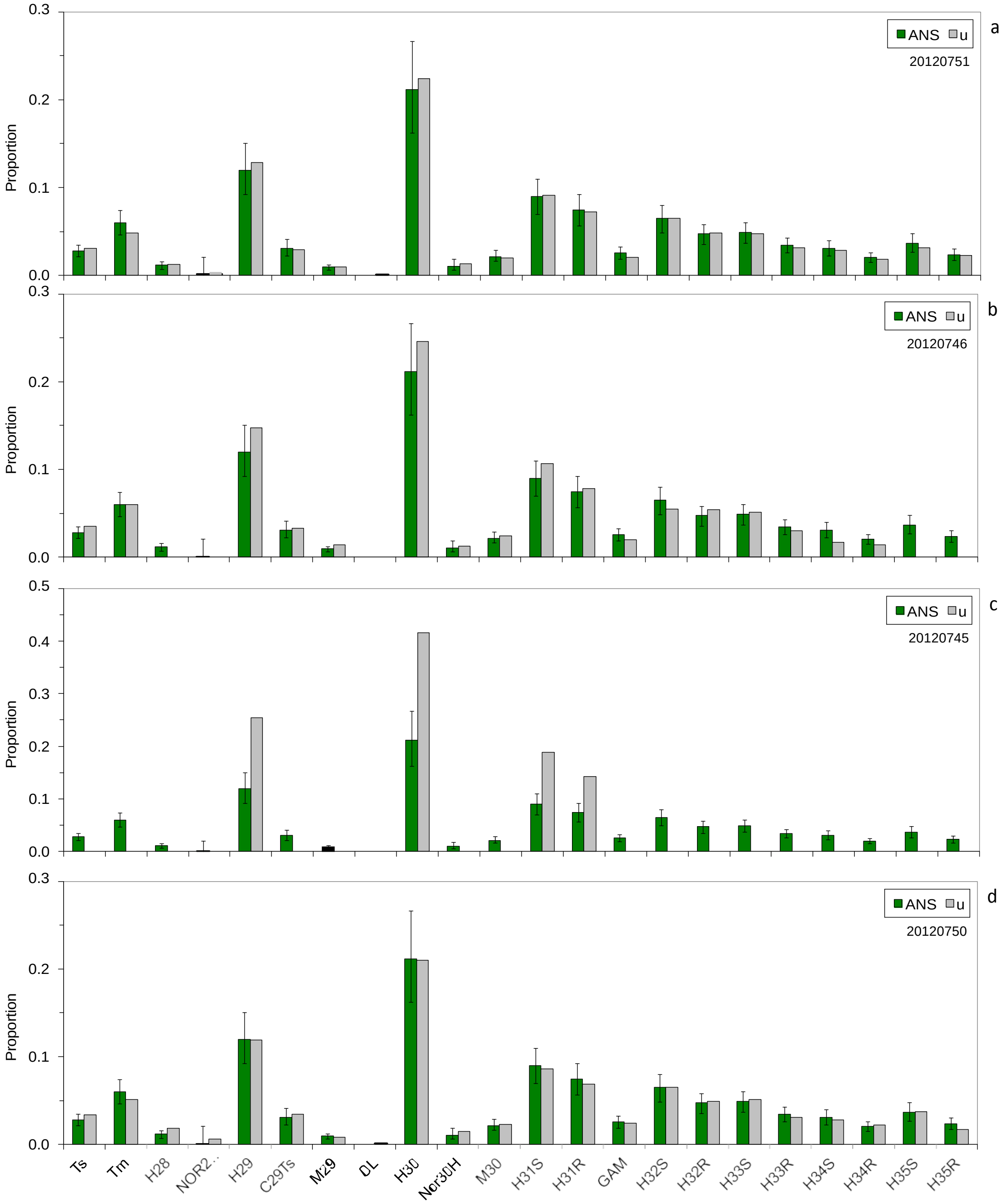

Figure 2. Hopane source-matching in 2012 GOA sediment. Green bars are source oil (i.e., EVO) with the vertical line representing the expected range of values; gray bars are the unknown sample in the comparison. (a) The McArthur Pass sediment (sample 70120751) is a match to EVO. (b) The fit for one of the Kashvik samples (sample 20120746) was similar to EVO, however, the overall hopane score was only 0.65 (Table 2). (c) The second sample from Kashvik (sample 20120745) is not consistent with EVO. Note that in 2012 Kashvik had no observable oil. (d) The Cape Gull sediment sample (sample 20120750) is consistent with EVO.

(a) normalized PAH

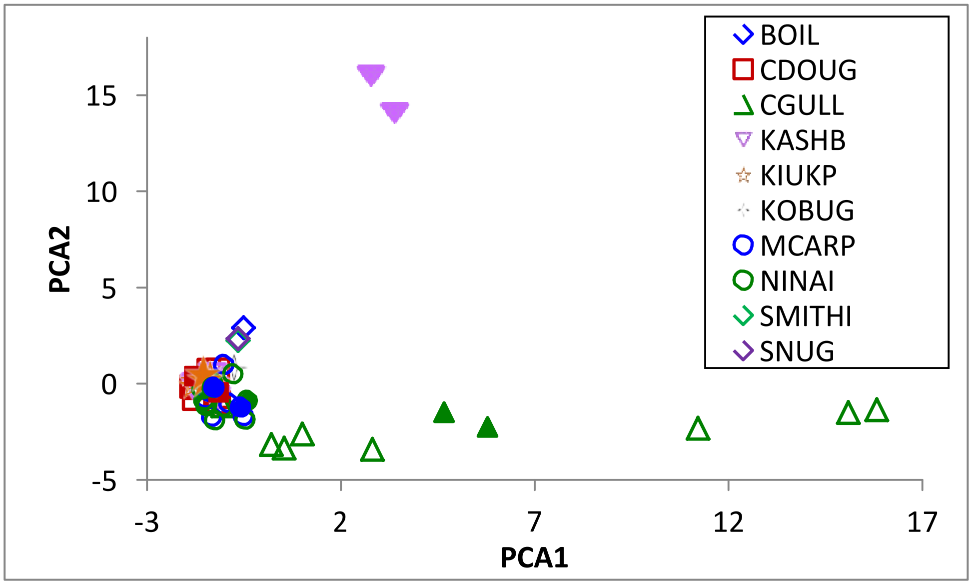

(b) normalized alkanes

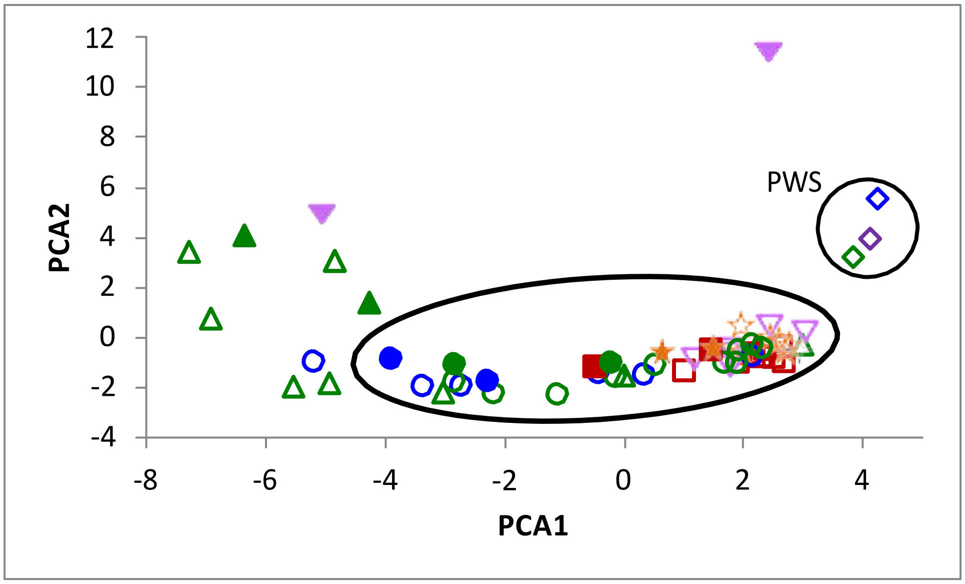

Figure 3. PCA of normalized PAH and normalized alkane data to determine source oil in sediment samples. Solid symbols identify samples collected in 2012; earlier samples are open. (a) normalized PAH results cluster around EVO, except for Cape Gull samples (green triangles) and the 2012 Kashvik samples (maroon triangles). (b) alkane results are similar but due to partial weathering of alkanes, larger scattering was observed.

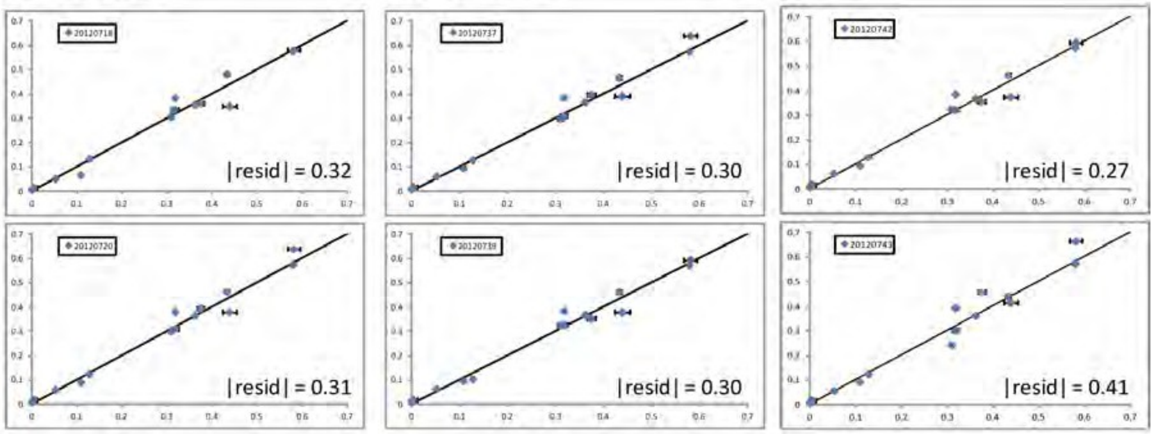

(a) Cape Douglas (b) Kiukpalik Is (c) Ninagiak Is

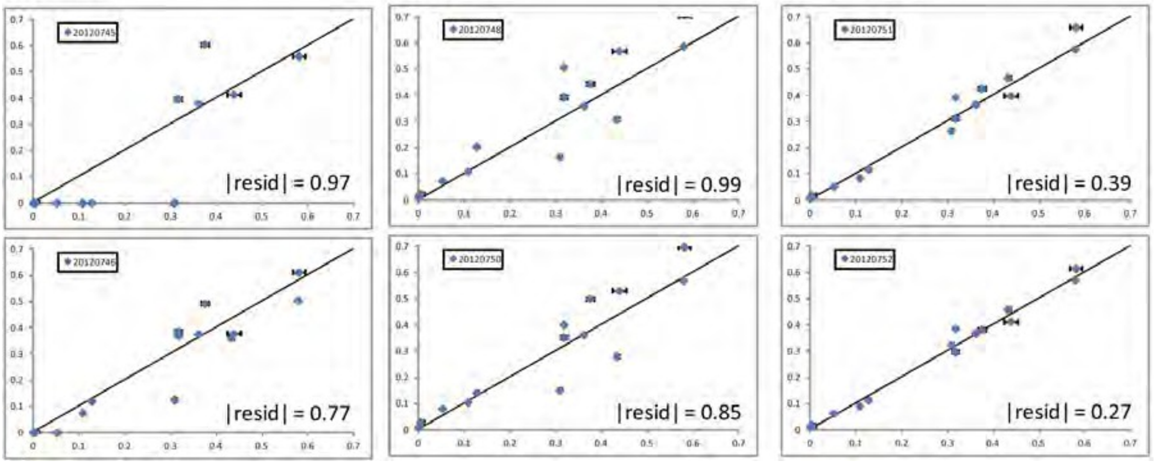

(d) Kashvik (e) Cape Gull (f) McArthur Pass

Figure 4. Nordtest biomarker ratio results of biomarker ratios determined from the oiled sediments collected in 2012. The biomarker ratios of the possible source oil (EVO) is given on the *x*-axis, the ratios of the samples on the y-axis. The values given are the residuals | resid |; a low value signified a probable match with EVO. The results from this test indicate that the oil at Kashvik and Cape Gull in 2012 is not likely EVO.

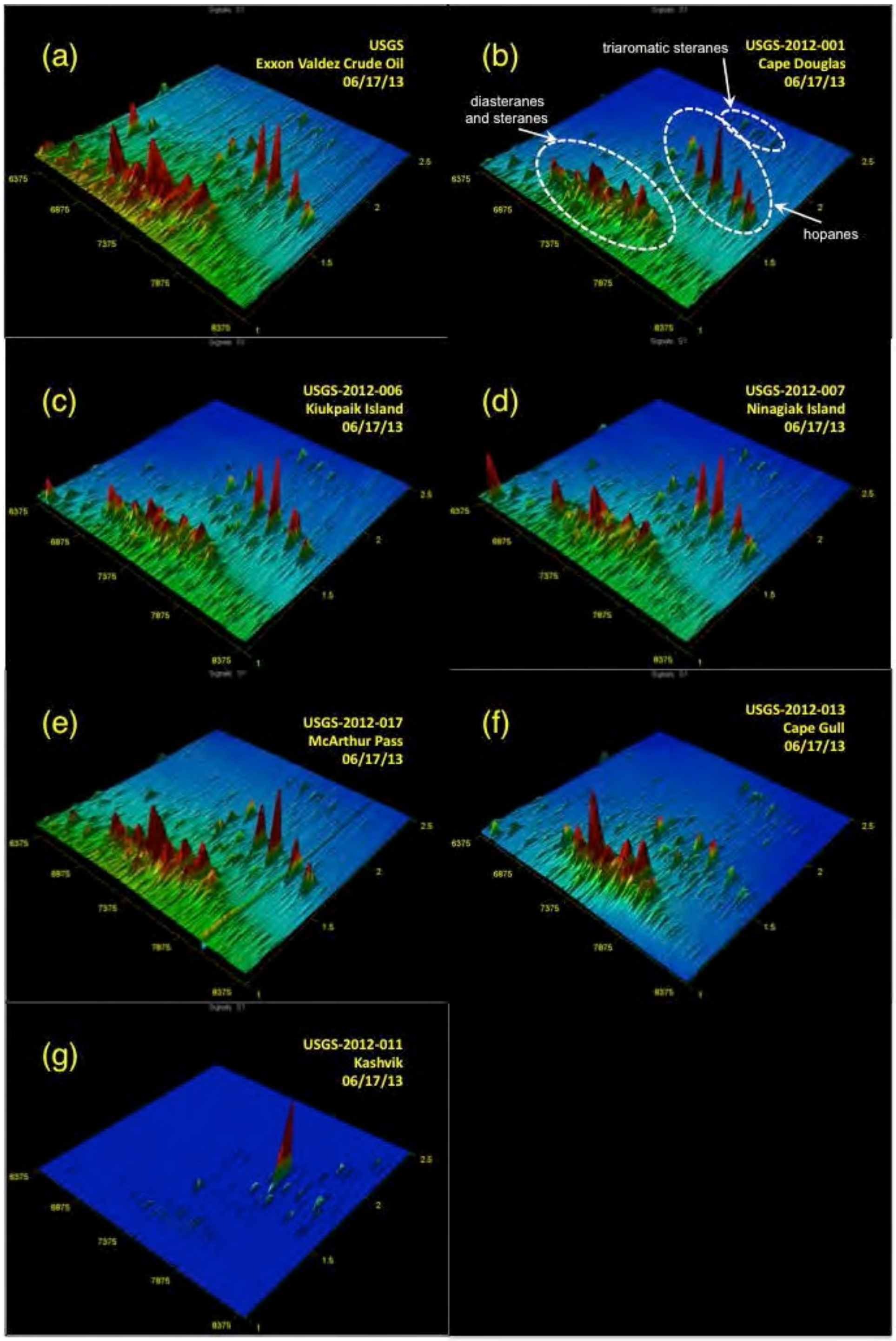

Figure 5. The biomarker region of a GCXGC-FID chromatogram for (a) EVO, and samples from (b) Cape Douglas, (c) Kiukpalik Is, (d) Ninagiak Is, (e) McArthur Pass, (f) Cape Gull, and (g) Kashvik.

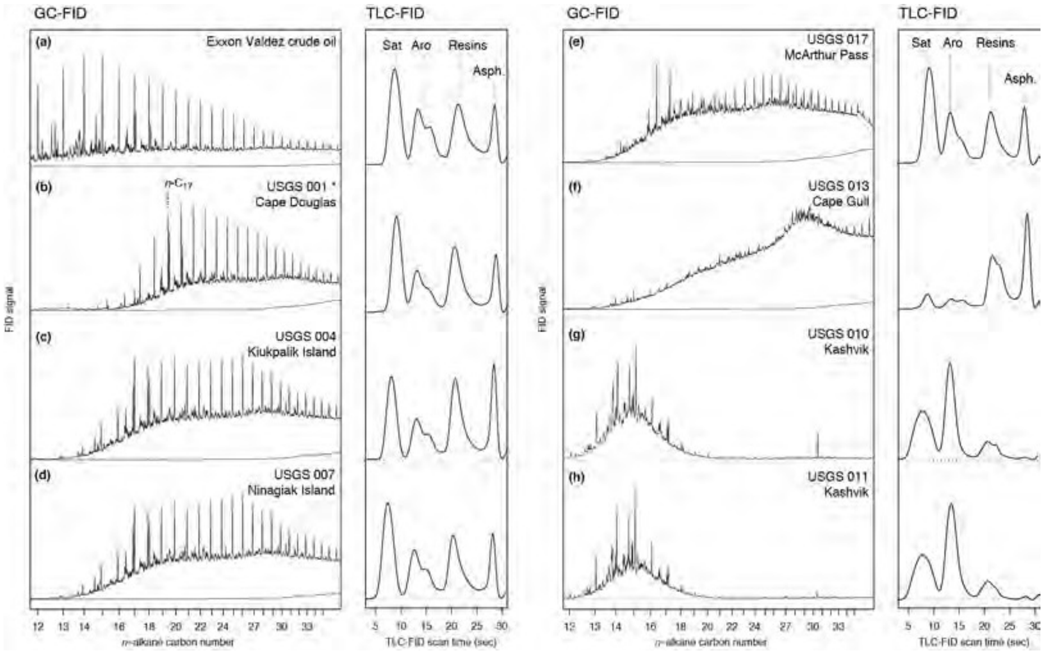

Figure 6. GC-FID and TLC-FID of (a) EVO and (b-h) sediment samples collected in 2012 at Cape Douglas, Kiukpalik Is, Ninagiak Is, McArthur Pass, Cape Gull and Kashvik. TLC-FID shows peaks for saturated (Sat), aromatic (Aro), resins and asphaltenes (Asph.). Note that resins and asphaltenes can also be referred to as “oxygenated hydrocarbons”. Note that the sample (b) was run with a slightly different GC-FID temperature program (see annotated n-C$_{17}$ for reference). Given is the blank run (baseline) as a grey line.

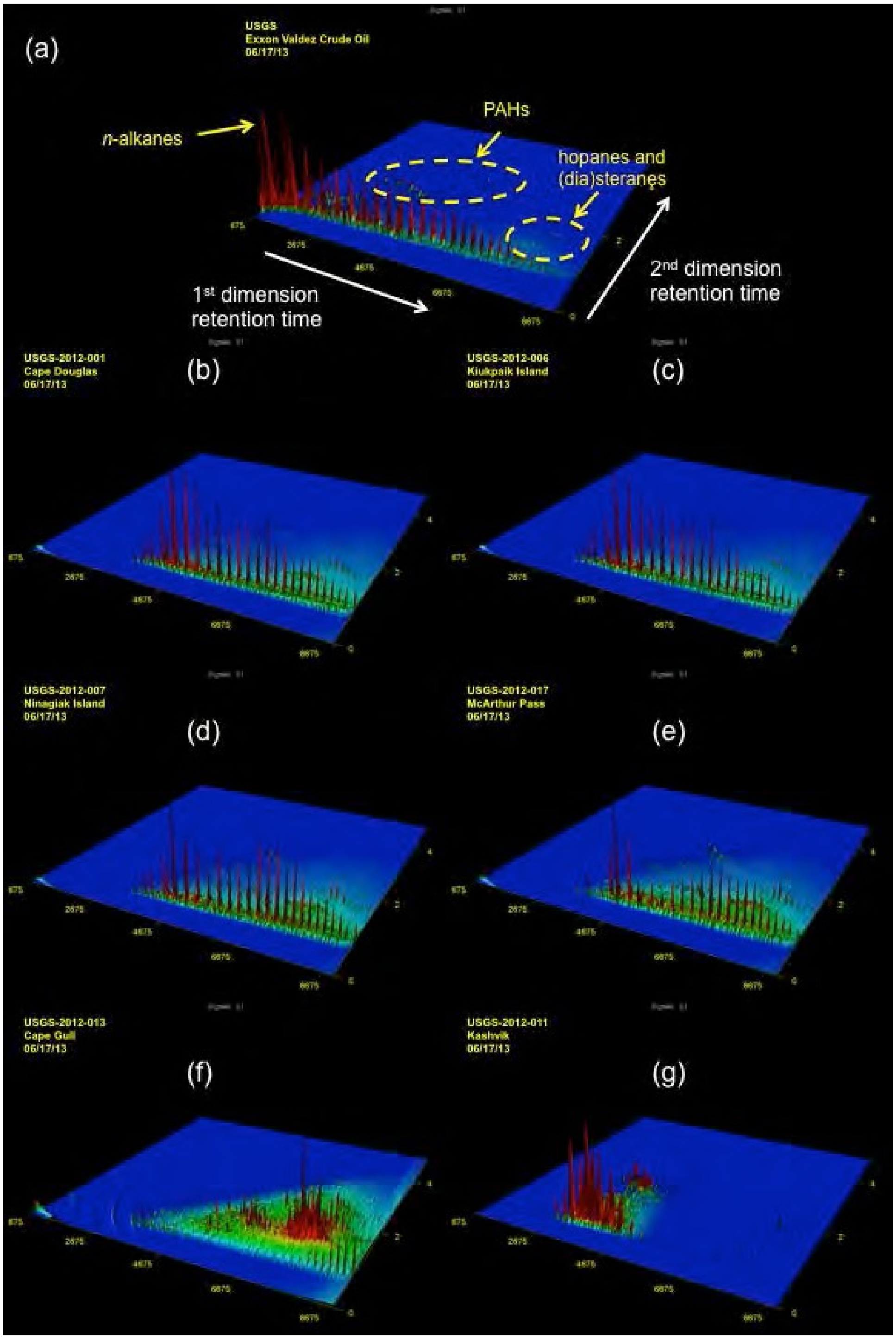

Figure 7. Mountain plot view of whole GC×GC chromatograms of (a) EVO, (b) Cape Douglas, (c) Kiukpalik Is, (d) Ninagiak Is, (e) McArthur Pass, (f) Cape Gull, (g) Kashvik.

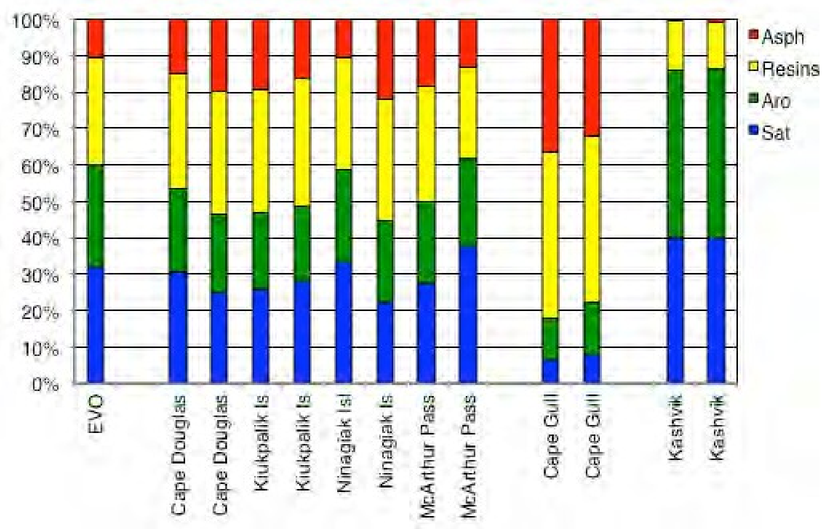

Figure 8. Results of TLC-FID for EVO and the 2012 site samples. Displayed are relative TLC-FID peak areas of saturated (Sat), aromatic (Aro) and two polar fractions, the resins and asphaltenes (Asph).

Supplemental 1 (Chapter 2)

Biomarker ratios for Nordtest as defined by Daling et al. (2002)

%27TS	100 x [27Ts(191)] / ([27Ts(191)] + [27Tm(191)])
%28ab	100 x [28ab(191)] / ([28ab(191)] + [30ab(191)])
%25nor30ab	100 x [25nor30ab(191)] / ([25nor30ab(191)] + [30ab(191)])
%29Ts	100 x [29Ts(191)] / ([29Ts(191)] + [30ab(191)])
%30o	100 x [300(191)] / ([300(191)] + [30ab(191)])
%30g	100 x [30G(191)] / ([30G(191)] + [30ab(191)])
%29ab	100 x [29ab(191)] / ([29ab(191)] + [30ab(191)])
%30d	100 x [30d(191)] / ([30d(191)] + [30ab(191)])
%32abS	100 x [32abS(191)] / ([32abS(191)] + [32abR(191)])
%27 dia	100 X ([27dbS(217)] + [27dbR(217)]) / ([27dbS(217)] + [27dbR(217)] + [27bbR(217)] + [27bbS(217)])
%29aaS	100 x [29aaS(217)] / ([29aaS(217)] + [29aaR(217)])
%29bb	100 x ([29bbR(217)] + [29bbS(217)]) / ([29bbS(217)] + [29bbR(217)] + [29aaS(217)] + [29aaR(217)])
%27bbSTER	100 x [27bb(S + R)(218)] / ([27bb(S + R)(218)] + [28bb(S + R)(218)] + [29bb(S + R)(218)])
%28bbSTER	100 x [28bb(S + R)(218)] / ([27bb(S + R)(218)] + [28bb(S + R)(218)] + [29bb(S + R)(218)])
%29bbSTER	100 x [29bb(S + R)(218)] / ([27bb(S + R)(218)] + [28bb(S + R)(218)] + [29bb(S + R)(218)])

APPENDICES – Chapter 1

Appendix A: Study Sites

Appendix B: GPS Coordinates

Appendix C: Supplemental 1

Appendix D: Surface Oil Percent Covers

Appendix E: Site Subsurface Oil Measurements

APPENDIX A. STUDY SITES

Cape Douglas

The Cape Douglas site (58^o 52' 44.8" N, 153^o 17' 32.9" W) is located on the peninsula that forms the northern side of Sukoi Bay. It is on an exposed beach facing northeast into lower Cook Inlet. In the low and middle intertidal zones, boulders overlie a wave-planed, bedrock surface terrace. Between the boulder armor at the surface and the bedrock beneath are 10-50 cm of cobble gravel. Higher on the shoreface small boulders and cobbles form a steep storm berm topped by masses of drift logs whose presence attest to the strength of storm waves here.

View northwest across the Cape Douglas site in August 2005. The boulders in the foreground are 75-150 cm in long diameter.

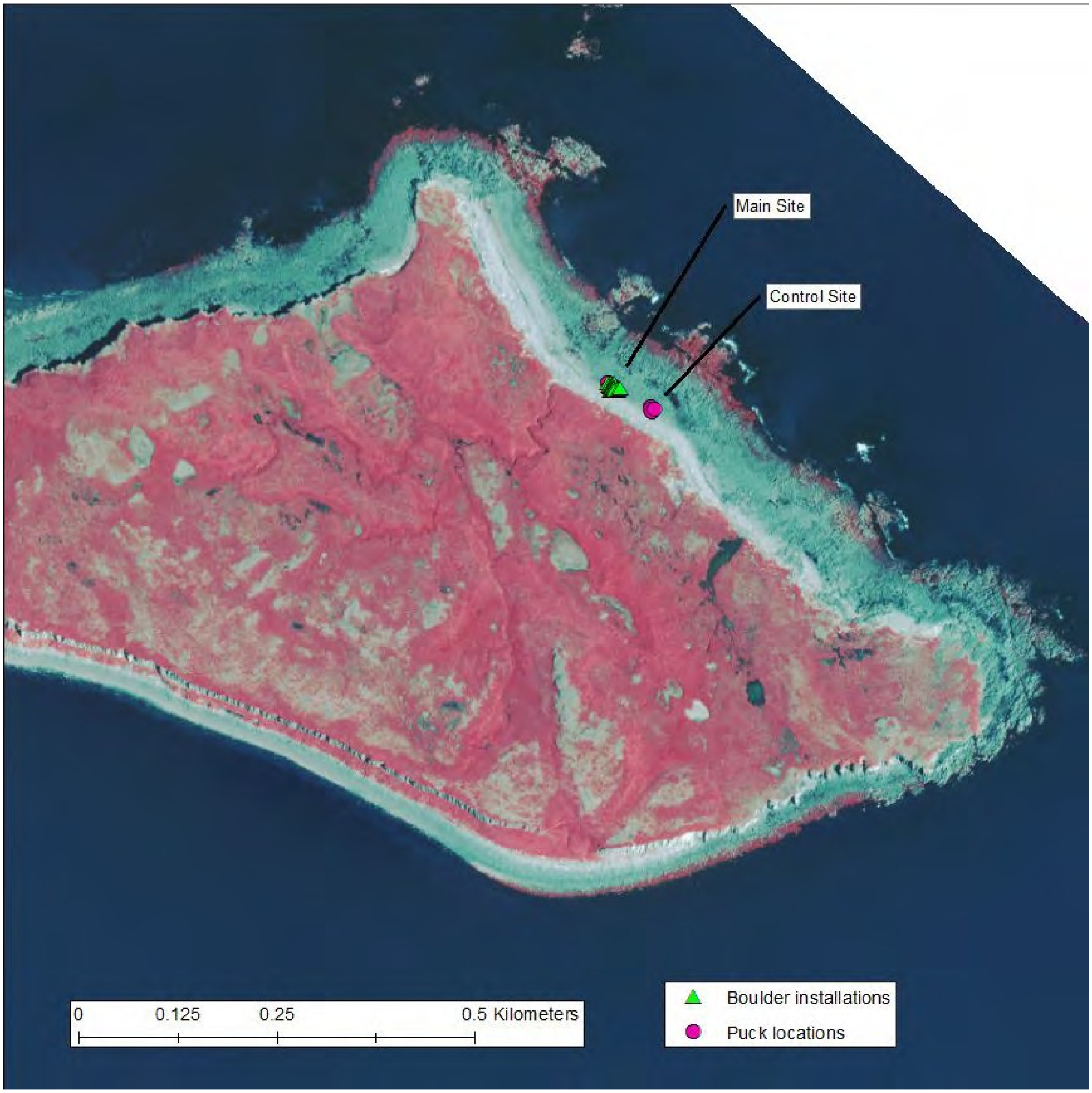

Vertical, color-infrared, aerial photograph of the peninsula where the Cape Douglas site is located. Sukoi Bay is the water body to the south. Note the lack of trees and even tall shrubs on this windswept peninsula. The prominent light-grey band along the shoreline behind the study site is the storm berm. This berm has dammed streams behind it. The "Control Site" is where PEMD samplers were deployed in 2012.

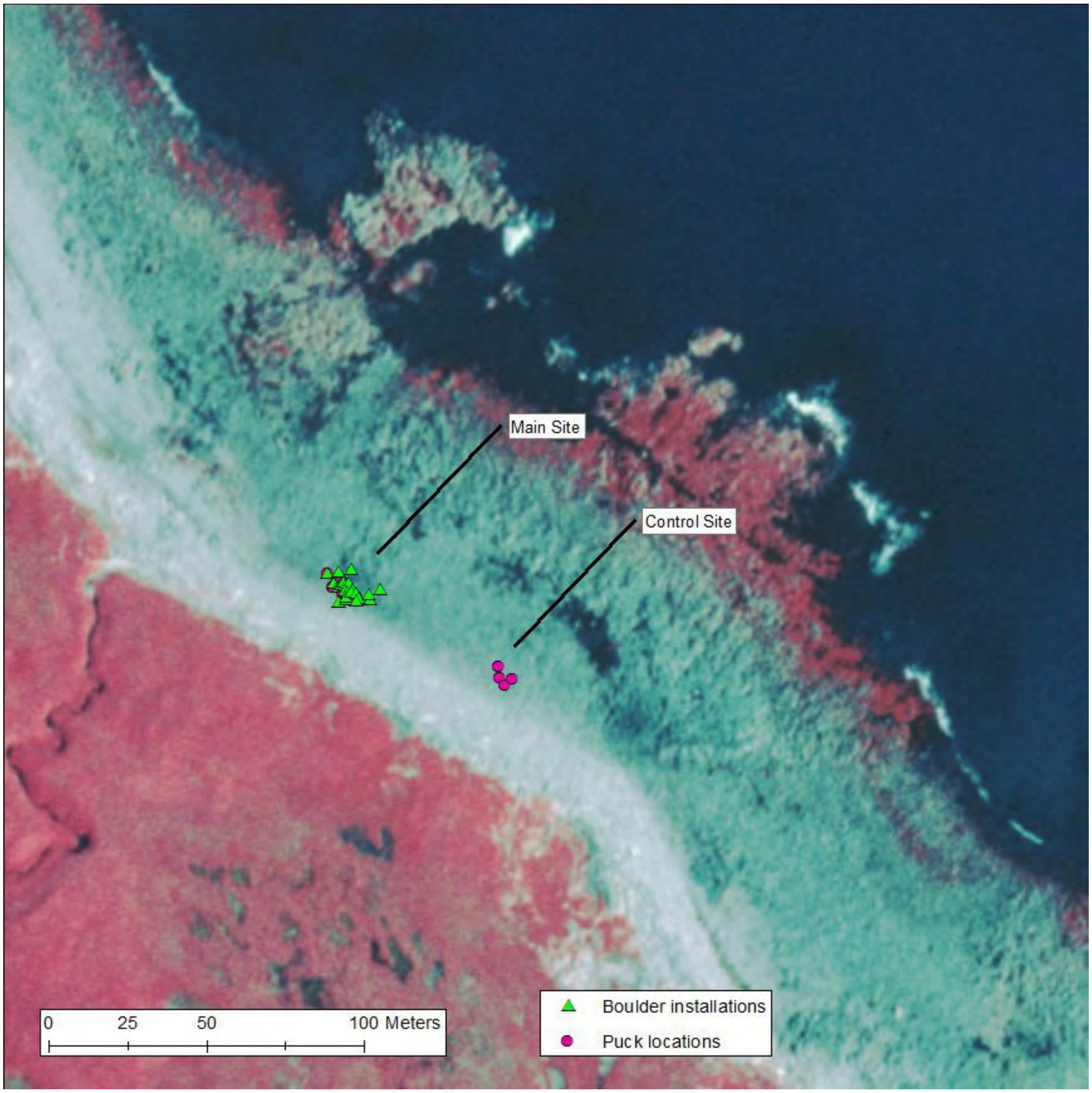

Blowup of the same aerial photograph showing locations of bolted boulders (green), PEMD samplers (red), and PEMD-control samplers (purple). Again, note the white band of the storm berm, the green hue of the lower-angled portion of the beach where boulder armors are well-developed, and the pink zone representing sea weed in the lower intertidal zone.

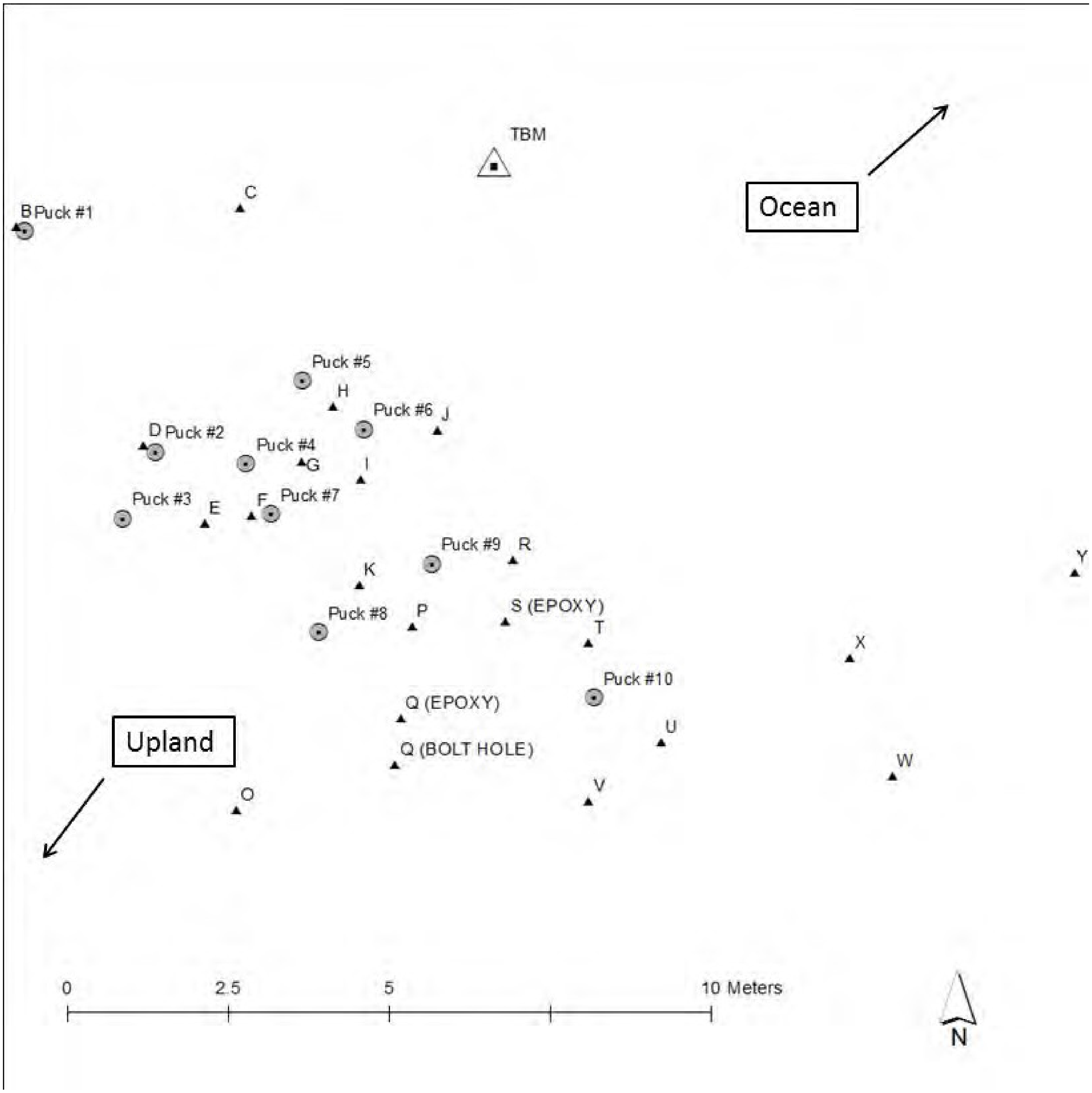

GPS-based map showing locations of bolts and PEMD samplers at the Cape Douglas site in 2012. "TBM" is the position of the surveying instrument. See Appendix B for exact GPS locations.

Kiukpalik Island

The Kiukpalik Island site (58° 35' 51.4" N, 153° 33' 3.7"W) faces Shelikof Strait on the southeastern shore adjacent to the only grove of Sitka spruce on the island. It has a less-developed geomorphology than the Cape Douglas site in that it lacks a well-developed storm berm. Instead, storm waves have eroded a bedrock scarp several meters in height along the top of the beach. The lower and middle intertidal zones are mainly exposed bedrock. Locally quarried boulders typically 1-2 m in long diameter have been thrown up along the base of the high tide scarp. In places these boulders form a well-integrated armor, in other places they are jumbles of boulders and driftwood.

View northeast across the Kiukpalik Island site in 2012. The dark color of the boulders near the person in blue is *Verrucaria* lichen.

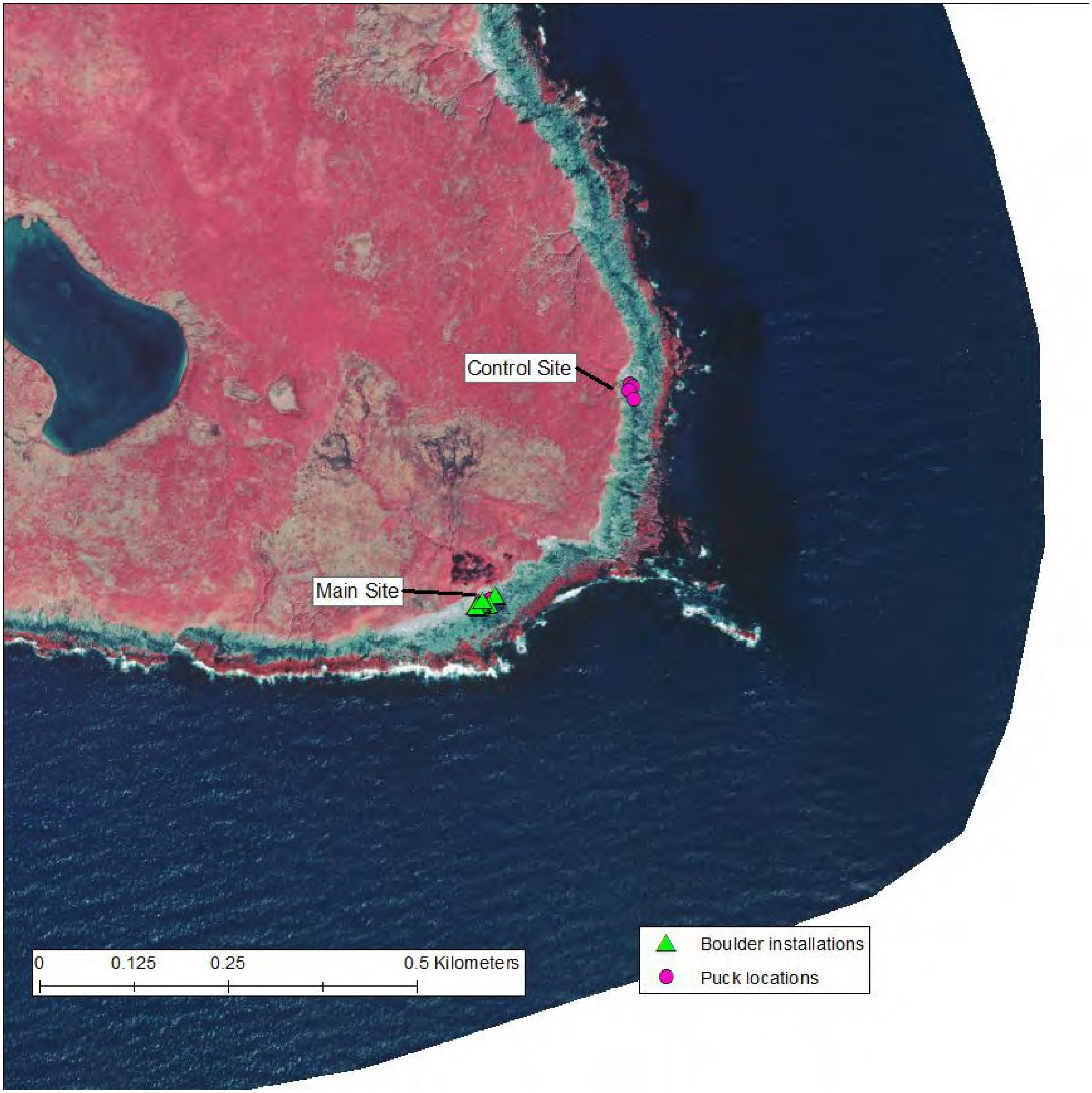

Color-infrared, vertical aerial photograph showing the location of bolted boulders (green) and of the control PEMD samplers (purple) at the Kiukpalik Island site in 2012.

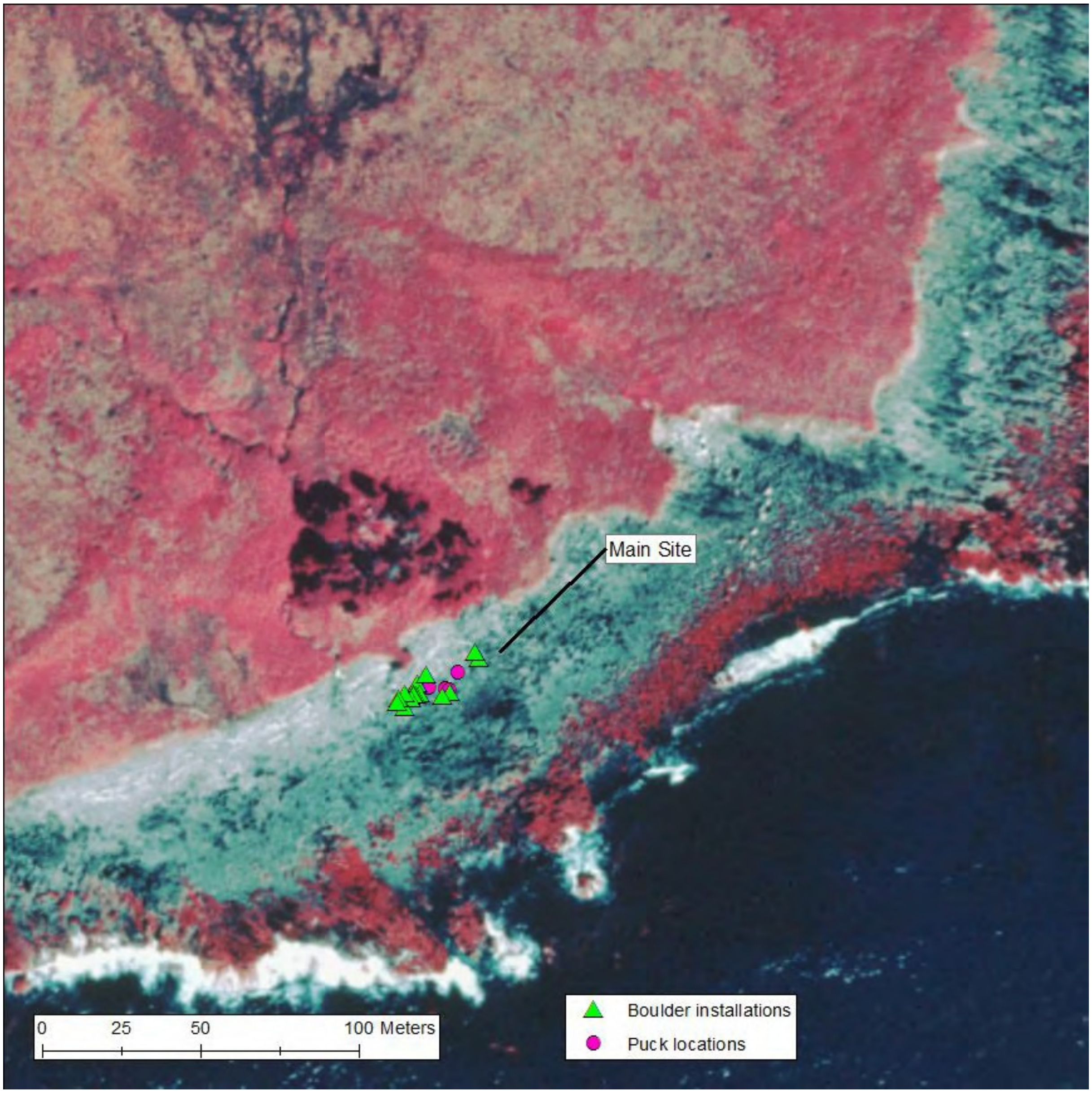

Blowup of the vertical aerial photograph of the Kiukpalik Island site. The dark objects onshore of the bolted boulders are spruce trees. Abundant driftwood is visible in the supratidal zone. Widespread seaweed cover in the lower intertidal zone appears as a red band nearest the sea.

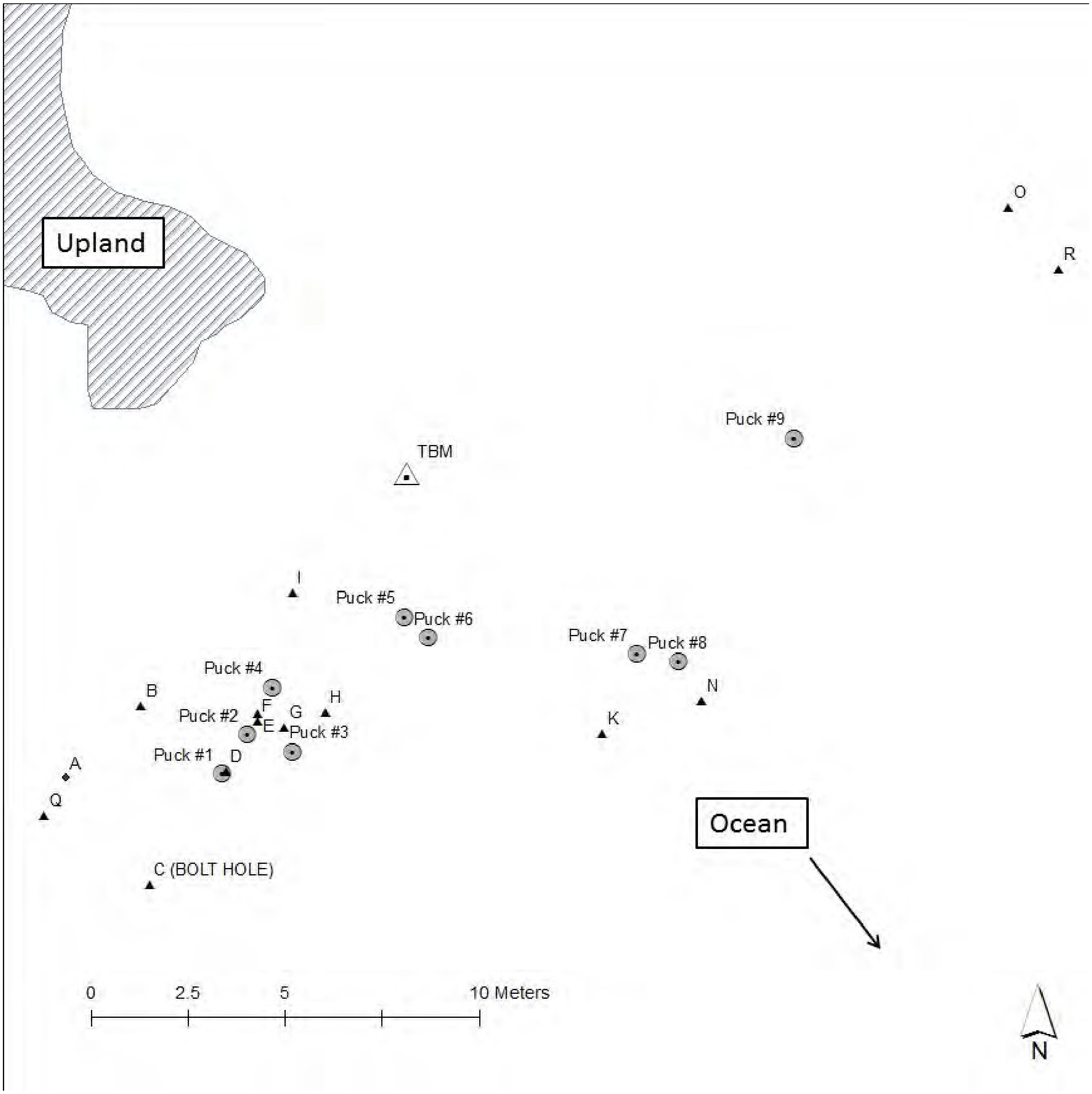

GPS-mapped positions of the marker bolts and the PMDS samplers in 2012 at the Kiukpalik Island site. See Appendix B for exact GPS locations.

Ninagiak Island

This site (58°27'17.54"N, 153°59'50.69"W) lies on the southeast shore of Ninagiak Island in Hallo Bay. The island is steep and densely vegetated with grasses and forbs. It is a sea-bird nesting island.

The Ninagiak Island site is located in a rocky cove. A gap in the cliffs to the rear opens onto a pebble beach marked by a prominent sea arch. The cliffs are covered with nesting gulls. There is no storm berm developed on this beach. As seen in this view taken in August 2012, boulders are crudely imbricated in the middle itertidal zone. The boulder armor is not particularly well-developed and overlies a rugged bedrock surface at shallow depth.

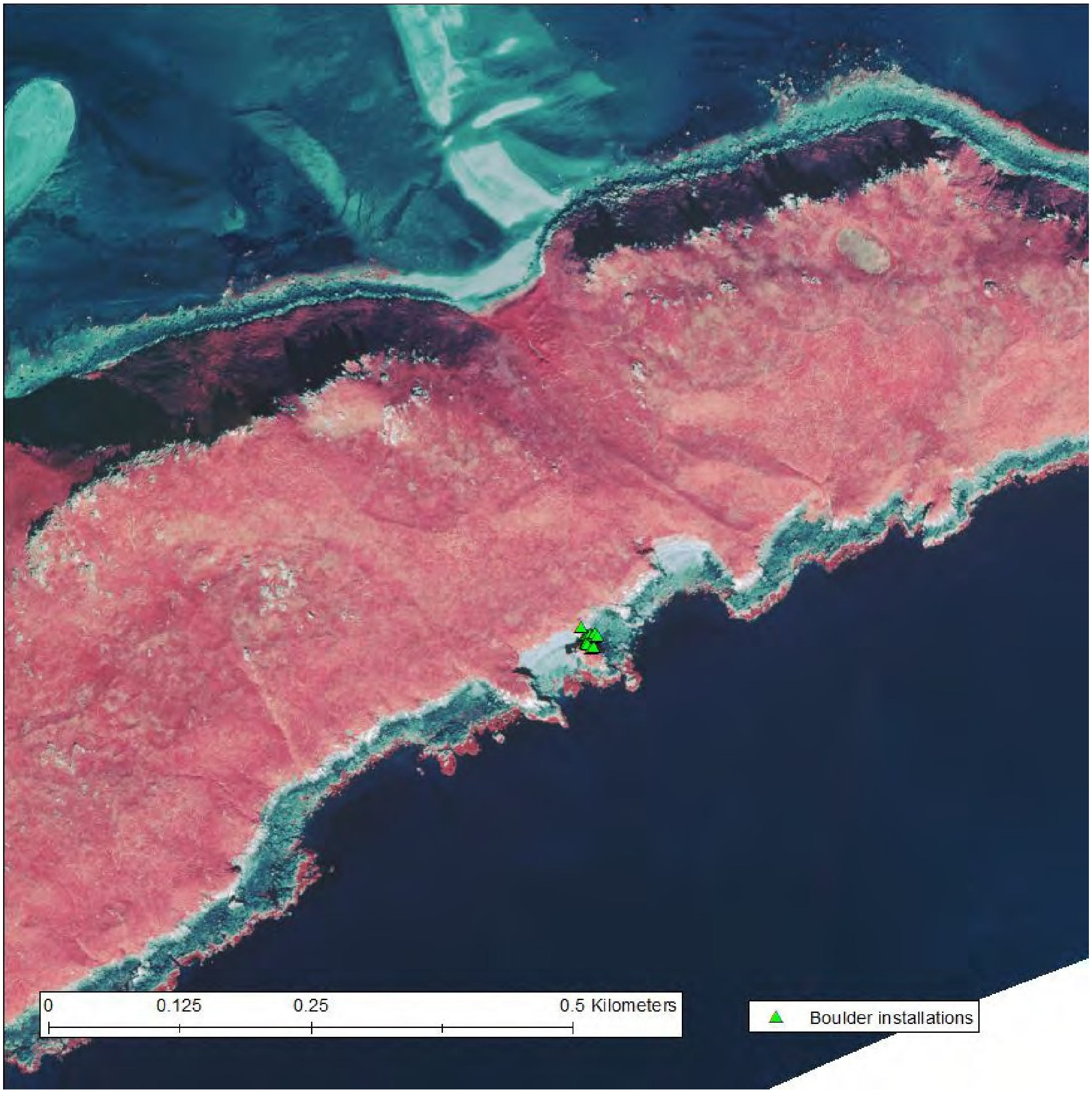

Color-infrared, vertical aerial photograph of the Ninagiak Island site. Locations of the marker bolts are shown in green.

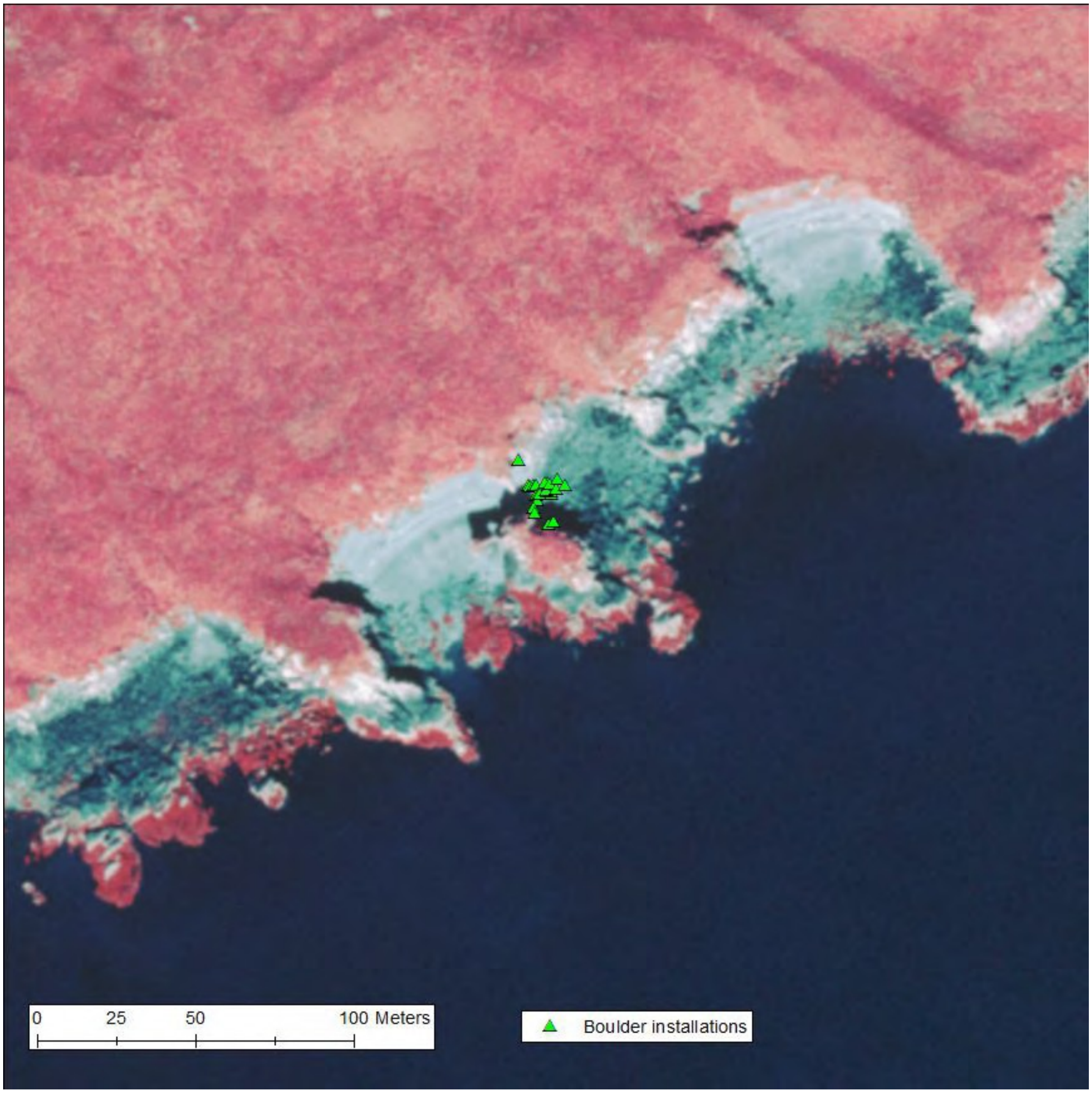

Blow-up of the color-infrared photograph showing the locations of the bolted boulders at the Ninagiak Island site. Note the contrast between the boulder beach we studied and the more sheltered, pebble beach to the west. This western beach was probably the source of the pebble sheet that obscured many boulders at this site at the time of the 2005 survey.

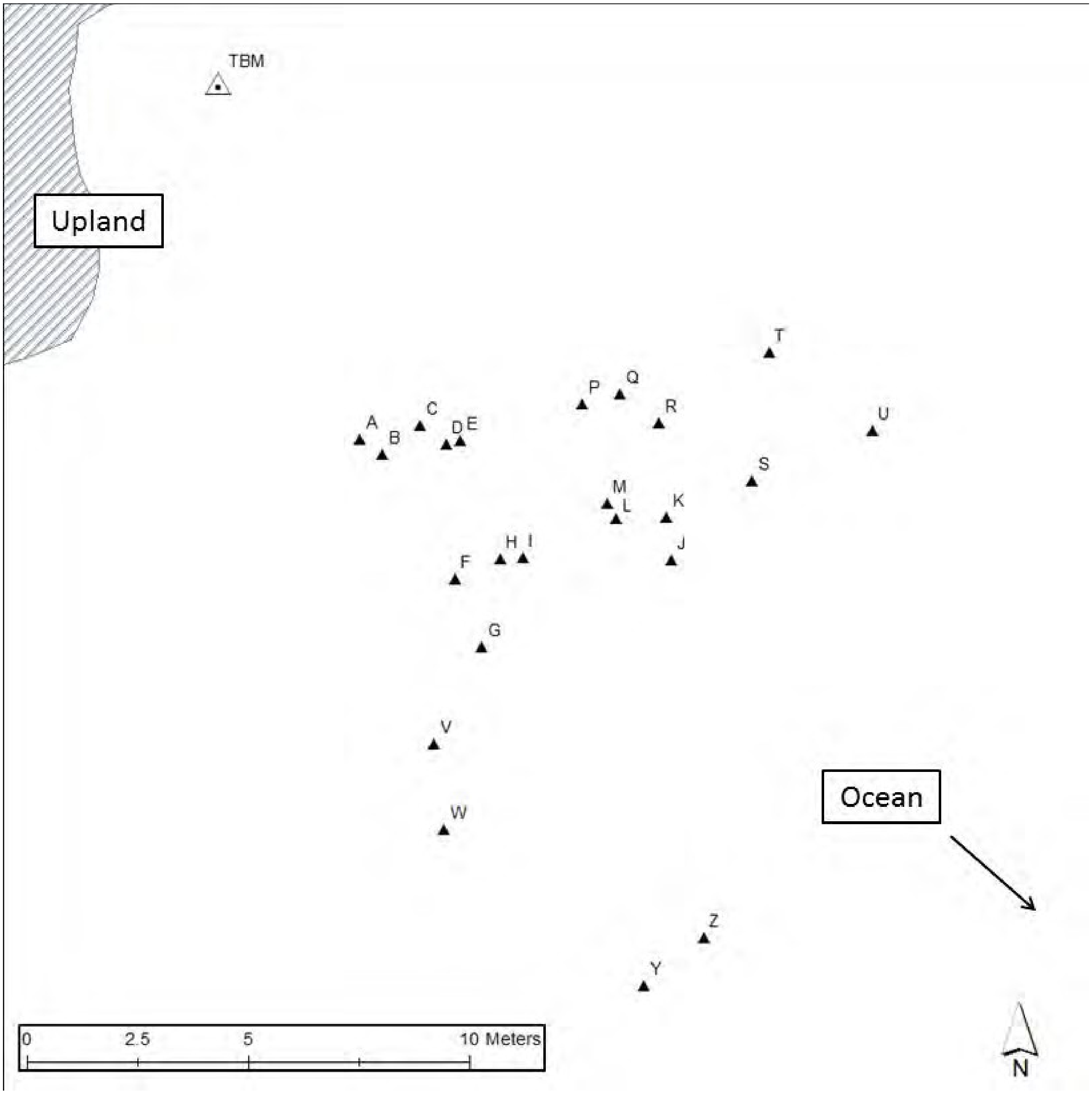

GPS-based map of the marker bolts at the Ninagiak Island site. See Appendix B for exact GPS locations.

Cape Gull

The Cape Gull site (58°14'6.87"N, 154° 9'8.69"W) is located in a relatively sheltered cove on the southern shore of Kaflia Bay. Locally quarried boulders, cobbles, and pebbles form the beach here. The storm berm is poorly developed. Boulders are smaller than at the preceding three sites with long diameters typically 30-100 cm. The surface armor is less developed here, and bedrock underlies the beach at shallow depths.

View over the Cape Gull site in August 2012.

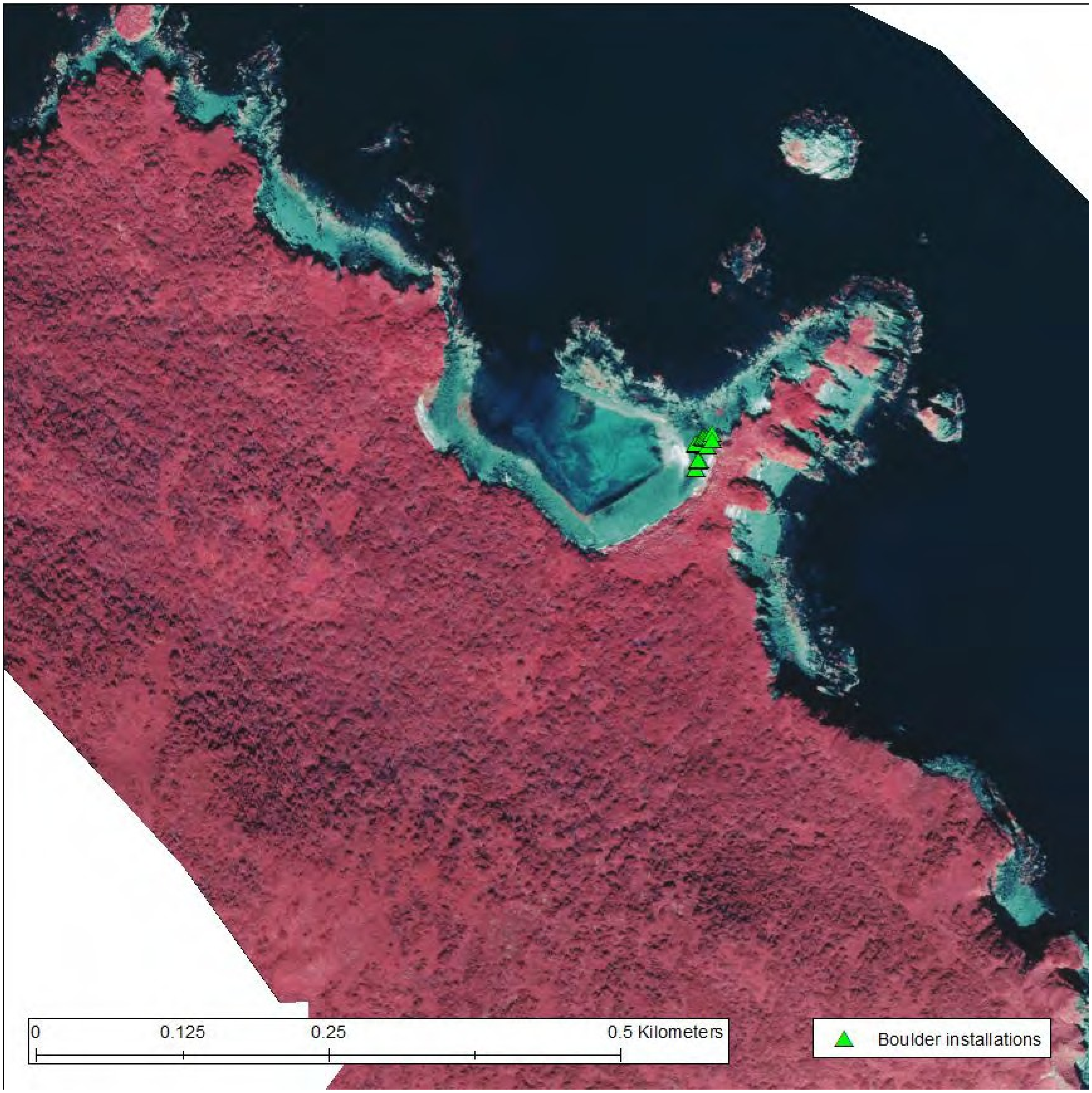

Color-infrared, vertical aerial photograph of the Cape Gull site showing locations of bolted boulders (green).

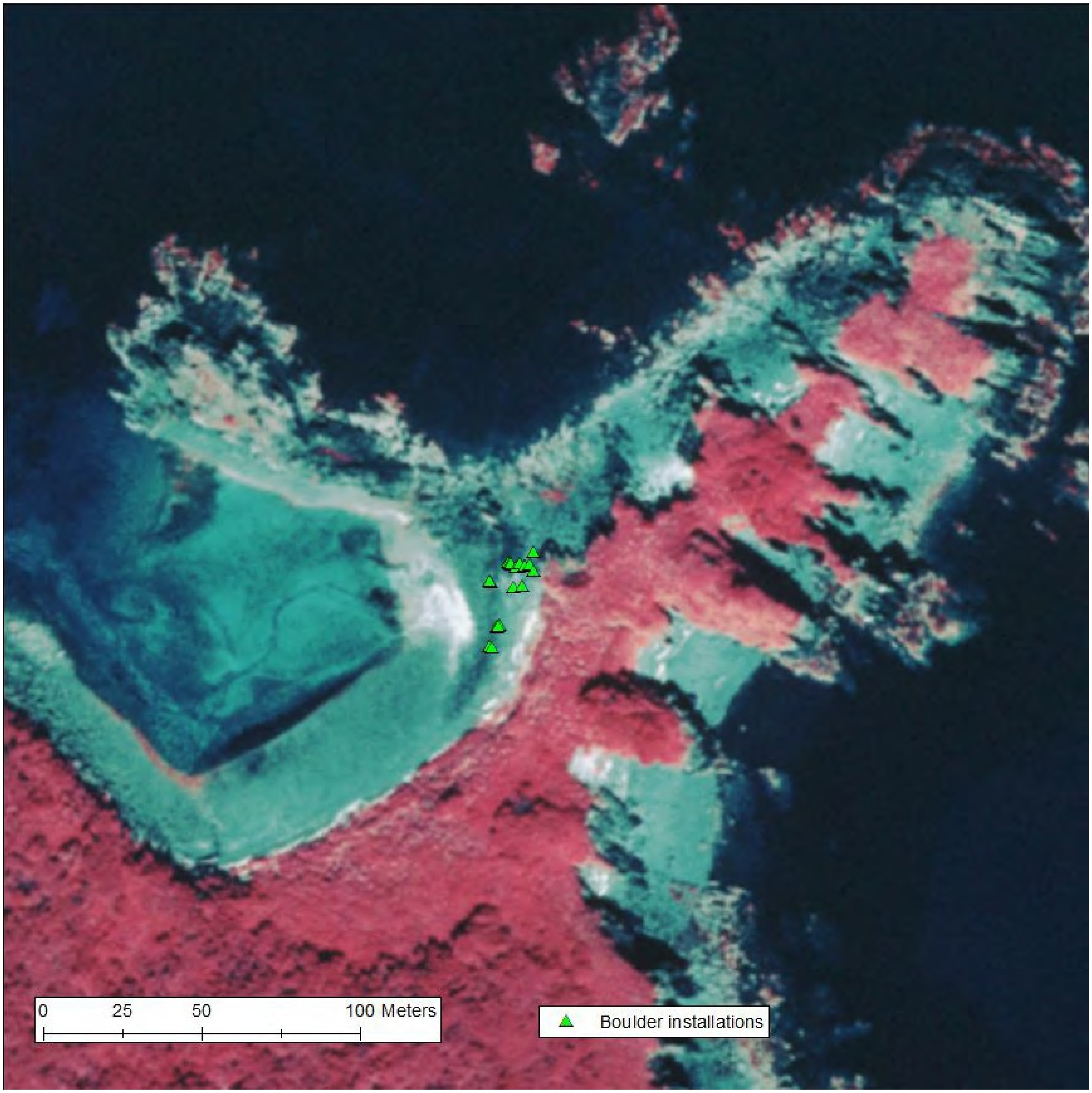

Closer view of the Cape Gull site. Bolted boulders are green triangles.

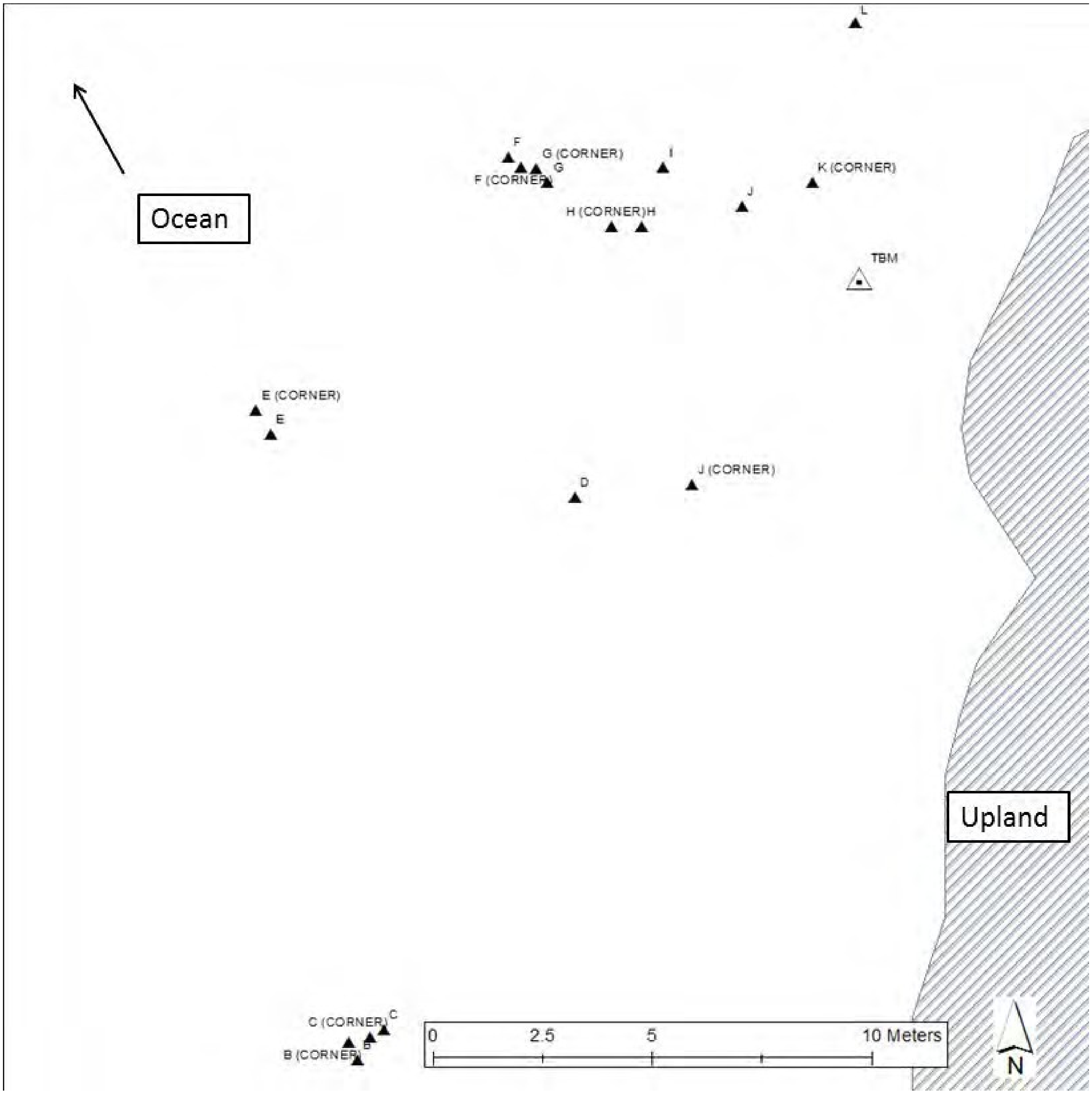

GPS-based map of bolt locations at the Cape Gull site. See Appendix B for exact GPS locations.

Kashvik Bay Site

The Kashvik Bay site (57°54'26.79"N, 155° 4'8.72"W) faces northeast into Shelikof Strait along the exposed, southern shore of Kashvik Bay. This is a windy, treeless portion of the coast.

View to the west across the Kashvik Bay site in August 2012. The beach here is composed of rounded, medium-sized boulders overlying a wave-planed bedrock strath at shallow depth. A boulder armor is present, but it is not well-organized, perhaps because the clasts are rounded and relatively small. As evident in this photograph, a predominant wave approach from the southeast has caused imbrication of some boulders. The storm berm is present but is poorly developed. Note the wave-cut scarp behind the beach. Our observations here indicate that waves of cobbles are sometimes swept in from the southeast across this boulder beach.

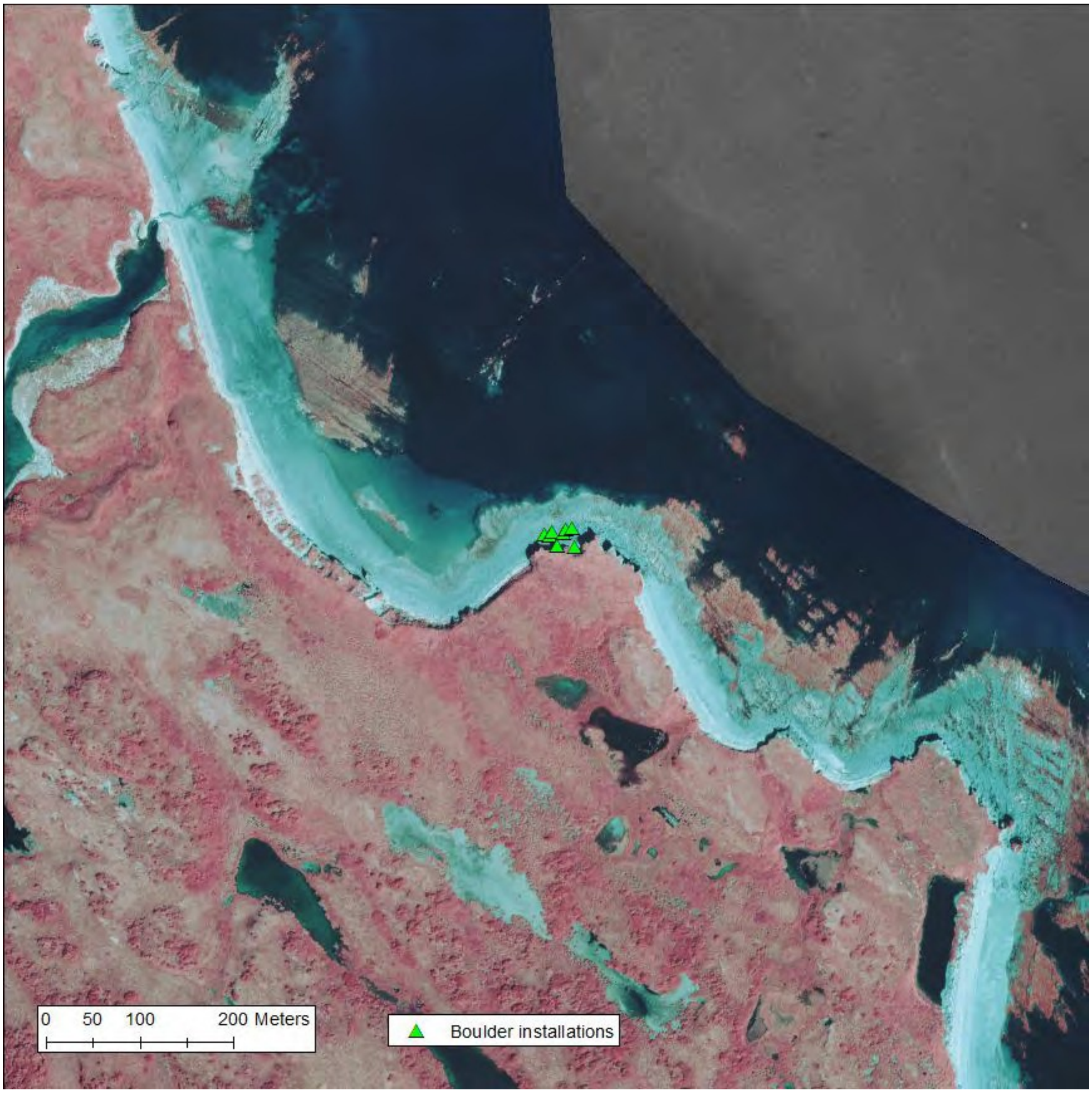

Vertical, color-infrared photograph of the Kashvik Bay site. Green triangles show the location of our bolt-marked transect line. The shallow, rocky nature of this area is clearly seen.

Blow-up of the previous photograph showing location of transect markers and of onshore bench marks at the Kashvik Bay site.

McArthur Pass site

Located in a relatively sheltered cove in Kenai Fjords National Park, the MR1 site (59°27'43.72"N, 150°22'46.90"W) differs from our other monitoring sites by lacking a boulder armor. Instead, it consists of shattered granitic bedrock lowered into the intertidal zone during the 1964 earthquake.

The MR1 site consists of shattered bedrock. The youthful nature of this beach is seen in the angularity of the clasts. The quadrat frame (40 x 50 cm) in the photo is set to assess surface oil cover at one of the permanently marked quadrat locations.

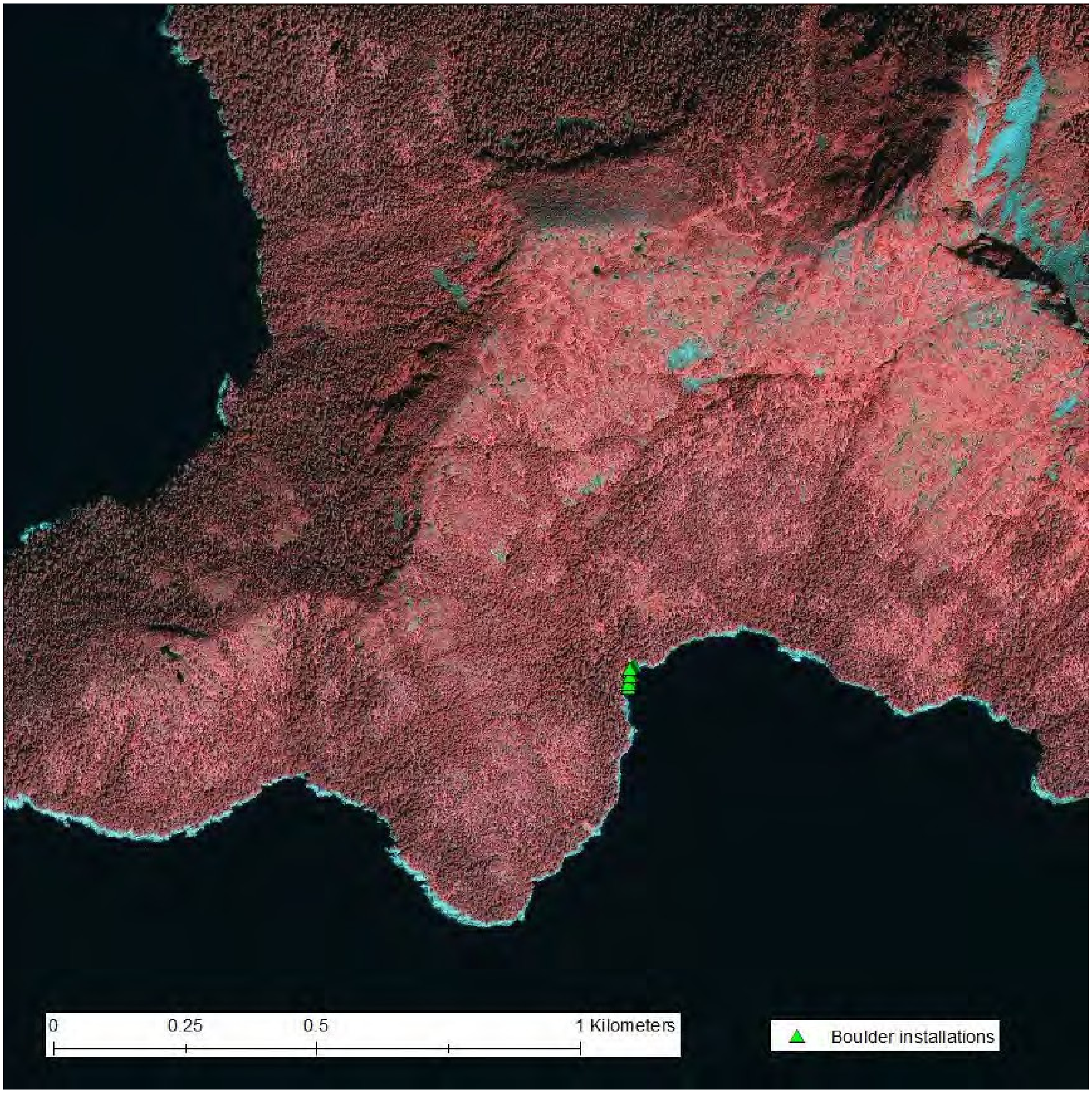

Vertical, color-infrared photograph of the McArthur Pass site. The surrounding hillsides are densely forested.

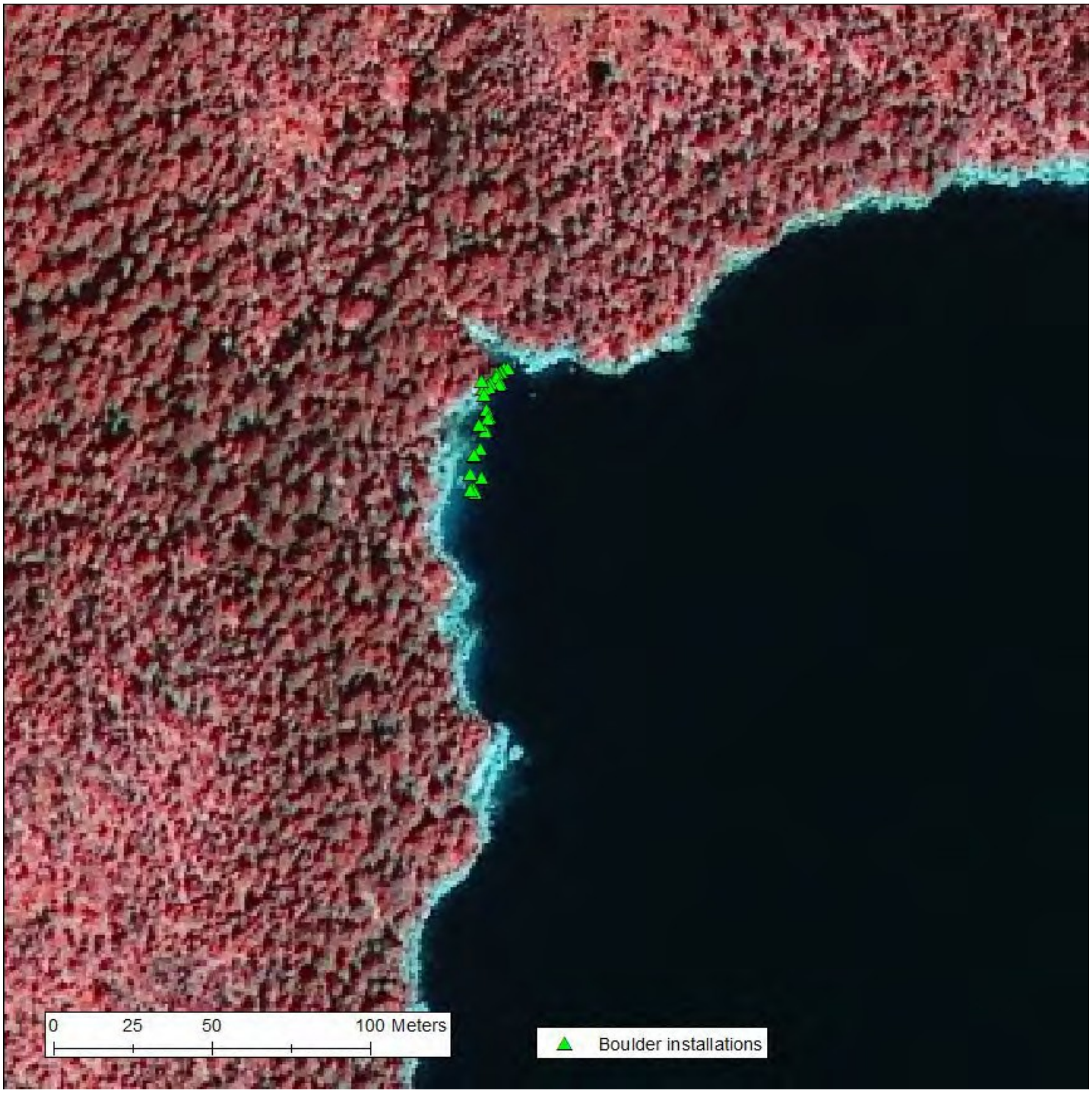

Blow-up of the preceding color-infrared photograph showing location of the survey bolts at the McArthur Pass site (green triangles). This coastline was lowered into the intertidal zone during the 1964 earthquake.

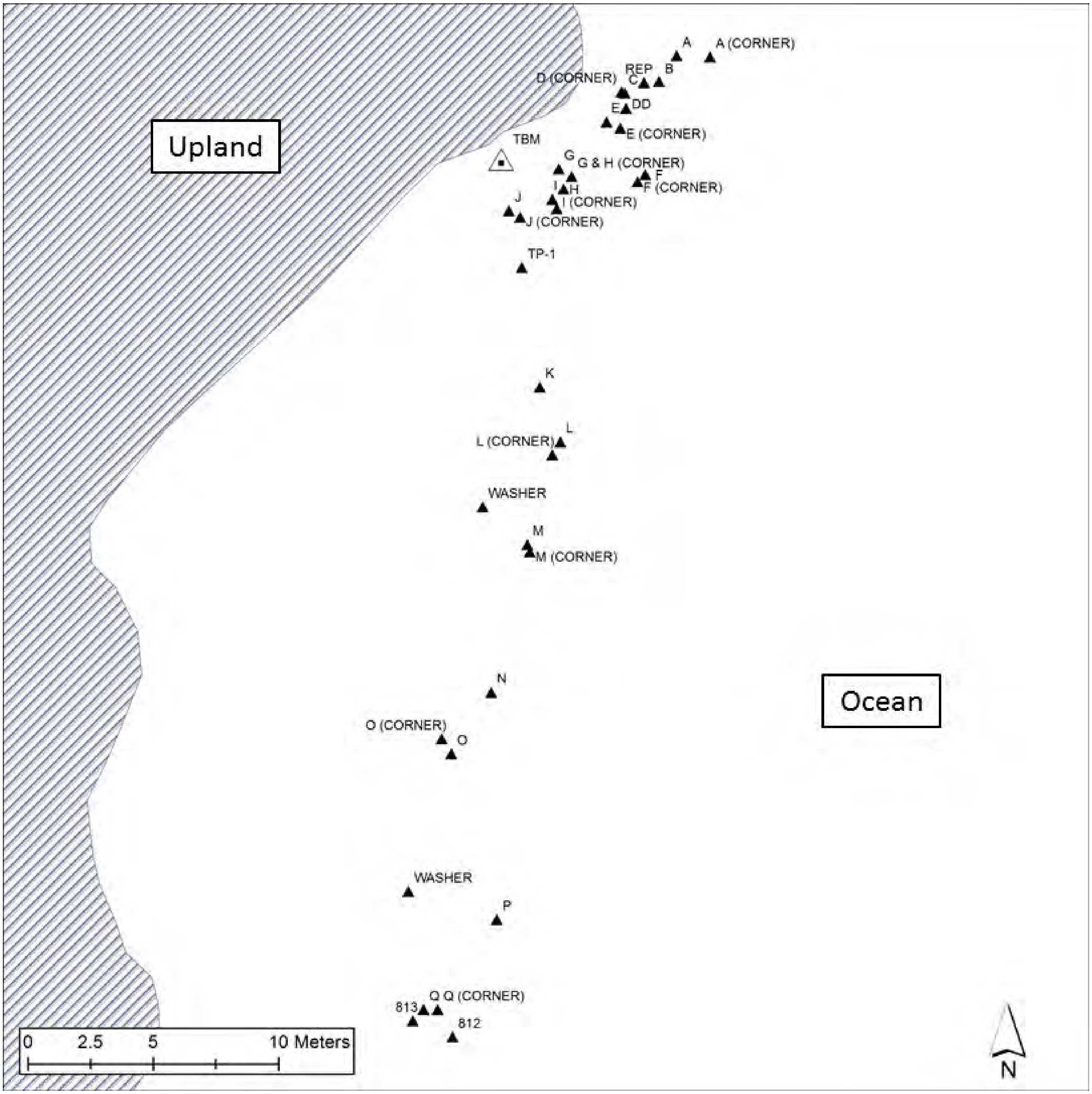

GPS-based map of bolts at the McArthur Pass site. See Appendix B for exact GPS locations.

APPENDIX B: GPS Coordinates

GPS Coordinates of temporary benchmarks (TBMs), quadrat bolts, puck (PEMD) bolts, other markers, taken in NAD83.

Name	Site	Puck	Label	POINT_X	POINT_Y
TBM	Cape Douglas	0		-153.29463	58.8784244
B	Cape Douglas	0		-153.29476	58.8784163
C	Cape Douglas	0		-153.29470	58.8784185
D	Cape Douglas	0		-153.29473	58.8783856
E	Cape Douglas	0		-153.29471	58.8783747
F	Cape Douglas	0		-153.29470	58.8783757
G	Cape Douglas	0		-153.29468	58.8783831
H	Cape Douglas	0		-153.29467	58.8783908
I	Cape Douglas	0		-153.29467	58.8783806
J	Cape Douglas	0		-153.29465	58.8783873
K	Cape Douglas	0		-153.29467	58.8783659
O	Cape Douglas	0		-153.29470	58.8783348
P	Cape Douglas	0		-153.29465	58.8783601
Q (BOLT HOLE)	Cape Douglas	0		-153.29466	58.8783409
Q (EPOXY)	Cape Douglas	0		-153.29466	58.8783474
R	Cape Douglas	0		-153.29463	58.8783691
S (EPOXY)	Cape Douglas	0		-153.29463	58.8783606
T	Cape Douglas	0		-153.29461	58.8783575
U	Cape Douglas	0		-153.29459	58.8783437
V	Cape Douglas	0		-153.29461	58.8783355
W	Cape Douglas	0		-153.29452	58.8783385
X	Cape Douglas	0		-153.29454	58.8783551
Y	Cape Douglas	0		-153.29447	58.8783666
	Cape Douglas	1	Puck #1	-153.29476	58.8784154
	Cape Douglas	2	Puck #2	-153.29472	58.8783845
	Cape Douglas	3	Puck #3	-153.29473	58.8783753
	Cape Douglas	4	Puck #4	-153.29470	58.8783828
	Cape Douglas	5	Puck #5	-153.29468	58.8783943
	Cape Douglas	6	Puck #6	-153.29467	58.8783874
	Cape Douglas	7	Puck #7	-153.29469	58.8783758
	Cape Douglas	8	Puck #8	-153.29468	58.8783593
	Cape Douglas	9	Puck #9	-153.29465	58.8783686
	Cape Douglas	10	Puck #10	-153.29460	58.8783498
	Cape Douglas	1	Control #1	-153.29383	58.8781491
	Cape Douglas	2	Control #2	-153.29382	58.8781153
	Cape Douglas	3	Control #3	-153.29379	58.8780951
	Cape Douglas	4	Control #4	-153.29375	58.8781118

A	Cape Gull	0	-154.15243	58.2348933
A (CORNER)	Cape Gull	0	-154.15242	58.2348924
B	Cape Gull	0	-154.15239	58.2349478
B (CORNER)	Cape Gull	0	-154.15239	58.2349515
C	Cape Gull	0	-154.15238	58.2349540
C (CORNER)	Cape Gull	0	-154.15239	58.2349526
D	Cape Gull	0	-154.15231	58.2350631
E	Cape Gull	0	-154.15242	58.2350758
E (CORNER)	Cape Gull	0	-154.15243	58.2350808
F	Cape Gull	0	-154.15233	58.2351325
F (CORNER)	Cape Gull	0	-154.15233	58.2351303
G	Cape Gull	0	-154.15232	58.2351272
G (CORNER)	Cape Gull	0	-154.15232	58.2351303
H	Cape Gull	0	-154.15228	58.2351185
H (CORNER)	Cape Gull	0	-154.15229	58.2351183
I	Cape Gull	0	-154.15227	58.2351306
J	Cape Gull	0	-154.15224	58.2351225
J (CORNER)	Cape Gull	0	-154.15226	58.2350656
K (CORNER)	Cape Gull	0	-154.15221	58.2351276
L	Cape Gull	0	-154.15220	58.2351602
TBM	Cape Gull	0	-154.15220	58.2351076
REP	Kashvik	0	-155.07028	57.9073906
TP-1	Kashvik	0	-155.07020	57.9073801
TP-2	Kashvik	0	-155.07015	57.9074168
TP-3	Kashvik	0	-155.06996	57.9074079
TP-4	Kashvik	0	-155.06991	57.9074444
LEP	Kashvik	0	-155.06979	57.9074615
BM	Kashvik	0	-155.07006	57.9072821
TBM	Kashvik	0	-155.06975	57.9072726
R	Kiukpalik Island	0	-153.55278	58.5969290
O	Kiukpalik Island	0	-153.55280	58.5969434
N	Kiukpalik Island	0	-153.55294	58.5968304
K	Kiukpalik Island	0	-153.55298	58.5968230
I	Kiukpalik Island	0	-153.55312	58.5968560
H	Kiukpalik Island	0	-153.55310	58.5968283
G	Kiukpalik Island	0	-153.55312	58.5968249
F	Kiukpalik Island	0	-153.55313	58.5968282
E	Kiukpalik Island	0	-153.55313	58.5968263
D	Kiukpalik Island	0	-153.55315	58.5968149
C (BOLT HOLE)	Kiukpalik Island	0	-153.55318	58.5967889
B	Kiukpalik Island	0	-153.55318	58.5968301

A	Kiukpalik Island	0		-153.55322	58.5968136
Q	Kiukpalik Island	0		-153.55323	58.5968051
TBM	Kiukpalik Island	0		-153.55307	58.5968830
	Kiukpalik Island	0	Control #1	-153.54967	58.5994307
	Kiukpalik Island	0	Control #2	-153.54962	58.5994018
	Kiukpalik Island	0	Control #3	-153.54969	58.5993671
	Kiukpalik Island	0	Control #4	-153.54958	58.5992603
	Kiukpalik Island	0	Puck #1	-153.55315	58.5968142
	Kiukpalik Island	0	Puck #2	-153.55314	58.5968231
	Kiukpalik Island	0	Puck #3	-153.55312	58.5968192
	Kiukpalik Island	0	Puck #4	-153.55313	58.5968339
	Kiukpalik Island	0	Puck #5	-153.55307	58.5968499
	Kiukpalik Island	0	Puck #6	-153.55306	58.5968451
	Kiukpalik Island	0	Puck #7	-153.55296	58.5968410
	Kiukpalik Island	0	Puck #8	-153.55295	58.5968392
	Kiukpalik Island	0	Puck #9	-153.55289	58.5968904
A	McArthur Pass	0		-150.37934	59.4620873
A (CORNER)	McArthur Pass	0		-150.37931	59.4620863
B	McArthur Pass	0		-150.37935	59.4620784
REP	McArthur Pass	0		-150.37936	59.4620782
C	McArthur Pass	0		-150.37937	59.4620749
DD	McArthur Pass	0		-150.37937	59.4620694
D (CORNER)	McArthur Pass	0		-150.37938	59.4620755
E	McArthur Pass	0		-150.37939	59.4620650
E (CORNER)	McArthur Pass	0		-150.37938	59.4620626
	McArthur Pass	0		-150.37936	59.4620455
F (CORNER)	McArthur Pass	0		-150.37937	59.4620431
G	McArthur Pass	0		-150.37942	59.4620492
H	McArthur Pass	0		-150.37942	59.4620419
G & H (CORNER)	McArthur Pass	0		-150.37942	59.4620462
I	McArthur Pass	0		-150.37943	59.4620385
I (CORNER)	McArthur Pass	0		-150.37943	59.4620350
J	McArthur Pass	0		-150.37946	59.4620352
J (CORNER)	McArthur Pass	0		-150.37945	59.4620327
TP-1	McArthur Pass	0		-150.37945	59.4620147
K	McArthur Pass	0		-150.37945	59.4619718
L	McArthur Pass	0		-150.37943	59.4619519
L (CORNER)	McArthur Pass	0		-150.37944	59.4619474
M	McArthur Pass	0		-150.37946	59.4619159
M (CORNER)	McArthur Pass	0		-150.37946	59.4619133
N	McArthur Pass	0		-150.37949	59.4618639

O	McArthur Pass	0	-150.37952	59.4618428
O (CORNER)	McArthur Pass	0	-150.37953	59.4618483
P	McArthur Pass	0	-150.37950	59.4617828
Q	McArthur Pass	0	-150.37955	59.4617521
Q (CORNER)	McArthur Pass	0	-150.37954	59.4617519
812	McArthur Pass	0	-150.37953	59.4617419
813	McArthur Pass	0	-150.37956	59.4617484
WASHER	McArthur Pass	0	-150.37956	59.4617945
WASHER	McArthur Pass	0	-150.37949	59.4619302
TBM	McArthur Pass	0	-150.37946	59.4620536
A	Ninagiak Island	0	-153.99737	58.4548153
B	Ninagiak Island	0	-153.99736	58.4548123
C	Ninagiak Island	0	-153.99735	58.4548180
D	Ninagiak Island	0	-153.99734	58.4548143
E	Ninagiak Island	0	-153.99733	58.4548149
F	Ninagiak Island	0	-153.99733	58.4547870
G	Ninagiak Island	0	-153.99732	58.4547733
H	Ninagiak Island	0	-153.99731	58.4547912
I	Ninagiak Island	0	-153.99731	58.4547914
J	Ninagiak Island	0	-153.99725	58.4547908
K	Ninagiak Island	0	-153.99725	58.4547996
L	Ninagiak Island	0	-153.99727	58.4547992
M	Ninagiak Island	0	-153.99727	58.4548023
Q	Ninagiak Island	0	-153.99727	58.4548244
P	Ninagiak Island	0	-153.99728	58.4548223
R	Ninagiak Island	0	-153.99725	58.4548185
S	Ninagiak Island	0	-153.99722	58.4548069
T	Ninagiak Island	0	-153.99721	58.4548328
U	Ninagiak Island	0	-153.99717	58.4548171
V	Ninagiak Island	0	-153.99734	58.4547537
W	Ninagiak Island	0	-153.99734	58.4547365
Y	Ninagiak Island	0	-153.99726	58.4547047
Z	Ninagiak Island	0	-153.99724	58.4547144
TBM	Ninagiak Island	0	-153.99742	58.4548870

Appendix C: Supplemental 1

Deuterated surrogate polynuclear aromatic hydrocarbon (PAH) standards and concentrations in spike used for passive samplers (PEMDs), tissue, and sediment. Spike volumes were 500 µL for tissue and sediments and half the equivalent for PEMDs, PAHs only. Spike solvent was hexane.

(µg/ml)	**Surrogate**
2.0	naphthalene-d_8
2.0	acenaphthene-d_{10}
2.0	phenanthrene-d_{10}
2.0	chrysene-d_{12}
2.0	perylene-d_{12}
2.0	benzo[*a*]pyrene-d_{12}
9.9	n-dodecane-d_{26}
9.7	n-hexadecane-d_{34}
9.7	n-eicosane-d_{42}
9.8	n-tetracosane-d_{50}
9.7	n-triacontane-d_{62}

APPENDIX D: Surface Oil Percent Covers

D1. Surface oil cover and description of the oil in quadrats at McArthur Pass Site (Segment MR-1) on 8/23/94, 7/28/99, 8/22/05, and 8/9/12

	1994		1999		2005		2012	
Quadrat	% Oil Cover	Oil Description	% Oil Cover	Oil Description	% Oil Cover	Oil Description	% Oil Cover	Oil Description
A	25	coat with minor asphalt	2	coat with minor asphalt	0		0	
B	14	coat with minor interstitial asphalt	4	coat with minor interstitial asphalt	1	asphalt	0	
C	13	coat, minor interstitial mousse	5	coat	0.5	asphalt	0	
D	12	coat, interstitial asphalt	10	asphalt	8		3	asphalt with embedded sediments
E	26	coat, minor interstitial mousse	3	asphalt	2	asphalt	1	asphalt with embedded sediments
F	13	coat	0.5	coat	0		0	
G	33	coat, asphalt	30	coat, asphalt	6	asphalt	5	asphalt with embedded sediments
H	17	coat, minor tar	16	coat, minor tar	6	asphalt	6	asphalt with embedded sediments
I	11	coat, interstitial tar	2	coat, interstitial tar	1.5	asphalt	0	
J	12	interstitial tar, trace of coat	6	tar	0.5		0	
K	9	interstitial tar	5	interstitial tar, trace of coat	0		0	
L	12	coat, interstitial tar	6	interstitial tar, trace of coat	1	asphalt	0	
M	22	interstitial tar, coat	4	interstitial tar, trace of coat	0.5		0	
N	30	interstitial tar	30	interstitial tar	8		1	asphalt with embedded sediments
O	13	interstitial tar	2	interstitial tar	6		0.5	asphalt with embedded sediments
P	12	interstitial tar	16	interstitial tar	1	asphalt	0	

Q	15	coat, interstitial tar	18	interstitial tar, trace of coat	12		1	asphalt with embedded sediments

D.2. Surface oil cover, quadrat arrangement and description of oil at the Cape Douglas site (Segment CD003A) on 8/7/94, 8/8/99, 8/16/05, and 8/3/12. Multiple values in 1999 are alternate quadrat positions necessitated by shifts in boulders/bolts. NA= Not Assessed; there may be multiple reasons why (e.g., bolt not found, boulders have moved and quadrat cannot be assessed, etc.).

Quadrat	1994 % Oil Cover	Oil Description	1999 % Oil Cover	Oil Description	2005 % Oil Cover	Oil Description	2012 % Oil Cover	Oil Description
A	12	soft asphalt, rainbow and grey sheening	0		NA		NA	
B	20	coat, stain, soft asphalt, grey sheen	0		0		0	
C	20	coat, soft asphalt, rainbow sheen	8, 2	hard asphalt	NA		0	
D	45	Interstitial mousse, soft asphalt, grey sheen	1	coat	18	asphalt	1	asphalt with embedded sediments
E	45	interstitial mousse, soft asphalt, grey sheen, coat, stain	<0.5	coat	8	asphalt and gray sheen	13	asphalt with embedded pebbles and granules
F	20	interstitial mousse, soft asphalt, grey sheen	4	coat and asphalt	11		8	asphalt with embedded sediments
G	15	coat, grey sheen	2, 5	coat	4	asphalt and gray sheen	4	tar and asphalt embedded with sediments
H	45	interstitial asphalt, interstitial mousse	34	hard asphalt	16	trace of coat, hard asphalt	3	asphaltic tar – thin and thick
I	35	coat, thick interstitial mousse, soft asphalt, grey	14	hard asphalt	0		1	clump of soft asphalt mixed with sediments

		sheen						
J	20	coat	0, 20	trace of coat, hard asphalt	14	trace of coat, hard asphalt	6	asphalt with embedded sediments
K	16	coat	3	trace of coat, hard asphalt	3	asphalt	0	
L	40	interstitial asphalt, coat	0		NA		NA	
M	40	coat, interstitial asphalt, rainbow sheen	22	asphalt	NA		NA	
N	13	interstitial asphalt, coat	0		NA		NA	
O	15	Interstitial asphalt, rainbow and grey sheen	0		0		0	
P	8	interstitial tar, coat	4	asphalt	2	asphalt	0	
Q	19	coat, stain, interstitial tar, grey sheen, interstitial mousse	4	asphalt	NA		0	
R	12	coat, interstitial tar	3,1	coat and asphalt	0		1	asphalt with embedded sediments
S	20	interstitial tar, coat, rainbow sheen, interstitial mousse	0		0		0	
T	16	interstitial mousse, rainbow sheen	1	coat and asphalt	0		0	
U	12	interstitial tar	10	coat and asphalt	0		0	
V	20	interstitial tar, coat	0		0		0	
W	9	interstitial mousse and tar	0		0		0	
X	8	coat	2, 4	coat	0		0	
Y	4	interstitial tar	0, 0.5	asphalt	0		0	

D.3. Surface oil cover and descriptions of the oil in quadrats at the Kiukpalik Island site (Segment SK-101) on 8/10/94, 8/9/99, 8/18/05, and 8/4/12. In 2005 much of the site, including quadrats, was infilled with cobbles and boulders. NA= Not Assessed; there may be multiple reasons why (e.g., bolt not found, boulders have moved and quadrat cannot be assessed, etc.).

Quadrat	1994 % Oil Cover	Oil Description	1999 % Oil Cover	Oil Description	2005 % Oil Cover	Oil Description	2012 % Oil Cover	Oil Description
A	28	coat	1	coat	0		0	
B	28	coat, interstitial tar	38	coat	NA		0	
C	20	stain, coat, interstitial tar, and mousse	8	stain, coat, interstitial tar, and mousse	NA		0	
D	38	stain, coat, interstitial tar	35	coat, asphalt	NA	coat	0	
E	38	interstitial tar and mousse, stain, coat	2	coat	0		13	asphalt with embedded sediments
F	30	stain, coat, interstitial tar	20	coat, tar	NA		0	
G	17	stain, coat, interstitial tar and mousse, grey sheen	33	minor coat, tar	NA	coat	1	asphalt with embedded sediments
H	58	coat, stain, interstitial mousse and tar	25	tar	NA		9	asphalt with embedded sediments, tar coating
I	36	stain, coat	4	coat, tar	NA		0	
J	<15		6	tar	NA		NA	
K	14	coat, interstitial tar and mousse	6	tar	NA		0	
L	36	coat, interstitial tar and mousse	4	coat	NA		NA	
M	<15		2	tar	NA		5	asphalt with embedded sediments, tar coating
N	12	coat, interstitial tar	6	tar	NA		3	asphalt with embedded sediments
O	16	coat, interstitial tar and mousse	6	coat, tar	NA	coat	0	
P	35	coat with spruce needles embedded	lost		NA		NA	

Q	16	coat	8	coat	NA		0	
R	12	stain, coat, interstitial tar and mousse	1	coat	NA		4	

D.4. Surface oil cover and description of the oil in quadrats at the Ninagiak Island site (Segment HB-050B) on 8/9/94, 8/10/99, 8/19/05 and 8/5/12. NA= *Not Assessed*; there may be multiple reasons why (e.g., bolt not found, boulders have moved and quadrat cannot be assessed, etc.).

Quadrat	1994% Oil Cover	Oil Description	1999 % Oil Cover	Oil Description	2005 % Oil Cover	Oil Description	2012 % Oil Cover	Oil Description
A	37	asphalt	6	asphalt	0		0	
B	55	asphalt, brown mousse, rainbow sheen	10	asphalt	NA		0	
C	45	asphalt, brown mousse, rainbow sheen	40	asphalt	NA		0	
D	30	brown mousse, asphalt	8	asphalt	0		0	
E	28	asphalt	7	asphalt	NA		0.5	asphalt with embedded sediments
F	21	asphalt	1	asphalt	NA		0	
G	12	asphalt	1	asphalt	NA		0	
H	27	asphalt	5	asphalt	NA		0	
I	28	asphalt	14	asphalt	0		0	
J	17	asphalt	2	asphalt	NA		5	asphalt with embedded sediments
K	17	asphalt	12	asphalt	NA		0	
L	23	asphalt	12	asphalt	NA		0	
M	28	asphalt	20	asphalt	NA		0	
N	25	asphalt	25	asphalt	NA		NA	
O	23	asphalt	16	asphalt	NA		NA	
P	11	asphalt	18	asphalt	NA		0	

Q	13	asphalt	10	asphalt	NA		0.5	asphalt with embedded sediments
R	37	asphalt	24	asphalt	NA		22	asphalt with embedded sediments
S	23	asphalt	6	asphalt and tar	NA		4	asphalt with embedded sediments
T	9	asphalt	8	asphalt	NA		6	asphalt with embedded sediments
U	14	asphalt, rainbow sheen	10	asphalt	NA		8	asphalt with embedded sediments
V	26	asphalt	14	asphalt	NA		10	asphalt with embedded sediments
W	11	asphalt	14	asphalt	NA		0	
X	25	asphalt	14	asphalt	NA		NA	
Y	18	asphalt	10	asphalt	0.5	asphalt	NA	
Z	16	asphalt	13	asphalt	13	asphalt	NA	

D.5. Surface oil cover and oil description in quadrats at the Cape Gull site (Segment K 0922-CG 1) on, 8/10/94, 8/10/99, 8/21/05 and 8/7/12. Quadrat A was assessed in two positions in 2012: the first position followed the 1994 orientation, the second position followed the 1999/2005 orientation.

Quadrat	1994% Oil Cover	Oil Description	1999 % Oil Cover	Oil Description	2005 % Oil Cover	Oil Description	2012 % Oil Cover	Oil Description
A	11	asphalt	0	asphalt	0		0, 0	
B	24	asphalt	1	asphalt	0		0	
C	11	asphalt	0	asphalt	0		0	
D	18	asphalt	0	asphalt	0		0	
E	12	asphalt	0	asphalt	0		0	
F	15	asphalt	20	asphalt	3	asphalt with shells	0	

G	30	asphalt	19	asphalt	9	asphalt with shells	0
H	14	asphalt	6	asphalt	0		0
I	12	asphalt	14	asphalt	0		0
J	14	asphalt	15	asphalt	2	asphalt with shells	0
K	18	asphalt	10	asphalt	2		0
L	14	asphalt	6	asphalt	0.5	asphalt with shells	0

APPENDIX E: SUBSURFACE OIL DEPTH

E.1 Subsurface oiling described by dip stones at McArthur Pass (Segment MR-1) on 8/23/94, 7/28/99, 8/22/05, and 8/9/12. “Clean” refers to absence of oil. List of conditions goes in stratigraphic sequence from surface downward. Symbol “>” indicates that oiling condition extends below lowest part of stone.

Stone Number	1994 Description of Oiling	Stone Number	1999 Description of Oiling	Stone Number	2005 Description of Oiling	Stone Number	2012 Description of Oiling
94-1	clean	99-1	2 cm tar and mousse	05-1	6 cm asphalt, underlain by buried soil	12-1	1 cm tar/ asphalt, >1 cm mousse
94-2	1.5 cm clean, 1 cm tar, 1cm mousse	99-2	1.5 cm tar	05-2	3 cm asphalt	12-2	1 cm tar/ asphalt, >2 cm mousse
94-3	>2 cm clean	99-3	3 cm tar	05-3	2 cm soft asphalt	12-3	1 cm tar/asphalt, >3 cm mousse
94-4	1 cm tar	99-4	2 cm tar	05-4	2 cm soft asphalt	12-4	3 cm, grey sheen in hole after removal
94-5	2 cm tar	99-5	4 cm tar	05-5	2 cm asphalt	12-5	3 cm
94-6	2 cm tar	99-6	2 cm tar	05-6	1 cm asphalt	12-6	1 cm
94-7	2 cm mousse			05-7	3 cm asphalt	12-7	2 cm
94-8	2 cm tar			05-8	>12 cm clean	12-8	2 cm asphalt
				05-9	1 cm asphalt	12-9	> 3 cm asphalt and brown mousse
				05-10	2 cm asphalt	12-10	>2 cm asphalt and brown mousse
				05-11	>2 cm asphalt	12-11	4 cm asphalt and brown mousse
				05-12	2 cm asphalt	12-12	1-2 cm asphalt, >1 cm mousse
				05-13	2 cm asphalt	12-13	>3 cm asphalt, oil below
				05-14	2 cm asphalt	12-14	>1 cm asphalt
				05-15	2 cm asphalt	12-15	1 cm asphalt, >2 cm mousse
				05-16	2 cm asphalt	12-16	0.5 cm asphalt, >2.5 cm mousse
						12-17	2 cm asphalt, >1 cm mousse
						12-18	4 cm asphalt
						12-19	2 cm asphalt, >6 cm mousse

E.2. Subsurface oiling described by dip stones at the Cape Douglas site (Segment CD003A) on 8/7/94, 8/8/99, 8/16/05, and 8/3/12. “Clean” refers to absence of oil. List of conditions goes in stratigraphic sequence from surface downward. Symbol “>” indicates that oiling condition extends below lowest part of dip stone.

Stone Number	1994 Description of Oiling	Stone Number	1999 Description of Oiling	Stone Number	2005 Description of Oiling	Stone Number	2012 Description of Oiling
94-1	2 cm mousse	99-1	4 cm mousse	05-1	>3 cm coat and mousse	12-1	>4 cm
94-2	3 cm mousse	99-2	2.5 cm mousse	05-2	6 cm coat and mousse	12-2	>4 cm
94-3	3 cm mousse	99-3	2 cm mousse	05-3	3 cm coat	12-3	>3 cm
94-4	3 cm mousse	99-4	1.5 cm mousse	05-4	>6 cm coat and asphalt	12-4	>8 cm
94-5	5 cm mousse	99-5	4.5 cm mousse	05-5	>4 cm asphalt and mousse	12-5	>2 cm
94-6	7 cm mousse	99-6	4 cm mousse	05-6	3 cm coat	12-6	>9 cm
94-7	>5 cm clean	99-7	>3 cm mousse	05-7	4 cm coat	12-7	>3 cm
94-8	>5 cm clean	99-8	2 cm mousse	05-8	4 cm asphalt	12-8	>4 cm
94-9	>5 cm clean	99-9	8 cm mousse	05-9	>4 cm asphalt and mousse	12-9	5 cm
94-10	>8 cm mousse	99-10	>5 cm mousse	05-10	>4 cm asphalt and mousse	12-10	>9 cm
94-11	>8 cm mousse	99-11	4.5 cm mousse	05-11	>4 cm asphalt and mousse	12-11	3 cm
94-12	>5 cm mousse	99-12	3.5 cm mousse	15-12	3 cm asphalt, 3 cm mousse	12-12	2 cm
94-13	9 cm mousse	99-13	2 cm mousse	05-13	1 cm asphalt, 2 cm mousse	12-13	>7 cm
94-14	>5 cm clean	99-14	5 cm mousse	05-14	1 cm asphalt, >6 cm mousse	12-14	5 cm
94-15	1 cm mousse	99-15	3 cm mousse	05-15	1 cm asphalt, >3 cm mousse	12-15	>3 cm
94-16	2.5 cm mousse	99-16	3.5 cm mousse	05-16	2 cm asphalt, 3 cm mousse	12-16	>3 cm
94-17	>3 cm mousse	99-17	7 cm mousse	05-17	1 cm asphalt, >9 cm mousse	12-17	>6 cm
94-18	7 cm mousse	99-18	>1 cm mousse	05-18	1 cm asphalt >3 cm mousse	12-18	>4 cm
94-19	>5 cm clean	99-19	>8 cm mousse	05-19	1 cm asphalt, >4 cm mousse	12-19	3 cm
		99-20	>5 cm clean	05-20	1 cm asphalt, >3 cm mousse	12-20	6 cm

E.3. Subsurface oiling described by dip stones at the Kiukpalik Island site (Segment SK-101) on 8/8/94, 8/9/99 and 8/4/12. In 2005, subsurface oil could not be samples because of infilling of the site by cobbles and small boulders.

Stone Number	1994 Description of Oiling	Stone Number	1999 Description of Oiling	Stone Number	2012 Description of Oiling
94-1	>10 cm clean	99-1	3 cm tar, 4 cm mousse	12-1	>5 cm
94-2	>10 cm clean	99-2	>2 cm mousse	12-2	4 cm
94-3	>2 cm clean	99-3	3 cm tar, >5 cm mousse	12-3	>3 cm
94-4	>3 cm clean	99-4	2 cm tar, >6 cm mousse	12-4	4 cm
94-5	>5 cm clean	99-5	2 cm tar, >3 cm mousse	12-5	6 cm
94-6	>7 cm mousse	99-6	>5 cm mousse	12-6	>2 cm
94-7	1 cm coat, 1 cm asphalt, >9 cm mousse	99-7	3 cm mousse	12-7	>6 cm
94-8	3 cm coat and mousse	99-8	2 cm tar, > 8 cm mousse	12-8	>9 cm
94-9	1 cm of tar, >4 cm mousse	99-9	2 cm tar, >1 cm mousse	12-9	>5 cm
94-10	>5 cm clean	99-10	1 cm tar, >1 cm mousse	12-10	>9 cm
94-11	3 cm coat, 1 cm mousse	99-11	2 cm tar, >3 cm mousse	12-11	>7 cm
94-12	4 cm tar, >4 cm mousse	99-12	2 cm asphalt, 3 cm tar, >3 cm mousse	12-12	3.5 cm
94-13	3 cm tar, >8 cm mousse	99-13	2 cm asphalt, 2 cm tar, 10 cm mousse	12-13	4 cm
94-14	>2 cm asphalt	99-14	3 cm tar, >1 cm mousse	12-14	2 cm
94-15	>2.5 cm asphalt	99-15	1 cm coat, 2 cm tar, >1 cm mousse	12-15	5 cm
94-16	1 cm tar, >7 cm mousse	99-16	2 cm tar, > 5 cm mousse	12-16	>5 cm
94-17	2 cm tar, >6 cm mousse	99-17	>3 cm mousse	12-17	>6 cm
94-18	3 cm tar, >8 cm mousse	99-18	>4 cm tar	12-18	>7 cm
94-19	1 cm tar, >4 cm mousse			12-19	>3 cm
				12-20	>9 cm

E.4. Subsurface oiling described by dip stones at the Ninagiak Island site (Segment HB-050B) on 8/9/94, 8/10/99, 8/19/05 and 8/5/12.

Stone Number	1994 Description of Oiling	Stone Number	1999 Description of Oiling	Stone Number	2005 Description of Oiling	Stone Number	2012 Description of Oiling
94-1	>10 cm clean	99-1	>6 cm clean	05-1	0.5 cm asphalt, 4 cm mousse	12-1	>3 cm
94-2	3 cm clean, >1 cm mousse	99-2	>9 cm clean	05-2	1 cm asphalt, >3 cm mousse	12-2	4 cm
94-3	2 cm coat, >5 cm mousse	99-3	>8 cm clean	05-3	2 cm asphalt, >2.5 cm mousse	12-3	4 cm
94-4	>3 cm clean	99-4	9 cm clean, 5 cm coat, 3 cm mousse	05-4	1 cm asphalt, >2.5 cm mousse	12-4	>4 cm
94-5	1 cm asphalt, >5 cm mousse	99-5	>3 cm tar	05-5	1.5 cm asphalt, 5 cm mousse	12-5	6 cm
95-6	4 cm tar, >3 cm mousse	99-6	1 cm clean, >2 cm mousse	05-6	12 cm clean	12-6	>3 cm
94-7	>3 cm mousse	99-7	>5 cm clean			12-7	2 cm
94-8	>2-7 cm mousse	99-8	>8 cm clean			12-8	3 cm
94-9	1 cm asphalt, 6 cm mousse	99-9	>5 cm clean			12-9	3 cm
94-10	>8 cm clean	99-10	>4 cm clean			12-10	2 cm
94-11	1 cm asphalt, >5 cm mousse	99-11	>2 cm asphalt			12-11	>2 cm
94-12	>5 cm clean	99-12	>2 cm mousse			12-12	>6 cm
94-13	>5 cm clean	99-13	12 cm clean, >2 cm mousse				
94-14	1 cm asphalt, 5 cm mousse	99-14	2 cm tar, 8 cm clean, >5cm mousse				
94-15	1 cm clean, 1 cm asphalt, 2 cm mousse	99-15	2 cm clean, 2 cm coat, >4 cm mousse				
94-16	>3 cm mousse	99-16	2 cm asphalt, 2 cm mousse				
94-17	>11 cm clean	99-17	2 cm asphalt, 2 cm mousse				
94-18	1 cm clean, 7 cm mousse	99-18	>5 cm clean				
		99-19	1 cm clean, >2 cm mousse				
		99-20	2 cm clean, 3 cm mousse				

E.5. Subsurface oiling described by dip stones at the Cape Gull site (Segment K 0922-CG 001) on 8/10/94, 8/10/99 and 8/21/05. No dipstones were sampled in 2012 because extremely little surface oil was observed at the site.

Stone Number	1994 Description of Oiling	Stone Number	1999 Description of Oiling	Stone Number	2005 Description of Oiling
94-1	>3 cm clean	99-1	>6 cm clean	05-1	>4cm clean
94-2	5 cm asphalt	99-2	>12 cm clean	05-2	>8 cm clean
94-3	>6 cm clean	99-3	>16 cm clean	05-3	>5 cm clean
94-4	7 cm mousse	99-4	>5 cm clean	05-4	2.5 cm shell mousse
94-5	>5 cm clean	99-5	6 cm asphalt	05-5	2 cm asphalt
94-6	>10 cm clean	99-6	1 cm tar, 8 cm asphalt	05-6	>2 cm shell mousse
94-7	>6 cm clean	99-7	2 cm tar	05-7	>2 cm shell mouse
94-8	>11 cm clean	99-8	2 cm mousse	05-8	>14 cm clean
94-9	>5 cm clean	99-9	>8cm clean	05-9	3 cm shell asphalt
94-10	1-3 cm mousse	99-10	3.5 cm asphalt	05-10	>3 cm shell asphalt
94-11	1-3 cm mousse	99-11	1 cm coat, 2.5 cm mousse		
94-12	0-1 cm clean, 3-9 cm mousse	99-12	>7 cm clean		
94-13	>4 cm clean	99-13	3 cm asphalt		
94-14	2 cm asphalt, 3 cm mousse	99-14	4 cm asphalt		
94-15	>4 cm clean	99-15	3 cm coat		
94-16	>3 cm clean	99-16	>3 cm coat		
94-17	>8 cm clean	99-17	>11 cm clean		
94-18	>2 cm clean				
94-19	>3 cm clean				

E.6. Subsurface oiling described by dip stones at the Kashvik Bay site (Segment KA-002) on 8/12/99. Dip stones could not be sampled in 1994 due to infilling of the site with cobbles, and the site could not be sampled in 2005 due to storm systems. In 2012, no surface or subsurface oil was observed at this site.

Stone Number	1999 Description of Oiling
99-1	5 cm mousse
99-2	2 cm tar, 2 cm mousse
99-3	1 cm tar, 1 cm mousse
99-4	3 cm mousse
99-5	8 cm mousse
99-6	2 cm mousse
99-7	4 cm mousse
99-8	2 cm mousse
99-9	2 cm mousse
99-10	4 cm mousse
99-11	4 cm mousse
99-12	1 cm tar, 2 cm mousse
99-13	1 cm tar, 2 cm mousse
99-14	3 cm tar
99-15	5 cm mousse